Vapor - liquid equilibrium of the carbon dioxide/methane mixture at three isotherms

Eirini Petropoulou[1*], Epaminondas Voutsas[1], Snorre Foss Westman[2], Anders Austegard[2], Hans Georg Jacob Stang[2], Sigurd Weidemann Løvseth[2]

[1]*Laboratory of Thermodynamics and Transport Phenomena*
School of Chemical Engineering, National Technical University of Athens
9, Heroon Polytechniou Str., Zografou Campus, 15780 Athens, Greece

[2]*SINTEF Energy Research*
Postboks 4761Torgard
N-7465 Trondheim
Norway

Abstract

Experimental vapor – liquid equilibrium data for the CO_2/CH_4 mixture have been measured at 293.13 K, 298.14 K and 303.15 K, with emphasis on the mixture critical area. The maximum estimated standard uncertainties are 3 mK in temperature, 2 kPa in pressure and 0.0008 in mole fraction. The scaling law of statistical thermodynamics has been fitted to the critical region data of each isotherm and very good estimation of the critical point is achieved with a maximum uncertainty of 10 kPa in critical pressure and 0.0009 in critical molar composition. The measurements have been validated against experimental data taken from the literature, where available, and against the prediction of the GERG-2008 model. The Soave-Redlich-Kwong (SRK) and Peng-Robinson (PR) Equations of State using the classic van der Waals one fluid mixing rules, the perturbed chain statistical association fluid theory (PC-SAFT) and the Universal Mixing Rule – Peng Robinson (UMR-PRU) model have been fitted to the data of each isotherm with very satisfactory results. UMR-PRU yields the lowest deviation, especially concerning the critical point area, with an overall absolute average deviation (AAD) of 0.18% in bubble point pressure and 0.43% in CO_2 mole fraction of the vapor phase. In the critical points, UMR-PRU results in an average % AAD equal to 1.55 in critical pressure and 0.99 in the critical point composition.

Keywords: vapor – liquid equilibrium, carbon dioxide, methane, equations of state, UMR-PRU

* Corresponding author. Tel.: (+30) 2107723230; fax: (+30) 2107723155
E-mail address: epetr@chemeng.ntua.gr (E. Petropoulou)

1. Introduction

The knowledge of vapor – liquid equilibrium (VLE) of binary mixtures is very important for validating thermodynamic models and tuning model parameters, rendering possible the accurate process design and operation. The carbon dioxide/methane mixture (CO_2/CH_4) is important both for carbon capture and storage (CCS) and the natural gas (NG) industry. In the case of CCS, methane can be found as an impurity in CO_2 captured from natural gas sweetening process, as well as from pre-combustion carbon capture in power plants [1]. On the other hand, CO_2 is one of natural gas components with typical concentration ranging, depending on the NG field, from 2% up to 30% [2]. Due to its importance for the natural gas industry the CO_2/CH_4 mixture has been studied since 1970 and according to NIST literature report [3], twenty three publications of VLE data are available in the literature covering a temperature range from close to the triple point up to the critical point of CO_2, i.e. from 153 K to 301 K, and pressures from 0.27 up to 8.74 MPa. Especially the region from 210 K up to 273.15 K is considered well covered with measurements over the whole phase boundary. However, from temperatures above 273.15 K, few experimental data are available and in most cases there is only one publication per isotherm, so no explicit validation of the data can occur. More specifically, experimental data covering both the liquid and vapor phase are reported in the work of Kaminishi et al. [4] for 283.15 K, without covering the critical mixture area and Nasir et al. [5] who reported several VLE measurements along the bubble and dew point lines. Despite that fact, much scattering is observed between those publications, as well as with the reported bubble points by Devlikamov et al. [6]. At the isotherm of 288.15 K, four data sources are available, Arai et al. [7], Xu et al. [8], Shi et al. [9] and Nasir et al. [5] which are in very good agreement with each other, especially in the area away from the critical point. Xu et al. [8] also reported data for the isotherm of 293.15 K, covering the whole phase boundary. Recently, Nasir et al. [5] reported the VLE of the CO_2/CH_4 binary for several isotherms ranging from 240 K up to 293 K. Yet, in their work a few data have been reported above 287 K. Meanwhile, the critical mixture area is not covered sufficiently in those isotherms. Finally, Bian et al. [10] measured the CO_2/CH_4 VLE close to the critical temperature of CO_2, at 301.15 K, but away of the critical mixture area. Apart from the publications covering both phases, Devlikamov et al. [6] reported the bubble points of CO_2/CH_4 mixture at four isotherms, which are stated at 278.15 K, 283.15 K, 293.15 K and 298.15 K.

According to Li et al. [1], CCS capture typically involves temperatures above 298.15 K, while the operating window for pipeline transportation is from 273.15 K to 317.15 K [11]. Therefore, new experimental data are required to cover the gaps in the higher temperature area and also to be used in order to extend the applicability of thermodynamic models. In the present work, VLE data for the CO_2/CH_4 mixture at three isotherms, 293.13 K, 298.14 K and 303.15 K are measured, following the work by Westman et al. [12, 13]. Emphasis is given in capturing the mixture behavior in the critical region. The experimental data obtained in this study are validated against the existing literature data at the isotherms of 293.13 K and 298.15 K, as well as against

the prediction of the state-of-the-art model for natural gas mixtures, GERG-2008 [14, 15] as calculated through the NIST RefProp software. The results and analysis are presented in accordance to the IUPAC guidelines for reporting phase equilibrium measurements [16], by performing estimation of the standard uncertainty as described in the Guide for the estimation of the Uncertainty in Measurements ("GUM") [17]. Finally, binary interaction parameters have been fitted to each isotherm of the experimental data obtained in this work using in-house software. For the correlation of the obtained experimental data, the Soave – Redlich – Kwong (SRK) [18, 19] and the Peng – Robinson (PR) [20, 21] Equations of State (EoS) combined with the van der Waals one fluid mixing rules (vdW1f) [22, 23] are examined. The above EoSs are selected since, due to their simplicity, they are commonly used in industrial practice. Furthermore, two more sophisticated approaches for the thermodynamic modelling of the VLE are also fitted to the experimental data obtained in this work. That is the Universal Mixing Rule – Peng Robinson (UMR-PRU) model, which combines the PR EoS with the UNIFAC [24] activity coefficient model, and an EoS with a more theoretical background derived from statistical thermodynamics, the Perturbed Chain – Statistical Associating Fluid Theory (PC-SAFT) [25, 26]. The performance of the different models is studied by fitting the model parameters to the liquid phase experimental data and comparing the description of the vapor phase solubility, as well as the critical point estimation.

The structure of the paper is as follows. In Section 2 the experimental apparatus and procedure are briefly described and in Section 3 the most important parameters for the uncertainty analysis are presented. The VLE experimental data are presented and the results of the thermodynamic modelling are discussed in Section 4. Finally, the conclusions reached are presented in Section 5. The models used to correlate the experimental data are briefly presented in Appendix A, while the detailed experimental data are given in tabulated form in the Supplementary Material.

2. Experimental Procedure

The apparatus used in this work [27] has been described in detail by Westman et al. [12]. The phase equilibrium cell has an internal volume of 100 ml and consists of a sapphire cylinder sealed by two titanium flanges, enclosed in a thermostatic bath. CO_2 and methane are injected separately into the cell using syringe pumps, enabling dynamic control of both the cell pressure and total composition. The injection pipelines are connected to valves embedded in the titanium flanges to minimize the dead volume of the cell. In order to monitor the temperature and ensure thermal uniformity, 25 Ω standard platinum resistance thermometers (SPRTs) are placed in each flange. The gas phase pressure inside the cell is measured by isolating a pressure sensor array from the fluid under test at various temperatures and level of aggressiveness using a differential pressure sensor setup. For composition measurements, small samples can be extracted from the cell using two capillaries. One capillary is used for the vapor sampling and has its inlet close to the top of the cell, while the other can be adjusted to the appropriate height to be used for the liquid sampling. To compensate for the cell pressure drop

caused by sampling, a bellows inside the cell can be expanded to decrease the cell volume. In order to reduce the time needed to reach equilibrium, the cell is equipped with a magnetic stirrer.

The temperature and pressure calibration was the one described by Ref. [12] and has been performed in-house in the SINTEF ER facilities. The temperature sensors have been calibrated against fixed point cells according to the International Temperature Scale of 1990 (ITS-90) [28] while the pressure sensors against a recently calibrated dead weight tester. The analytical procedure along with the respective uncertainty analysis are given in detail in Ref. [12]. The gas chromatograph (GC) has been calibrated against gravimetrically prepared calibration gas mixtures, which have been prepared in-house using a custom-built apparatus for such preparation. The purity of the source gases as given by the manufacturer is reported in Table 1, while no further analysis has been performed. Details about the GC calibration are given in Section 3.3.4.

2.1. General

The measurements have been performed using an isothermal analytical method with a variable volume cell with the temperature and the pressure as independent variables. The equilibrium cell is kept at constant temperature using a thermostat bath and is filled with CO_2 and a mixture of CO_2/CH_4 until the target pressure is obtained. The coexistence of the two phases is confirmed visually through a borescope, which is directly connected to a monitor. The experimental procedure is similar to the one followed by Westman et al. [12, 13] and will be briefly described in the following. Before the start of a VLE experiment, the whole system is evacuated through a vacuum pump to ensure no contamination of the pipelines, the pumps or the equilibrium cell. More specifically, the CO_2 pump, the impurity mixture pump and their respective lines are evacuated once and then are flushed with their respective gas. The flushing and evacuation procedure is repeated five times in total to remove any impurities remaining in the cell. After the final flushing and evacuation, the gases are filled to their respective lines and pumps and remain at a pressure of at least 0.5 MPa to prevent any contamination. Then, the same procedure is repeated for the equilibrium cell. After setting the required temperature of the thermostatic bath, the cell is filled with CO_2 until the liquid level is about 40% of the cell volume. The stirrer runs until the temperature and pressure are stabilized. If the measured vapor pressure is within the uncertainty limits of the Span-Wagner [29] EoS, the setting of the bath is deemed appropriate.

After the CO_2 vapor pressure measurements, methane, in the form of a CO_2/CH_4 mixture, is injected to the cell by an injection pump, until the specified pressure is obtained. The liquid level of the cell is adjusted either by injecting more CO_2 or by venting out some liquid from the bottom of the cell. The mixture is stirred to equilibrium and when the temperature and the pressure indications are stabilized for about thirty minutes, the stirrer is turned off and the mixture is left to settle before starting the sampling. The settling time ranges from thirty minutes to three hours, depending on the proximity to the critical region. More specifically, where the density difference between the vapor and the liquid phase is significant, that is away from the critical region, the settling time is set to thirty minutes, while when approaching the

critical region the settling time is increased to one hour. During the settling time, the borescope is inserted into the bath to check the liquid level and then is quickly removed to ensure that no additional heat transfer affects the equilibrium. When the settling period has been completed, the sampling of both phases starts, beginning with the liquid phase and continuing with the vapor phase, by taking six samples from the liquid phase and seven from the vapor one. The samples are withdrawn from the cell every 32 minutes, which is sufficient time to capture the whole CO_2 peak in the chromatogram, as well as for the two phases to settle after the restoration of equilibrium. During sampling, nitrogen in overpressure from the auxiliary circuit is injected through a specific pump to the bellows plate in the cell to compensate for the decrease in pressure caused from the removal of the sample volume. At the isotherm of 303.15 K, the use of the bellows seems to have no significant effect. This is probably due to the high CO_2 concentration, as well as the small differences in density between the two phases. Hence, the bellows' pressure control system does not work and the bellows are not used in the measurements. The selection of the appropriate sample volume in each temperature and pressure is predicted through GERG-2008 EoS, following the methodology proposed by Westman et al. [12]. The first sample of each phase is discarded as flushing sample, while no specific ascending or descending trend has been observed in the series of the remaining samples, which indicates that there is sufficient settling time between each sample.

The pressure readings are retrieved from the sensors every second and the resistance values of the temperature sensors are recorded approximately every 20 seconds. The temperature and pressure measurements from the stable period before the withdrawal of the first sample until the end of sampling is used to calculate the VLE data set, following a procedure that will be discussed in detail in Section 3.2.

2.2. Critical Region

A special procedure suggested by Westman et al. [12, 13] has been followed for pressures close to the critical region for each isotherm, which permits the accurate capturing of the critical area and thus the overall shape of the phase boundary. In this case, the pressure was increased conventionally, by injecting the CO_2/CH_4 mixture into the cell using the impurity pump. The proximity to the critical point is established by a step-by-step increase of the pressure up to the point that the supercritical region is temporarily reached and the mixture reverts to the two-phase region upon reaching the equilibrium. This way, the critical pressure is identified within a narrow interval, of the order of 0.01 MPa. Having established the two-phase region at a point close to the critical one, the stirrer runs from 45 minutes to about 1 hour and then the mixture is left to settle for 2-3 hours. The increased settling time is justified because of the proximity to the critical region, where the densities of both phases are very similar. After the settling period, five or six samples are taken from the liquid phase, and seven samples are taken from the vapor phase with a 32 minutes period between the opening of the ROLSI™ samplers (Rapid On Line Sampler – Injector). During sampling, the bellow plate system is used to compensate for the pressure decrease, with the exception of the isotherm of 303.15 K where this procedure is not necessary as discussed above. After the completion of the VLE measurement, the pressure is slightly decreased by taking samples from the vapor and the liquid phase without using the bellows. The same

procedure, that is stirring to the new equilibrium VLE point, waiting for the two phases to settle and finally sampling of the liquid and vapor phase, is repeated until the critical region is sufficiently captured.

3. Uncertainty Analysis

3.1. Definitions

The terms and the definitions of the "GUM" [17] are used in the uncertainty analysis. The uncertainty components are evaluated as standard uncertainties, with symbol $u(y)$, where y is the estimate of the measurand, Y, that is the measurement result. $s(y)$ is the standard deviation calculated from the samples of y, and is the estimate for minimum contribution to standard uncertainty from random errors in y. The propagation of the standard uncertainties in the input quantities, X_i, to the standard uncertainty in the final measurand, Y, is expressed through the combined standard uncertainty, $u_c(y)$.

3.2. Temperature and Pressure

The uncertainty analysis for the pressure and the temperature measurements has been given in detail by Westman et al. [12] and only the respective results will be reported in this work. The detailed uncertainty results for the mean temperature and pressure values are reported along with their respective VLE measurements in Tables 2 and 3, and for each sample in Tables S.1 and S.2 in the Supplementary Material. The resulted standard uncertainties in the pressure measurement are illustrated in Figure 1(a) and in temperature in Figure 1(b). As it is observed, the standard uncertainty in pressure is estimated to be below 0.03% of the measured pressure. Similarly ~~from the reported values~~, the maximum uncertainty ~~in pressure is 2 kPa while~~ in temperature ~~the maximum uncertainty~~ is 3 mK.

3.3. Composition

The VLE composition and uncertainty analysis has been performed following the same procedure as the one described in detail by Westman et al. [12]. The gas chromatograph (GC) used for determining the compositions of each component in the VLE point is the same that was used in Ref. [12], with the calibration mixtures gravimetrically prepared in a custom built apparatus on the SINTEF ER premises [30].

The uncertainty in the composition derives from a range of sources, which are described in the following subsections. Those include the impurities of the gases used for the calibration mixture preparation, the uncertainty in molar masses, inaccuracies in weighted masses, CO_2 adsorption, repeatability, uncertainties caused at sampling as well as GC analysis and the consistency between the calibration function and data.

3.3.1. Source gas composition and molar mass

The composition and the corresponding uncertainty of the calibration gas mixtures are results of the purity and the molar mass of the source gases used for its preparation. The molar masses of CO_2 and CH_4 have been calculated along with their respective uncertainties from the molar masses of the monoatomic carbon, C, oxygen, O, and hydrogen, H, as given by Wieser et al. [31, 32] and are reported in Table S.3 in the Supplementary Material.

The minimum certified purities of the source gases are given in Table 1, along with their specifications for certain impurities. Since the source gases were not entirely pure, estimates for their molar masses, M_{CO_2+imp} and M_{CH_4+imp}, were calculated as described by Westman et al. [12] by assuming the hydrocarbon impurity to be formed entirely from methane, in the case of CO_2 and ethane for CH_4. The calculated molar masses of the source gases, along with the effective molar masses including the impurities, $M_{CO_2,eff}$ and $M_{CH_4,eff}$ are presented in Table S.3.

3.3.2. Gravimetric preparation

The methodology followed for the gravimetric preparation of the calibration gas mixtures, as well as for the estimation of their uncertainty is the one described in detail by Westman et al. [12, 30]. Two calibration CO_2/CH_4 mixtures with molar compositions, in terms of CO_2, ranging between 0.85 and 0.95, which is the expected range of the compositions for the isotherms in study, have been prepared. The detailed compositions along with the corresponding uncertainties are reported in Table S.4 in the Supplementary Material.

3.3.3. Composition calibration procedure and estimated composition uncertainty

The calibration of the GC has been performed as described in detail by Westman et al. [12] in Appendix A.3.1, with emphasis in the prevention of CO_2 adsorption. Then, samples of varying sizes have been extracted from the cell in two different pressures, 6 MPa and 8 MPa, which are the ranges of the expected pressures at the VLE in the isotherms of interest. These samples formed the basis for the calibration of the composition analysis, giving a relation between the CO_2 mole fraction of the calibration gas mixtures and the GC detector response.

The uncertainty contribution from the calibration mixture reaching the GC could be calculated from:

$$u_c\left(y_{CO_2,cal}\right) = \sqrt{u^2\left(y_{CO_2,cal}, m\right) + u^2\left(y_{CO_2,cal}, M_{eff}\right) + u^2\left(y_{CO_2,cal}, ads\right)}\,, \quad \text{Eq. (1)}$$

where $u\left(y_{CO_2,cal}, m\right)$ and $u\left(y_{CO_2,cal}, M_{eff}\right)$ are the contributing uncertainties in the masses of CO_2 and CH_4 in the gas mixture and in the effective molar masses. The term $u\left(y_{CO_2,cal}, ads\right)$ is the uncertainty contribution from adsorption and is calculated by assuming higher adsorption of CO_2 compared to that of methane. As it is observed from Table S.4, where the uncertainty terms of the calibration mixtures are presented, the different uncertainty contributions are of the same order of magnitude. The uncertainty contribution, $u\left(y_{CO_2,cal}, M_{eff}\right)$, dominates the combined total uncertainty, $u_c\left(y_{CO_2,cal}\right)$, but still it is an order of magnitude lower compared to the uncertainty derived from the calibration function error, which will be shown in Section 3.3.4.

3.3.4. GC integration and calibration function

The GC column, method and detector are those used by Westman et al. [12], using helium as carrier gas with the supplier specifications given in Table 1. The CO_2 and CH_4 peaks in the GC chromatogram using this setup are very distinct, leading to very good separation. The areas under the CO_2 and CH_4 GC peaks, A_{CO_2} and A_{CH_4} respectively, have been obtained for each sample after numerical integration. The GC

thermal conductivity detector (TCD) response was non-linear with respect to the number of moles of CO_2 and CH_4 that passed through it. The following calibration function correlates the area of each component to the mole number passed through the detector.

$$\hat{n}_{CO_2} \cdot k = A_{CO_2} + c_1 \cdot {A_{CO_2}}^{c_2} \quad \text{Eq. (2)}$$

$$\hat{n}_{CH_4} \cdot k = c_3 \cdot A_{CH_4} + c_4 \cdot {A_{CH_4}}^{c_5} \quad \text{Eq. (3)}$$

$$\hat{y}_{CO_2,cal} = \frac{\hat{n}_{CO_2}}{\hat{n}_{CO_2} + \hat{n}_{CH_4}} \quad \text{Eq. (4)}$$

where $\hat{y}_{CO_2,cal}$ is the estimator of the CO_2 mole fraction of a calibration gas mixture given the corresponding integrated peak areas from the GC chromatogram of a specific sample and *k* is a constant factor denoting the areas to the number of moles. The value of *k* is not of interest since it is eliminated when the mole fraction is calculated, as per Eq. (4).

The parameters c_i, with *i* taking values from 1 up to 5 have been fitted per phase by performing a weighted least squares minimization of the objective function *S*, as it is described by Equation A.32 by Westman et al. [12]. The mean value, $\hat{y}_{CO_2,cal}$, of the estimators calculated for each of the 26 series of 5 valid samples have been fitted to the calibration mixture mole fractions, $y_{CO_2,cal}$, and the results along with the standard deviation are presented in Table S.5 in the Supplementary Material. The need for fitting different values of the parameters for the liquid and the vapor phase is justified from the fact that the liquid sampler extracts helium at a slower rate than the vapor sampler. Thus, using the same opening times yields slightly different sample concentration in the column for the two samplers. As it can be observed from Figure ~~1~~2, the errors between the calibration gas CO_2 mole fraction and the mole fraction measured by the GC, $e = y_{CO_2,cal} - \hat{y}_{CO_2,cal}$, are randomly scattered around zero for the two values of $y_{CO_2,cal}$, which indicates that the fit is reasonable. It should be noted, that due to the small number of calibration gas mixtures, a linear correlation had been tested initially, but it failed to accurately describe the relation between the areas and the molar composition of the mixtures, probably due to the high difference in the TCD detector response of CO_2 and CH_4. $s(e)$ is about 10 times higher than $u_c(y_{CO_2,cal})$, and hence the former completely dominates the total systematic uncertainty of the composition measurements.

3.3.5. Total uncertainty in liquid and vapor phase mole fractions

For a set of VLE measurements, the uncertainty in the measurement of temperature, *T*, and pressure, *p*, contributes to the total uncertainty in composition at *T* and *p*, so that the final total uncertainty in composition is given by Eq. (5).

$$u_{tot}(z_{CO_2}) = \sqrt{u^2(z_{CO_2}) + \left(u_c(\bar{T})\frac{\partial z_{CO_2}}{\partial T}\right)^2 + \left(u_c(\bar{p})\frac{\partial z_{CO_2}}{\partial p}\right)^2} \quad \text{Eq. (5)}$$

where z_{CO_2} stands for the composition either for the liquid, x_{CO_2}, or the vapor phase, y_{CO_2}, and $u_c(\bar{T})$ and $u_c(\bar{p})$ are the temperature and pressure uncertainties respectively, as described in detail by Westman et al. [12].

The derivatives of the composition with regard to temperature and pressure, $\frac{\partial z_{CO_2}}{\partial T}$ and $\frac{\partial z_{CO_2}}{\partial p}$, have been calculated numerically from the UMR-PRU thermodynamic model fitted to the data of each isotherm, as it is described in detail in Section 4.5. For data close to the critical region, the calculation of the derivatives with respect to pressure, $\frac{\partial z_{CO_2}}{\partial p}$, are calculated analytically from the fitted scaling law, as it is described in detail in Section 4.3, since the latter fits the experimental data better in this particular region.

3.4. Data Reduction

The same procedure as the one followed by Westman et al. [12, 13] is used in the current work and thus only a brief summary as well as the definition of the symbols used will be given here.

As it was described in Section 2.3, the bellows restore and stabilize the pressure 1-3 minutes after the extraction of the sample for the isotherms of 293.13 and 298.14 K. For the isotherm of 303.15 K the use of the bellows is not required, as discussed in Section 2.1. In the latter case, the pressure returns to its original value after 1-3 minutes, probably due to the high concentration in CO_2. After the return to its original value, the pressure remains stable for 25 to 27 minutes, until the withdrawal of the next sample.

In each series of consecutive liquid or vapor composition samples, x_{CO_2} or y_{CO_2}, at a nominal temperature and pressure, it is assumed that each composition sample has the equilibrium composition at the temperature, *T*, and pressure, *p*. For each of these series of samples, the average mean values of the temperature and pressure and the trimmed mean values for the liquid and vapor phase compositions are calculated, denoted as $\bar{T}_f$, $\bar{p}_f$, $\bar{x}_{CO_2}$, and $\bar{y}_{CO_2}$, respectively. The subscript *f* is used to differentiate between the temperature and pressure values associated with each composition sample, x_{CO_2} or y_{CO_2}, and of those associated with the average compositions, $\bar{x}_{CO_2}$ or $\bar{y}_{CO_2}$. The details concerning the methodology for describing and calculating the propagation of the uncertainty in the measured variables *T*, *p*, x_{CO_2}, and y_{CO_2} into resulting estimates associated with each composition sample are given by Westman et al. [12], and the symbols used are summarized in Table S.6 in the Supplementary Material along with the data for the individual composition samples.

The propagation of uncertainty from the data of an individual sample, $\bar{T}$, $\bar{p}$, x_{CO_2}, and y_{CO_2}, into the mean values for a series of samples, $\bar{T}_f$, $\bar{p}_f$, $\bar{x}_{CO_2}$, and $\bar{y}_{CO_2}$, is defined by Eqs. (11) - (14) in Westman et al. [12] and the symbols are defined in the footnotes of Tables 2 and 3.

4. Results and discussion

4.1. VLE experimental results

VLE measurements at three isotherms of the CO_2/CH_4 binary system at the average temperature of 293.13 K, 298.14 K and 303.15 K have been conducted. Both the dew point and bubble point curves have been mapped, starting from CO_2 vapor pressure up to the critical point of the mixture.

The data for each series of samples are given in terms of mean temperature, $\bar{T}_f$, mean pressure, $\bar{p}_f$, and mean mole fractions for the liquid phase, $\bar{x}_{CO_2}$, or the vapor phase, $\bar{y}_{CO_2}$, in Tables 2 and 3, respectively. These averaged VLE data are plotted in Figure ~~2~~3 along with the other available experimental data close in temperature, where available, and the predictions of the GERG-2008 model.

The temperature, $\bar{T}$, pressure, $\bar{p}$, and mole fractions for the liquid phase, x_{CO_2}, and the vapor phase, y_{CO_2}, for each individual sample are given in Tables S.1 and S.2 in the Supplementary Material, together with their uncertainty estimates. The composition derivatives with respect to pressure, $\frac{\partial x_{CO_2}}{\partial p}$ and $\frac{\partial y_{CO_2}}{\partial p}$, along with the total standard uncertainties in the composition of the samples, $u_{tot}(x_{CO_2})$ and $u_{tot}(y_{CO_2})$, are also reported in Tables S.1 and S.2 in the Supplementary Material.

4.2. Summary and analysis of uncertainty estimates

As it can be retrieved from Table 2, the maximum and average standard deviation of the measurements in terms of CO_2 composition in the liquid phase is $2.5 \cdot 10^{-5}$ and $9.6 \cdot 10^{-6}$, respectively. For the vapor phase, as can be extracted from Table 3, the maximum and average standard deviation is $1.7 \cdot 10^{-4}$ and $1.5 \cdot 10^{-5}$, which indicates that there is higher dispersion in the vapor phase compared to the liquid one. Except from the maximum values, the estimated standard deviation in the mean mole fractions are significantly lower than the systematic uncertainty of the composition measurement. It is also apparent from Figure ~~2~~3, that the relative uncertainty in composition is low for the isotherms of 293.13 K and 298.14 K, while it is higher for the isotherm of 303.15 K, where the CH_4 solubility in CO_2 is extremely low. Still, even if we take into account the uncertainty estimates, the data provide a very good description of the phase boundary.

The estimated standard uncertainty of the VLE measurement in terms of mole fractions as described in Section 3.3.5, $u_{tot}(\bar{x}_{CO_2})$ and $u_{tot}(\bar{y}_{CO_2})$, shows an increasing trend with pressure in general for each isotherm. The maximum of $u_{tot}(\bar{x}_{CO_2})$ is $8.2 \cdot 10^{-4}$ for the series in the critical region, and approximately $1.2 \cdot 10^{-4}$ for the series outside the critical region. $u_{tot}(\bar{y}_{CO_2})$, has a maximum value of $7.9 \cdot 10^{-4}$ for the series in the critical region, and approximately $1.4 \cdot 10^{-4}$ for the series outside the critical region.

The combined standard uncertainty of the measured pressure, $u_c(\bar{p})$, has an average value of 1.1 kPa, with a maximum value equal to 1.2 kPa. This corresponds to approximately 0.02% for the lowest measured pressure and 0.01% for the highest one.

4.3. Critical Point Estimation

The critical point estimation in terms of temperature and composition is based on the scaling law of statistical mechanics [33-35] as described by Westman et al. [12]

$$z_{CO_2} = \hat{z}_{CO_2,C} + \left(\lambda_1 + \varepsilon\frac{\lambda_2}{2}\right)(\hat{p}_c - p) + \varepsilon\frac{\mu}{2}(\hat{p}_c - p)^{\beta} \; . \qquad \text{Eq. (6)}$$

Here, ε equals 1 for bubble points and -1 for dew points, z_{CO_2} is the bubble point or dew point composition at pressure p measured in an area close to the critical point as discussed in Section 2.2, $\hat{z}_{CO_2,C}$ is the estimated composition in the critical point, $\hat{p}_c$ the estimated critical point pressure and λ_1, λ_2, μ and β the scaling law parameters.

According to Sengers et al. [36] a constant value of β equal to 0.325 is appropriate, leaving three parameters, λ_1, λ_2 and μ to be fitted to the data for each isotherm. The regression has been performed to the VLE data indicated in Table 4, along with the estimated results, using the ordinary unweighted least squares method.

The uncertainty in the estimated critical composition and pressure, $u(\hat{z}_{CO_2,C})$ and $u(\hat{p}_c)$ respectively, are calculated according to the Eqs. (7) and (8), following the methodology proposed by Westman et al. [12] and it is based on the uncertainties in the composition and pressure of the VLE data used for the fitting, as well as the standard errors of regression for the critical pressure and composition, $S_E(\hat{p}_C)$ and $S_E(\hat{z}_{CO_2,C})$.

$$\mathrm{u}(\hat{z}_{CO_2,c}) = \sqrt{S_E^2(\hat{z}_{CO_2,c}) + \left[\frac{1}{n_p}\sum_{i=1}^{n_p} u_c(\bar{z}_{i,CO_2})\right]^2} \qquad \text{Eq. (7)}$$

$$\mathrm{u}(\hat{\mathrm{p}}_c) = \sqrt{S_E^2(\hat{p}_c) + \left[\frac{1}{n_p}\sum_{i=1}^{n_p} u_c(\bar{p}_{i,f})\right]^2} \qquad \text{Eq. (8)}$$

The total uncertainty in the composition has been calculated, as mentioned beforehand, using the derivatives of the composition with respect to pressure, which are calculated numerically by utilizing the scaling law. The detailed values are reported in Tables S.1 and S.2 in the Supplementary Material, indicated with the marker $^{+}$.

The estimated critical point pressure and composition are given along with their respective uncertainties in Table 4 and are presented graphically in Figure ~~3~~4.

Although the fitting of the scaling law is straightforward, one parameter of importance is the selection of the experimental points close to the critical area to be included in the fitting. For the estimation of the critical point all VLE measurements close to the critical area have been included in order to better attain the trend of the experimental data. As shown in Figure ~~3~~4(c), only a single vapor phase point has been excluded from the fitting, since it appears to be somewhat of an outlier.

4.4. Comparison with the literature data and GERG-2008 EoS

As it is stated in the introduction, very few experimental data are available at the temperatures of interest. At the isotherm of 293.15 K, the experimental isothermal VLE

data of Xu et al. [8], Nasir et al. [5] and Devlikamov et al. [6] are available and they are plotted along with the measurements of this work in Figure ~~2~~3(a). In general, fairly good agreement is observed between the data of Xu et al. [8] and our measurements, especially in the vapor phase, in the areas away of the critical. It should be noted that the uncertainties reported by Xu et al. [8] are an order of magnitude higher than those in this work, namely, 0.01 K in temperature, 0.02 MPa in pressure and 0.001 in the composition. Furthermore, much scattering is observed especially for the vapor phase measurements, indicating that at those points the uncertainty is much higher. For the liquid phase, although there is generally good agreement between the datasets, Xu et al. [8] systematically reported slightly lower CO_2 mole fraction in the liquid phase compared to this work. The most distinctive differences are reported in the vicinity of the critical area, where Xu et al. [8] report significantly lower CO_2 mole fraction. Maybe this is attributed to the difference in the purity between the source chemicals used; that is 99.95% for methane and 99.97% for CO_2, compared to 99.9995% for methane and 99.9992% for CO_2 used in this work. This difference in the pure chemicals may cause this shift of the phase boundary to lower CO_2 concentrations in both phases due to the existence of higher molecular weight compounds, rendering the VLE data measured in this work more accurate. Nasir et al. [5] recently reported three VLE measurements at the isotherm of 293.65 K. As it is observed in Figure ~~2~~3(a), our data are in agreement with the reported measurements of Nasir et al. [5] in both phases. Furthermore, the data by Devlikamov et al. [6] for pressure higher than 7 MPa, show significantly lower methane content in the liquid phase as compared to the data by Xu et al. [8], Nasir et al. [5], the data measured in this work as well as the predictions of the GERG-2008 model. Similar behavior is observed at the isotherm of 283.15 K for the bubble point measurements of Devlikamov et al. [6], where they present lower methane solubility compared to the data measured by Kaminishi et al. [4] and Nasir et al. [5]. For the above mentioned reasons, the data by Devlikamov et al. [6] are considered as inaccurate. Finally, for the non-critical area, the experimental data obtained in this work are in good agreement with the predictions of the GERG-2008 model.

At the mean temperature of 298.14 K, only the data by Devlikamov et al. [6] for the liquid phase exist, which, as discussed above, are generally considered inaccurate and thus cannot be used to evaluate the data obtained in our work. Therefore, the only comparison of value can occur with the prediction of an accurate thermodynamic model. As it is presented in Figure ~~2~~3(b), the obtained data are in good agreement with the prediction of GERG-2008 and thus are considered to be of reasonable accuracy.

To the best of our knowledge, VLE data at 303.15 K for the CO_2/CH_4 mixture have not been presented in the literature and thus, the comparison of the data obtained in this work is limited to the prediction of the GERG-2008 model. As it is observed in Figure ~~2~~3(c), the GERG-2008 prediction for both phases is within the limits of the experimental accuracy.

4.5. Model fitting

Following the work by Westman et al. [12, 13], the GERG-2008 model has been used for the VLE prediction of the isotherms of interest in order to evaluate the experimental data obtained in this work. As mentioned in section 4.4, the GERG-2008 prediction for

both phases is in good accordance with the data obtained in this work away from the critical area. Despite from the fact that the specific model is state-of-the-art for natural gas mixtures such as mixtures including methane, it overpredicts significantly the pressure at the critical region.

Since equations of state are usually used for the design and control of process simulations, the SRK and the PR EoSs, the latter with the vdW1f and with advanced mixing rules (UMR-PRU), as well as the PC-SAFT EoS are used to correlate the experimental data of each isotherm. All EoSs used in this work are well-documented in the literature and their theory and equations will be briefly described in Appendix A. The critical properties (T_c, p_c, ω) required for the pure components for the cubic EoSs and the UMR-PRU model are presented in Table 5. It should be noted that although there are various versions of PC-SAFT documented in the literature, in this work, the original PC-SAFT proposed by Gross and Sadowski [25] has been considered, treating CO_2 as a non-associating compound. Especially for the case of PC-SAFT, the pure component parameters had to be refitted to vapor pressure and liquid density data taken from DIPPR [37], with enforced critical temperature and pressure, in order to be able to describe the critical area quite accurately. The new pure component parameters obtained for the PC-SAFT EoS through the fitting procedure are presented along with their respective deviations in Table 6.

The models' binary interaction parameters have been determined by fitting the bubble point pressure experimental data presented in Table 2, using the objective function of Eq. (9). The respective results for each isotherm along with the absolute average deviation are tabulated in Table 7.

$$S = \frac{1}{n_p}\sum_{i=1}^{n_p} 100\,\frac{abs(p_i^{exp} - p_i^{calc})}{p_i^{exp}} \qquad \text{Eq. (9)}$$

where S is the objective function to be minimized, n_p the number of experimental data points used for the fitting of the parameters, p_i^{exp}, the experimental pressure of a VLE point, as determined in Table 2 and p_i^{calc} the bubble point pressure calculated from the thermodynamic model.

As it can be observed from the results presented in Table 7 and Figure ~~4~~5, all models describe accurately the bubble point pressures even at the 303.15 K, which is close to the critical temperature of pure CO_2. The more theoretically strong PC-SAFT equation of state does not pose any advantage compared to the cubic EoSs. Instead, it needed refitting of the pure component parameters in order to be able to describe accurately the CO_2 vapor pressure and the critical area. This can be attributed to the fact that the potential and reference fluid used in PC-SAFT have been developed initially for polymers and thus are more accurate for larger, chain-like molecules, while both CO_2 and CH_4 deviate from that consideration. SRK and PR combined with the vdW1f mixing rules, on the other hand, resulted in an overall absolute average deviation (AAD) equal to 0.34% and 0.38% respectively, which is lower than the one expressed by PC-SAFT EoS, namely 0.42%. It should be noted that although the vapor phase has been not included in the fitting of the models' parameters, very satisfactory results are obtained for all the examined models. Finally, UMR-PRU yields the best correlation results especially with reference to the critical point estimation. This can be attributed

to the fact that UMR-PRU has two adjusting parameters, u_{nm} and u_{mn}, due to the local composition nature of UNIFAC, which provides more flexibility as compared to the one k_{ij} value required for the cubic EoSs and PC-SAFT. Table 8 presents the deviations of the UMR-PRU model, which provides the most accurate results with respect to the critical point, against the critical pressure and composition values estimated with the scaling law. The maximum deviation in critical pressure obtained with the UMR-PRU model is 2.37% and in the critical point composition 1.73%. Since the UMR-PRU model yields the lower deviation compared to the experimental data, it is used for the calculation of the derivative of the composition with respect to temperature and pressure, as it is discussed in Section 3.3.5, in order to calculate the total uncertainty in composition.

5. Conclusions

Vapor-liquid equilibrium data for the CO_2/CH_4 binary mixture have been measured at the mean temperatures of 293.13 K, 298.14 K and 303.15 K. The reported data map both the bubble point and dew point curves for each isotherm, ranging from the CO_2 vapor pressure up to the critical point of the mixture, with emphasis given to the critical region. The critical point of the mixture has been estimated for each isotherm by fitting the scaling law to the VLE data obtained in the proximity of the critical area. The vapor pressure of the pure CO_2 is consistent with the values calculated with the Span - Wagner equation of state, which is a reference EoS for CO_2 properties. Due to the lack of experimental data in the measured isotherms, comparison with other data available in literature has only been possible for the isotherm of 293.13 K. It was shown that our measurements are in fairly good agreement with the reported literature data. Very good agreement between the GERG-2008 predictions and the measurements of this work in the vapor and liquid phase for the non-critical area has also been observed.

New binary interaction parameters have been fitted to the experimental data of each isotherm for four models; the cubic EoSs SRK and PR combined with the classic van der Waals one fluid mixing rules, the PC-SAFT EoS and the UMR-PRU model. Very satisfactory correlation results have been obtained for all models outside the critical region. In the bubble point pressure, PR yields an overall deviation at the three examined isotherms equal to 0.34%, the corresponding number for SRK is 0.38%, PC-SAFT yields slightly higher deviation equal to 0.42%, while UMR-PRU results in a 0.18% deviation. In the prediction of the vapor phase composition, all examined models yield satisfactory and similar results. More specifically, PR yields a deviation equal to 0.55%, SRK 0.58%, PC-SAFT 0.52%, while again UMR-PRU gives the lowest deviation equal to 0.43%. Finally, the accuracy of the models has been also evaluated in the prediction of the critical point of the mixture, where PR, SRK and PC-SAFT yield similar results, while UMR-PRU predicts slightly better the critical point both in terms of critical point pressure and critical point composition with an overall deviation equal to 1.15% and 0.99% respectively.

As a concluding remark, the data obtained in this work improve the data situation for the CO_2/CH_4 mixture at temperatures of interest to various CCS and NG applications, and can be used as a basis for extending the applicability of several thermodynamic models.

Acknowledgements

This work has been supported by ECCSEL, project number 675206, funded by the Horizon 2020 programme of the European Union.

List of symbols

a	Helmoltz free energy
A_i	area covered in the GC chromatogram for the component *i*, derived after numerical integration.
c_i	fitted parameters to correlate the area covered in the GC chromatogram to number of moles passed through the detector, i = 1 to 5. (-)
e	error between the calibration gas CO_2 mole fraction and the mole fraction calculated through the GC adaptation. (-)
k	constant factor denoting the areas to the number of moles in Eqs. (2), (3)
k_{ij}	binary interaction parameter between the components i and j for the attractive term of SRK and PR EoS and the segment-segment interaction of unlike chains in the Berthelot-Lorentz mixing rules in PC-SAFT EoS.
M	molar mass (kg·kmol^{-1})
m_i	PC-SAFT segment number of component i (-)
n	number of data series used to correlate the area covered in the GC chromatogram to number of moles passed through the detector
n_p	number of data points used for the fitting of model parameters used in Eq. (9).
p	pressure at VLE (MPa)
p_c	estimated critical pressure, defined in Section 4.3 (MPa)
$\bar{p}$	pressure at VLE: mean pressure before one composition sample in Tables S.1 and S.2 in the Supplementary Material. (MPa)
$\bar{p}_f$	pressure at VLE: mean of the pressures $\bar{p}$ for a series of composition samples in Tables 2 and 3. (MPa)
Q_i	relative van der Waals surface area of group i (-)
R	universal ideal gas constant (83.14 bar cm^3 mol^{-1} K^{-1})
R_i	relative van der Waals volume of group i (-)
$s(z)$	sample standard deviation of variable z.

607	$s(\bar{z})$	sample standard deviation of the mean of variable z.
608	S	model fitting objective function to be minimized.
609	S_E	standard error of regression.
610 611	$\bar{T}$	ITS-90 temperature at VLE: mean temperature before one composition sample in Tables S.1 and S.2 in the Supplementary Material. (K)
612 613	$\bar{T}_f$	ITS-90 temperature at VLE: mean of the temperatures $\bar{T}$ for a series of composition samples in Tables 2 and 3. (K)
614	$u(z)$	standard uncertainty of variable z.
615	$u_c(z)$	combined standard uncertainty of variable z.
616	u_{nm}	UNIFAC binary interaction parameter between groups *n* and *m*.
617	$u_{tot}(z)$	total standard uncertainty of variable z = x_{CO_2} or y_{CO_2} from Eq. (5). (-)
618 619	x_{CO_2}	liquid phase CO_2 mole fraction at VLE given in Table S.1 in the Supplementary Material. (-)
620 621	$\bar{x}_{CO_2}$	liquid phase CO_2 mole fraction at VLE: mean mole fraction a series of composition samples in Table 2. (-)
622 623	$x_{CO_2,calc}$	liquid phase CO_2 mole fraction at VLE, calculated from the fitted UMR-PRU. See Section 4.5. (-)
624 625	y_{CO_2}	vapor phase CO_2 mole fraction at VLE given in Table S.2 in the Supplementary Material. (-)
626 627	$\bar{y}_{CO_2}$	vapor phase CO_2 mole fraction at VLE: mean mole fraction a series of composition samples in Table 3. (-)
628 629	$\bar{y}_{CO_2,calc}$	vapor phase CO_2 mole fraction at VLE, calculated from the fitted UMR-PRU. See Section 4.5. (-)
630	z_{CO_2}	liquid or vapor phase CO_2 mole fraction
631 632	$z_{CO_2,c}$	estimated critical composition in terms of CO_2 mole fraction, defined in Section 4.3. (-)

633

634 Abbreviations

635

AAD	Absolute Average Deviation, $\%AAD = 100 \cdot \frac{1}{n_p} \sum_{i=1}^{n_p} \frac{\left\| x^{exp} - x^{calc} \right\|}{x^{exp}}$, where n_p is the number of points, exponent *exp* indicates the experimental value of the size *x* and exponenent *calc* indicates the calculated value of the size *x* by the respective thermodynamic model
CCS	Carbon capture and storage
EoS	Equation of State
GC	Gas chromatograph
GERG-2008	Equation of state for natural gas mixtures [14, 15]
GUM	ISO Guide for the estimation of Uncertainty in Measurement [16]
ITS-90	International Temperature Scale of 1990 [28]
NG	Natural gas
PR	Peng – Robinson EoS
ROLSI	Rapid On Line Sampler Injector
SPRT	Standard platinum resistance thermometer
SRK	Soave-Redlich-Kwong EoS
SW	Span-Wagner EoS for CO_2
TCD	Thermal conductivity detector in GC
UMR-PRU	Universal Mixing Rule combined with PR and UNIFAC
UNIFAC	UNIQUAC Functional-Group Activity Coefficients
vdW1f	van der Waals one fluid mixing rules
VLE	Vapor – liquid equilibrium

Greek symbols

β	universal critical exponent of scaling law in Eq. (6) (-)
ε	scaling law parameter in Eq. (6) (-)
ε_i/k	PC-SAFT segment energy parameter of component *i* (K)
λ_i	scaling law parameter in Eq. (6), *i* = 1 to 2 (MPa^{-1})
μ	scaling law parameter in Eq. (6) ($MPa^{-\beta}$)

σ_i	PC-SAFT segment diameter of component *i* (Å)
ω	acentric factor

Superscripts and Subscripts

c	critical property
Calc	Calculated
disp	dispersion contribution for the PC-SAFT EoS
Exp	Experimental
f	subscript to denote the average mean value of temperature and pressure for a VLE measurement
hc	hard-chain contribution for the PC-SAFT EoS
p	points
r	reduced value of temperature ($T_r=T/T_c$)
res	residual

References

[1] H. Li, J.P. Jakobsen, Ø. Wilhelmsen, J. Yan, PVTxy properties of CO2 mixtures relevant for CO2 capture, transport and storage: Review of available experimental data and theoretical models, Applied Energy, 88 (2011) 3567-3579.

[2] K.S. Pedersen, P.L. Christensen, J.A. Shaikh, Phase behavior of petroleum reservoir fluids, CRC press, 2014.

[3] http://trc.nist.gov/thermolit/main/home.html#home, last accessed on 07/17/2017.

[4] G.-I.A. Kaminishi, Y.; Saito, S.; Maeda, S., Vapor-liquid equilibria for binary and ternary systems containing carbon dioxide, J. Chem. Eng. Jpn., 1 (1968).

[5] Q. Nasir, K.M. Sabil, K.K. Lau, Measurement of isothermal (vapor + liquid) equilibria, (VLE) for binary (CH4 + CO2) from T = (240.35 to 293.15) K and CO2 rich synthetic natural gas systems from T = (248.15 to 279.15) K, Journal of Natural Gas Science and Engineering, 27, Part 1 (2015) 158-167.

[6] V.V.S. Devlikamov, L. V.; Repin, N. N., Solubility of methane in liquid carbon dioxide, Izv. Vyssh. Uchebn. Zaved., 8 (1982).

[7] Y.K. Arai, G.-I.; Saito, S., The experimental determination of the p-v-t-x (pressure-volume-temperature-composition) relations for the carbon dioxide - nitrogen and the carbon dioxide - methane systems, J. Chem. Eng. Jpn., (1971).

[8] N.D. Xu, J.; Wang, Y.; Shi, J., High pressure vapor liquid equilibria at 293 K for systems containing nitrogen, methane and carbon dioxide, Fluid Phase Equilibria, 81 (1992).

[9] m.W. Shi, m.; Zhang, j.; Wang, L., Shi, m.; Wei, m.; Zhang, j.; Wang, L., Chemical Engineering(China), 6 (1984).

[10] B. Bian, Y. Wang, J. Shi, E. Zhao, B.C.Y. Lu, Simultaneous determination of vapor-liquid equilibrium and molar volumes for coexisting phases up to the critical temperature with a static method, Fluid Phase Equilibria, 90 (1993) 177-187.

[11] J.M. Joana Serpa, Evangelos Tzimas, Technical and Economic Characteristics of a CO2 Transmission Pipeline Infrastructure in: JRC Scientific and Technical Reports, Luxembourg: Publications Office of the European Union 2011, DOI: 10.2790/30861.

[12] S.F. Westman, H.G.J. Stang, S.W. Løvseth, A. Austegard, I. Snustad, S.Ø. Størset, I.S. Ertesvåg, Vapor–liquid equilibrium data for the carbon dioxide and nitrogen (CO2 + N2) system at the temperatures 223, 270, 298 and 303 K and pressures up to 18 MPa, Fluid Phase Equilibria, 409 (2016) 207-241.

[13] S.F. Westman, H.G.J. Stang, S.W. Løvseth, A. Austegard, I. Snustad, I.S. Ertesvåg, Vapor-liquid equilibrium data for the carbon dioxide and oxygen (CO2 + O2) system at the temperatures 218, 233, 253, 273, 288 and 298 K and pressures up to 14 MPa, Fluid Phase Equilibria, 421 (2016) 67-87.

[14] O. Kunz, W. Wagner, The GERG-2008 wide-range equation of state for natural gases and other mixtures: an expansion of GERG-2004, Journal of chemical & engineering data, 57 (2012) 3032-3091.
[15] K.O.K.R.W.W.J. M., The GERG-2004 Wide-Range Equation of State for Natural Gases and Other Mixtures GERG TM15 2007 TECHNICAL MONOGRAPH, VDI Verlag GmbH 2007.
[16] D. Chirico Robert, W. de Loos Theodoor, J. Gmehling, R.H. Goodwin Anthony, S. Gupta, M. Haynes William, N. Marsh Kenneth, V. Rives, D. Olson James, C. Spencer, F. Brennecke Joan, J.P.M. Trusler, Guidelines for reporting of phase equilibrium measurements (IUPAC Recommendations 2012), in: Pure and Applied Chemistry, 2012, pp. 1785.
[17] I. BIPM, I. IFCC, I. ISO, Iupap and oiml 2008, Evaluation of Measurement Data—Guide to the Expression of Uncertainty in Measurement, (2008).
[18] O. Redlich, J. Kwong, On the Thermodynamics of Solutions. V. An Equation of State. Fugacities of Gaseous Solutions, Chemical Reviews, 44 (1949) 233-244.
[19] G. Soave, Equilibrium constants from a modified Redlich-Kwong equation of state, Chemical Engineering Science, 27 (1972) 1197-1203.
[20] D.-Y. Peng, D.B. Robinson, A new two-constant equation of state, Industrial & Engineering Chemistry Fundamentals, 15 (1976) 59-64.
[21] D.-Y. Peng, D.B. Robinson, Two and three phase equilibrium calculations for systems containing water, The Canadian Journal of Chemical Engineering, 54 (1976) 595-599.
[22] J.D. Van der Waals, Over de Continuiteit van den Gas-en Vloeistoftoestand, Sijthoff, 1873.
[23] J.D. Van Der Waals, On the continuity of the gaseous and liquid states, Courier Corporation, 2004.
[24] A. Fredenslund, R.L. Jones, J.M. Prausnitz, Group-contribution estimation of activity coefficients in nonideal liquid mixtures, AIChE Journal, 21 (1975) 1086-1099.
[25] J. Gross, G. Sadowski, Perturbed-Chain SAFT: An Equation of State Based on a Perturbation Theory for Chain Molecules, Industrial & Engineering Chemistry Research, 40 (2001) 1244-1260.
[26] J. Gross, G. Sadowski, Application of the perturbed-chain SAFT equation of state to associating systems, Industrial & engineering chemistry research, 41 (2002) 5510-5515.
[27] H.G. Jacob Stang, S.W. Løvseth, S.Ø. Størset, B. Malvik, H. Rekstad, Accurate Measurements of CO2 Rich Mixture Phase Equilibria Relevant for CCS Transport and Conditioning, Energy Procedia, 37 (2013) 2897-2903.
[28] H. Preston-Thomas, The international temperature scale of 1990 (ITS-90), metrologia, 27 (1990) 3.
[29] R. Span, W. Wagner, A New Equation of State for Carbon Dioxide Covering the Fluid Region from the Triple-Point Temperature to 1100 K at Pressures up to 800 MPa, Journal of Physical and Chemical Reference Data, 25 (1996) 1509-1596.
[30] S.F. Westman, H.J. Stang, S.Ø. Størset, H. Rekstad, A. Austegard, S.W. Løvseth, Accurate Phase Equilibrium Measurements of CO 2 Mixtures, Energy Procedia, 51 (2014) 392-401.
[31] M.E. Wieser, N. Holden, T.B. Coplen, J.K. Böhlke, M. Berglund, W.A. Brand, P. De Bièvre, M. Gröning, R.D. Loss, J. Meija, Atomic weights of the elements 2011 (IUPAC Technical Report), Pure and Applied Chemistry, 85 (2013) 1047-1078.
[32] E. Wieser Michael, B. Coplen Tyler, Atomic weights of the elements 2009 (IUPAC Technical Report), in: Pure and Applied Chemistry, 2010, pp. 359.
[33] L.P. Kadanoff, W. Götze, D. Hamblen, R. Hecht, E. Lewis, V.V. Palciauskas, M. Rayl, J. Swift, D. Aspnes, J. Kane, Static phenomena near critical points: theory and experiment, Reviews of Modern Physics, 39 (1967) 395.
[34] M.S. Green, M. Vicentini-Missoni, J.L. Sengers, Scaling-law equation of state for gases in the critical region, Physical Review Letters, 18 (1967) 1113.
[35] M.E. Fisher, The theory of equilibrium critical phenomena, Reports on progress in physics, 30 (1967) 615.
[36] J.V. Sengers, J.M.H. Levelt Sengers, A universal representation of the thermodynamic properties of fluids in the critical region, International Journal of Thermophysics, 5 (1984) 195-208.
[37] T.E. Daubert, R.P. Danner, Physical and Thermodynamic Properties of Pure Chemicals: Data Compilation, 2003.
[38] M. Wertheim, Fluids with highly directional attractive forces. II. Thermodynamic perturbation theory and integral equations, Journal of statistical physics, 35 (1984) 35-47.
[39] M. Wertheim, Fluids with highly directional attractive forces. I. Statistical thermodynamics, Journal of statistical physics, 35 (1984) 19-34.
[40] W.G. Chapman, K.E. Gubbins, G. Jackson, M. Radosz, New reference equation of state for associating liquids, Industrial & Engineering Chemistry Research, 29 (1990) 1709-1721.

Appendix A: Brief presentation of thermodynamic models

All thermodynamic models used in this work are well established in literature, so they are only briefly presented here.

A.1 Cubic EoS

The cubic EoS expression in a generalized form are given in Eqs. A.1 - A.5, with the universal constant r_1 equal to zero in the case of SRK and 1 for PR. The temperature dependency of the attractive term parameter is given from the Soave[19] expression as described in Eqs. A.2 – A.3, where T_c, p_c and ω are the critical properties for each compound which are presented in Table 5.

$$p = \frac{RT}{v-b} - \frac{a_c a(T)}{v(v+b) + r_1 b(v-b)} \quad \text{Eq. A.1}$$

$$a(T) = \left(1 + m(1 - T_r^{0.5})\right)^2 \quad \text{Eq. A.2}$$

$$m = d_0 + d_1\omega + d_2\omega^2 \quad \text{Eq. A.3}$$

$$a_c = d_3 \frac{(RT_c)^2}{p_c} \quad \text{Eq. A.4}$$

$$b = d_4 \frac{RT_c}{p_c} \quad \text{Eq. A.5}$$

The specific parameters d_0-d_4 for each EoS are tabulated in Table A.1.

For the extension of the PR to mixtures, the classic van der Waals[22, 23] one fluid (vdw1f) mixing and combining rules are considered, as presented in Eqs A.6 – A.8.

$$a = \sum\sum x_i x_j a_{ij} \left(1 - k_{ij}\right) \quad \text{Eq. A.6}$$

$$b = \sum x_i b_i \quad \text{Eq. A.7}$$

$$a_{ij} = \left(a_i a_j\right)^{1/2} \quad \text{Eq. A.8}$$

A.2 UMR-PRU

The Universal Mixing Rule – Peng Robinson (UMR-PRU) belongs to the class of the so-called EoS/G^E models. UMR-PRU is based on the PR EoS and uses the following mixing rules for the dimensionless parameter $\alpha = \frac{a}{bRT}$, where a is the attractive term, as given in Eq. A.9, and b the co-volume parameter of the EoS.

$$a = \frac{1}{-0.53}\left(\frac{G^E_{comb-SG} + G^E_{residual}}{RT}\right) + \sum_i \frac{a_i}{b_i} \qquad \text{Eq. A.9}$$

Additionally, $G^E_{comb-SG}$ and $G^E_{residual}$ are the Staverman-Guggenheim term of the combinatorial part and the residual part of the UNIFAC activity coefficient model respectively.

For the co-volume parameter, *b*, the following mixing and combining rules are applied:

$$\mathrm{b} = \sum_i \sum_j x_i x_j b_{i,j} \qquad \text{Eq. A.10}$$

$$b_{ij} = \left(\frac{b_i^{1/2} + b_j^{1/2}}{2}\right)^2 \qquad \text{Eq. A.11}$$

A.3 PC-SAFT EoS

One of the most successful attempts to correct the weaknesses of cubic equations of state is the Statistical Associating Fluid Theory (SAFT) family of equations of state. SAFT is based on the perturbation theory of Wertheim[38, 39] and was originally developed by Chapman et al.[40].

In this study, the Perturbed-Chain SAFT (PC-SAFT) proposed by Gross and Sadowski[25] is considered, which is one of the most successful modifications of the SAFT theory. The main difference between original SAFT and PC-SAFT is the reference fluid used. Specifically, PC-SAFT uses the hard-chain reference fluid to account for the dispersion interactions unlike SAFT, that uses the hard-sphere reference fluid. In the PC-SAFT equation, for non-associating compounds, the residual Helmholtz energy $a^{res}(T,V,N)$ is given as the summation of two terms, the hard-chain (a^{hc}) and the dispersion (a^{disp}), each one representing contributions from the corresponding kind of intermolecular forces, as presented in Eq. A.12.

$$a^{res}(T,V,N) = a(T,V,N) - a^{ideal}(T,V,N) = a^{hc} + a^{disp} \qquad \text{Eq. A.12}$$

The hard-chain term (a^{hc}) is given by Eq. A.13.

$$\frac{a^{hc}}{RT} = \bar{m}\frac{a^{hs}}{RT} - \sum_i x_i(m_i - 1) ln g^{hs}_{ii}(\sigma_{ii}) \qquad \text{Eq. A.13}$$

where m_i is the number of segments in a chain of component *i*, $\overline{m}$ is the mean segment number in the mixture ($\overline{m} = \sum_i x_i m_i$).

The hard-sphere contribution (a^{hs}) is given by Eqs. A.14-A.16.

$$\frac{a^{hs}}{RT} = \frac{1}{\zeta_0}\left[\frac{3\zeta_1\zeta_2}{1-\zeta_3} + \frac{{\zeta_2}^3}{\zeta_3(1-\zeta_3)^2} + \left(\frac{{\zeta_2}^3}{{\zeta_3}^2} - \zeta_0\right) ln(1-\zeta_3)\right] \qquad \text{Eq. A.14}$$

$$\zeta_n = \frac{\pi}{6}\rho \sum_i x_i m_i \, d_i^n \qquad \text{Eq. A.15}$$

$$d_i = \sigma_i \left[1 - 0.12exp\left(-3\frac{\varepsilon_i}{kT}\right)\right] \qquad \text{Eq. A.16}$$

where $\sigma_i$is the segment diameter, and ε_i is the depth of the potential for the component *i*.

The radial distribution function of the hard sphere fluid (g_{ii}^{hs}) is calculated as in Eq. A.17.

$$g_{ii}^{hs} = \frac{1}{1-\zeta_3} + \left(\frac{d_i d_j}{d_i + d_j}\right)\frac{3\zeta_2}{(1-\zeta_3)^2} + \left(\frac{d_i d_j}{d_i + d_j}\right)^2 \frac{2{\zeta_2}^2}{(1-\zeta_3)^3} \qquad \text{Eq. A.17}$$

The dispersion term is modeled using a second order perturbation theory on chain molecules rather than hard spheres, using the expression given by Eq. A.18.

$$\frac{a^{disp}}{RT} = -2\pi\rho I_1(n,\overline{m})\overline{m^2\varepsilon\sigma^3} - \pi\rho\overline{m}C_1(n,\overline{m})I_2(n,\overline{m})\overline{m^2\varepsilon^2\sigma^3} \qquad \text{Eq. A.18}$$

where the integrals I_1 and I_2 and the compressibility expression C_1 are functions of $\overline{m}$ and the packing fraction n (or ζ_3), while n is the reduced density.

The dispersion term is extended to mixtures by assuming the van der Waals one-fluid theory approximation, as presented in Eqs. A.19-A.20.

$$\overline{m^2\varepsilon\sigma^3} = \sum_i \sum_j x_i x_j m_i m_j \left(\frac{\varepsilon_{ij}}{kT}\right)\sigma_{ij}^3 \qquad \text{Eq. A.19}$$

$$\overline{m^2\varepsilon^2\sigma^3} = \sum_i \sum_j x_i x_j m_i m_j \left(\frac{\varepsilon_{ij}}{kT}\right)^2 \sigma_{ij}^3 \qquad \text{Eq. A.20}$$

The parameters for a pair of unlike segments are obtained by the conventional Berthelot-Lorentz combining rules, as given in Eqs, A,21-A.22.

$$\sigma_{ij} = \frac{1}{2}\left(\sigma_i + \sigma_j\right) \qquad \text{Eq. A.21}$$

$$\varepsilon_{ij} = \sqrt{\varepsilon_i \varepsilon_j}\left(1 - k_{ij}\right) \qquad \text{Eq. A.22}$$

The binary interaction parameter, k_{ij}, is introduced to correct the segment-segment interactions of unlike chains. Actually, it is a binary adjustable parameter that is determined by fitting binary phase equilibrium data, similarly to cubic EoS.

PC-SAFT requires three parameters for pure non-associating compounds: the segment number (m), the segment diameter (σ) and the segment energy parameter (ε/k), which for the components involved in this work are given in Table 6.

Figure Captions

Figure 1. (a) Pressure standard uncertainty relative to the measured pressure for the VLE measurements performed, expressed as $100 \cdot \bar{u}_c(\bar{p})/\bar{p}_f$. $\bar{p}_f$ stands for the measured pressure and $\bar{u}_c(\bar{p})$ for the standard uncertainty. (b). Temperature deviations for each VLE measurement from isotherm mean temperature, and temperature standard uncertainty, expressed together as $\bar{T}_f \pm \bar{u}_c(\bar{T}) - isotherm\ mean\ temperature$, versus the VLE experimental pressure $\bar{p}_f$. $\bar{T}_f$ stands for the VLE experimental mean temperature and $\bar{u}_c(\bar{T})$ for the standard uncertainty in temperature. Blue colour indicates the isotherm at the mean temperature of 293.130 K, red colour indicates the isotherm at the mean temperature of 298.142 K and green colour indicates the isotherm at the mean temperature of 303.145 K. (For interpretation of the references to colour in this figure legend, the reader is referred to the web version of this article.)

Figure ~~1~~2. Error between actual compositions in Table S.4 and the composition determined by the GC using the fit of Eqs. (2)-(4). Composition analysis uncertainty $u(x_{CO_2}) = u(y_{CO_2}) = s(e)$ as reported in Table S.5.

Figure ~~2~~3. VLE pressure – composition diagram for the CO_2/CH_4 for the different isotherms measured in this work. Blue colour indicates the liquid phase and red colour the vapor one. (x) indicates the experimental data measured in this work along with the estimated uncertainties (black uncertainty bars). (◇) Indicates the critical point of the mixture as estimated by the fitting of the Scaling Law (See Eq. (6)). The solid line is the prediction of the GERG-2008 model. (a). Mean temperature 293.130 K. (○) indicates the data by Xu et al. [8], (Δ) indicates the data by Nasir et al. [5]. and (□) indicates the data by Devlikamov et al. [6] (b). Mean temperature 298.142 K. (□) indicates the data by Devlikamov et al. [6] (c). Mean temperature 303.145 K. Please note that the scaling in (c) is very narrow due to the proximity in CO_2 critical temperature.

Figure ~~3~~4. Pressure-composition phase behavior in the critical region estimated by the scaling law model in Eq. (6). (+) indicates the points used for the fitting of the scaling law (see Table 4), (x) indicates the points not used in the fitting of scaling law and solid line indicates the scaling law correlation. Blue colour indicates the liquid phase and red colour the vapor one. Please note that the scales of the graphs are very different from each other.

Figure ~~4~~5. Binary VLE correlation results for the CO_2/CH_4 mixture at (a) 293.13 K, (b) 298.14 K and (c) 303.15 K, with the: PR (blue solid line), SRK (green long dashed line), PC-SAFT (grey dashed line) and UMR-PRU (black solid line). (○) indicates the experimental data of this work as presented in Tables 2 and 3. Note that the critical point estimated through the scaling law from the experimental data is marked as a green (◇) while the predicted critical point of the models as a (✶) of the same coloring as the respective model.

Table 1: Characteristics of pure chemicals used.

Chemical Name	Cas No	Source	Initial mol fraction purity	Purification method	Final mol fraction purity	Analysis method
Carbon dioxide[a]	124-38-9	AGA	0.999992	None	0.999992	None
Methane[b]	74-82-8	AGA	0.999995	None	0.999995	None
Helium[c]	7440-59-7	AGA	0.999999	None	0.999999	None

[a] Maximum specified impurity content by volume is less than 3 ppm H_2O, 1 ppm O_2, 2 ppm N_2, 1 ppm and hydrocarbons C_nH_m.

[b] Maximum specified impurity content by volume is less than 2 ppm H_2O, 0.5 ppm O_2, 4 ppm N_2, 1 ppm other hydrocarbons C_nH_m and 0.1 ppm H_2.

[c] GC carrier gas.

Table 2: Liquid phase: Experimental VLE data for CO_2 and CH_4 at mean temperature, $\bar{T}_f$, mean pressure, $\bar{p}_f$, and mean liquid phase mole fraction, $\bar{x}_{CO_2}$.[a]

ID	Data			Temperature (K)			Pressure (MPa)			Composition (-)			
	$\bar{T}_f$ (K)	$\bar{p}_f$ (MPa)	$\bar{x}_{CO_2}$ (-)	$s(\bar{T}_f)$	$\bar{u}_c(\bar{T})$	$\bar{u}_c(\bar{T}_f)$	$s(\bar{p}_f)$	$\bar{u}_c(\bar{p})$	$\bar{u}_c(\bar{p}_f)$	$s(\bar{x}_{CO_2})$	$\bar{u}_{tot}(\bar{x}_{CO_2})$	$\bar{u}_c(\bar{x}_{CO_2})$	$\bar{x}_{CO_2,calc}$
P1	293.130	5.7273[b]	0.99999	1.3e-3	1.1e-3	1.7e-3	1.3e-3	1.7e-3	1.2e-3				
L1	293.130	6.1348	0.98472	6.8e-4	1.1e-3	1.3e-3	3.1e-5	1.1e-3	1.1e-3	3.3e-6	9.9e-5	9.9e-5	0.98537
L2	293.129	6.6459	0.96439	1.6e-4	1.4e-3	1.4e-3	2.1e-5	1.1e-3	1.1e-3	5.2e-6	1.0e-4	1.0e-4	0.96486
L3	293.130	6.8401	0.95611	3.2e-4	1.3e-3	1.4e-3	8.0e-6	1.1e-3	1.1e-3	1.2e-5	1.0e-4	1.0e-4	0.95629
L4	293.130	6.9756	0.95018	5.9e-4	1.1e-3	1.3e-3	1.1e-5	1.1e-3	1.1e-3	1.2e-5	1.0e-4	1.0e-4	0.95000
L5	293.129	7.1183	0.94364	2.5e-4	1.2e-3	1.2e-3	1.5e-5	1.1e-3	1.1e-3	8.1e-6	1.1e-4	1.1e-4	0.94307
L6	293.130	7.3508	0.93240	2.0e-4	1.2e-3	1.2e-3	7.5e-6	1.1e-3	1.1e-3	1.5e-5	1.1e-4	1.1e-4	0.93096
L7	293.130	7.5758	0.92024	7.2e-5	1.3e-3	1.3e-3	1.1e-5	1.1e-3	1.1e-3	5.3e-6	1.1e-4	1.1e-4	0.91800
L8	293.130	7.7962	0.90568	2.1e-4	1.3e-3	1.3e-3	2.4e-5	1.2e-3	1.2e-3	9.4e-6	1.2e-4	1.2e-4	0.90350
L9	293.130	7.9091	0.89394	4.4e-4	1.2e-3	1.3e-3	1.4e-5	1.2e-3	1.2e-3	4.7e-6	2.1e-4[+]	2.1e-4[+]	0.89390
L10	293.130	7.9135	0.89309	8.9e-5	1.1e-3	1.1e-3	2.3e-5	1.2e-3	1.2e-3	2.5e-5	2.5e-4[+]	2.5e-4[+]	0.89311
L11	293.128	7.9179	0.89220	5.9e-5	1.3e-3	1.3e-3	9.6e-6	1.2e-3	1.2e-3	2.5e-5	2.7e-4[+]	2.7e-4[+]	0.89223
L12	293.129	7.9219	0.89123	8.3e-4	1.2e-3	1.5e-3	1.7e-5	1.2e-3	1.2e-3	2.2e-5	3.2e-4[+]	3.2e-4[+]	0.89127
L13	293.130	7.9266	0.88982	7.6e-5	1.1e-3	1.1e-3	9.1e-6	1.2e-3	1.2e-3	2.2e-5	5.1e-4[+]	5.1e-4[+]	0.88982
L14	293.129	7.9308	0.88782	3.4e-4	1.2e-3	1.2e-3	5.9e-6	1.2e-3	1.2e-3	2.0e-5	8.3e-4[+]	8.3e-4[+]	0.88778
P2	298.141	6.4316[c]	0.99999	6.7e-4	1.4e-3	1.6e-3	1.0e-3	1.5e-3	1.1e-3				
L15	298.142	6.6411	0.99200	1.9e-4	1.9e-3	1.9e-3	1.0e-5	1.1e-3	1.1e-3	8.2e-7	9.9e-5	9.9e-5	0.99271
L16	298.142	6.9755	0.97855	1.5e-4	1.9e-3	1.9e-3	1.4e-5	1.1e-3	1.1e-3	1.7e-6	1.0e-4	1.0e-4	0.97936
L17	298.142	7.3114	0.96361	1.1e-4	1.8e-3	1.8e-3	9.8e-6	1.1e-3	1.1e-3	9.2e-6	1.1e-4	1.1e-4	0.96361
L18	298.141	7.5079	0.95359	5.2e-4	1.8e-3	1.9e-3	1.8e-5	1.1e-3	1.1e-3	5.0e-6	1.1e-4	1.1e-4	0.95277
L19	298.142	7.6250	0.94622	1.5e-4	2.0e-3	2.0e-3	7.5e-6	1.1e-3	1.1e-3	1.9e-5	1.4e-4	1.4e-4	0.94594
L20	298.141	7.6599	0.94337	3.6e-4	1.8e-3	1.8e-3	5.7e-5	1.1e-3	1.1e-3	6.1e-6	1.3e-4	1.3e-4	0.94328
L21	298.141	7.6783	0.94150	1.5e-4	1.7e-3	1.7e-3	1.0e-5	1.1e-3	1.1e-3	7.5e-6	1.6e-4[+]	1.6e-4[+]	0.94149
L22	298.142	7.6886	0.94016	3.0e-4	1.8e-3	1.8e-3	3.3e-6	1.1e-3	1.1e-3	1.4e-5	1.9e-4[+]	1.9e-4[+]	0.94017
L23	298.142	7.6938	0.93924	7.9e-5	1.8e-3	1.8e-3	1.5e-5	1.1e-3	1.1e-3	1.7e-5	1.3e-4[+]	1.3e-4[+]	0.94046
L24	298.141	7.6978	0.93835	3.3e-4	1.8e-3	1.8e-3	1.4e-5	1.1e-3	1.1e-3	5.4e-6	1.3e-4[+]	1.3e-4[+]	0.94015
P3	303.144	7.2121[d]	0.99999	4.2e-4	2.4e-3	2.4e-3	1.1e-3	1.6e-3	1.2e-3				
L25	303.144	7.2625	0.99791	2.4e-4	2.3e-3	2.4e-3	3.2e-5	1.1e-3	1.1e-3	1.9e-6	1.0e-4	1.0e-4	0.99778
L26	303.145	7.3064	0.99600	6.0e-4	2.4e-3	2.5e-3	8.7e-5	1.1e-3	1.1e-3	2.1e-6	1.0e-4	1.0e-4	0.99589

L27	303.144	7.3611	0.99350	4.3e-4	2.4e-3	2.5e-3	4.6e-5	1.1e-3	1.1e-3	1.3e-6	1.1e-4	1.1e-4	0.99337
L28	303.144	7.4156	0.99073	4.3e-4	2.5e-3	2.5e-3	2.7e-5	1.1e-3	1.1e-3	2.4e-6	1.1e-4	1.1e-4	0.99068
L29	303.145	7.4256	0.99009	4.4e-5	2.5e-3	2.5e-3	2.9e-5	1.1e-3	1.1e-3	1.7e-5	1.2e-4[+]	1.2e-4[+]	0.99010
L30	303.145	7.4289	0.98988	6.6e-5	2.6e-3	2.6e-3	3.4e-5	1.1e-3	1.1e-3	2.8e-6	1.2e-4[+]	1.2e-4[+]	0.98987
L31	303.145	7.4306	0.98975	6.9e-5	2.6e-3	2.6e-3	2.1e-5	1.1e-3	1.1e-3	4.2e-6	1.3e-4[+]	1.3e-4[+]	0.98974
L32	303.145	7.4318	0.98963	1.9e-4	2.5e-3	2.5e-3	4.0e-5	1.1e-3	1.1e-3	4.7e-6	1.4e-4[+]	1.4e-4[+]	0.98963
L33	303.145	7.4331	0.98950	1.6e-4	2.6e-3	2.6e-3	1.7e-5	1.1e-3	1.1e-3	5.6e-6	1.7e-4[+]	1.7e-4[+]	0.98949
L34	303.144	7.4341	0.98934	1.2e-4	2.5e-3	2.5e-3	4.2e-5	1.1e-3	1.1e-3	1.1e-5	2.3e-4[+]	2.3e-4[+]	0.98934

[+] The derivatives $\frac{\partial x_{CO_2}}{\partial p}$ used in Eq. (5) to obtain $\bar{u}_{tot}(\bar{x}_{CO_2})$ were calculated using the scaling law in Eq. (6) with the parameters in Table 4 instead of the UMR-PRU fitted model. See Table S.1 in the Supplementary Material for the values of the derivatives, and Section 4.3 for details.

[a] Sample standard deviation of the mean of the temperatures, $s(\bar{T}_f)$, mean of the standard systematic uncertainty of the temperature, $\bar{u}_c(\bar{T})$, total standard uncertainty of the temperature, $\bar{u}_c(\bar{T}_f)$, sample standard deviation of the mean of the pressures, $s(\bar{p}_f)$, mean of the standard systematic uncertainty of the pressures, $\bar{u}_c(\bar{p})$, total standard uncertainty of the pressure, $\bar{u}_c(\bar{p}_f)$, sample standard deviation of the mean mole fractions, $s(\bar{x}_{CO_2})$, mean of the total standard uncertainty of the mole fractions, $\bar{u}_{tot}(\bar{x}_{CO_2})$, the combined uncertainties of the mean mole fractions, $\bar{u}_c(\bar{x}_{CO_2})$, and UMR-PRU calculated mole fraction, $\bar{x}_{CO_2,calc}$.

[b] Span-Wagner CO_2 vapor pressure is 5.7256 ± 0.0017 MPa.

[c] Span-Wagner CO_2 vapor pressure is 6.4317 ± 0.0019 MPa.

[d] Span-Wagner CO_2 vapor pressure is 7.2131 ± 0.0021 MPa.

Table 3: Vapor phase: Experimental VLE data for CO_2 and CH_4 at mean temperature, $\bar{T}_f$, mean pressure, $\bar{p}_f$, and mean vapor phase mole fraction, $\bar{y}_{CO_2}$.[a]

ID	Data			Temperature (K)			Pressure (MPa)			Composition (-)			
	$\bar{T}_f$ (K)	$\bar{p}_f$ (MPa)	$\bar{y}_{CO_2}$ (-)	$s(\bar{T}_f)$	$\bar{u}_c(\bar{T})$	$\bar{u}_c(\bar{T}_f)$	$s(\bar{p}_f)$	$\bar{u}_c(\bar{p})$	$\bar{u}_c(\bar{p}_f)$	$s(\bar{y}_{CO_2})$	$\bar{u}_{tot}(\bar{y}_{CO_2})$	$\bar{u}_c(\bar{y}_{CO_2})$	$\bar{y}_{CO_2,calc}$
P1	293.130	5.7273[b]	0.99999	1.3e-3	1.1e-3	1.7e-3	1.3e-3	1.7e-3	1.2e-3				
V1	293.129	6.1346	0.96030	3.3e-4	1.2e-3	1.2e-3	4.7e-5	1.1e-3	1.1e-3	3.6e-5	1.4e-4	1.4e-4	0.96186
V2	293.130	6.6458	0.91971	2.8e-4	1.4e-3	1.4e-3	1.5e-5	1.1e-3	1.1e-3	7.5e-6	1.2e-4	1.2e-4	0.92147
V3	293.129	6.8401	0.90679	4.1e-4	1.5e-3	1.5e-3	5.3e-6	1.1e-3	1.1e-3	5.9e-6	1.2e-4	1.2e-4	0.90827
V4	293.130	6.9755	0.89863	1.4e-4	1.1e-3	1.1e-3	9.1e-6	1.1e-3	1.1e-3	2.0e-5	1.1e-4	1.1e-4	0.89981
V5	293.129	7.1183	0.89070	2.4e-4	1.2e-3	1.2e-3	2.2e-5	1.1e-3	1.1e-3	2.6e-5	1.1e-4	1.1e-4	0.89150
V6	293.130	7.3508	0.87979	3.3e-4	1.2e-3	1.2e-3	9.9e-6	1.1e-3	1.1e-3	2.7e-5	1.1e-4	1.1e-4	0.87947
V7	293.130	7.5758	0.87189	1.5e-4	1.2e-3	1.2e-3	6.4e-6	1.1e-3	1.1e-3	2.2e-5	1.0e-4	1.0e-4	0.86978
V8	293.130	7.7961	0.86866	1.0e-4	1.1e-3	1.2e-3	5.7e-6	1.1e-3	1.1e-3	7.4e-6	9.5e-5	9.5e-5	0.86268
V9	293.130	7.9091	0.87303	1.1e-4	1.1e-3	1.1e-3	9.2e-6	1.2e-3	1.2e-3	9.3e-6	1.8e-4[+]	1.8e-4[+]	0.87301
V10	293.130	7.9135	0.87361	1.1e-4	1.1e-3	1.1e-3	7.3e-6	1.2e-3	1.2e-3	6.6e-6	1.9e-4[+]	1.9e-4[+]	0.87358
V11	293.128	7.9179	0.87424	2.9e-4	1.3e-3	1.3e-3	8.7e-6	1.2e-3	1.2e-3	9.0e-6	2.2e-4[+]	2.2e-4[+]	0.87427
V12	293.130	7.9219	0.87499	5.9e-4	1.2e-3	1.3e-3	7.8e-6	1.2e-3	1.2e-3	9.3e-6	2.7e-4[+]	2.7e-4[+]	0.87504
V13	293.130	7.9266	0.87626	9.8e-5	1.1e-3	1.1e-3	6.5e-6	1.2e-3	1.2e-3	4.4e-6	3.8e-4[+]	3.8e-4[+]	0.87626
V14	293.130	7.9308	0.87817	1.5e-4	1.2e-3	1.2e-3	7.2e-6	1.2e-3	1.2e-3	1.5e-5	7.9e-4[+]	7.9e-4[+]	0.87813
P2	298.141	6.4316[c]	0.99999	6.7e-4	1.4e-3	1.6e-3	1.0e-3	1.5e-3	1.1e-3				
V15	298.142	6.6410	0.98297	1.6e-4	1.9e-3	1.9e-3	1.7e-5	1.1e-3	1.1e-3	3.7e-6	1.2e-4	1.2e-4	0.98448
V16	298.141	6.9754	0.95917	2.8e-4	1.8e-3	1.9e-3	1.9e-5	1.1e-3	1.1e-3	2.4e-6	1.2e-4	1.2e-4	0.96113
V17	298.142	7.3114	0.93993	1.1e-4	1.8e-3	1.8e-3	8.4e-4	1.8e-3	1.6e-3	9.1e-6	1.3e-4	1.3e-4	0.94114
V18	298.143	7.5078	0.93180	5.3e-5	2.0e-3	2.0e-3	1.1e-5	1.1e-3	1.1e-3	9.1e-6	1.1e-4	1.1e-4	0.93141
V19	298.142	7.6250	0.92917	2.2e-4	1.9e-3	1.9e-3	8.0e-6	1.1e-3	1.1e-3	1.6e-5	9.8e-5	9.9e-5	0.92867
V20	298.142	7.6599	0.92928	1.5e-4	1.9e-3	1.9e-3	7.5e-6	1.1e-3	1.1e-3	9.7e-6	1.1e-4	1.1e-4	0.92914
V21	298.142	7.6783	0.92979	2.6e-4	1.7e-3	1.7e-3	7.0e-6	1.1e-3	1.1e-3	1.6e-5	1.1e-4[+]	1.1e-4[+]	0.92978
V22	298.142	7.6886	0.93044	7.7e-5	1.7e-3	1.7e-3	7.1e-6	1.1e-3	1.1e-3	1.3e-5	2.4e-4[+]	2.4e-4[+]	0.93046
V23	298.142	7.6938	0.93103	8.0e-5	1.8e-3	1.8e-3	4.4e-4	1.2e-3	1.2e-3	1.7e-4	2.0e-4[+]	2.6e-4[+]	0.92451
V24	298.142	7.6977	0.93175	5.2e-5	1.8e-3	1.8e-3	1.7e-5	1.1e-3	1.1e-3	1.6e-5	9.8e-5[+]	9.9e-5[+]	0.92441
P3	303.144	7.2121[d]	0.99999	4.2e-4	2.4e-3	2.4e-3	1.1e-3	1.6e-3	1.2e-3				
V25	303.144	7.2625	0.99695	1.9e-4	2.4e-3	2.4e-3	1.3e-5	1.1e-3	1.1e-3	2.5e-6	1.1e-4	1.1e-4	0.99697
V26	303.144	7.3064	0.99438	2.1e-4	2.4e-3	2.4e-3	1.2e-5	1.1e-3	1.1e-3	2.3e-6	1.1e-4	1.1e-4	0.99455

V27	303.141	7.3607	0.99142	9.2e-4	2.4e-3	2.6e-3	9.0e-6	1.1e-3	1.1e-3	5.8e-6	1.1e-4	1.1e-4	0.99164
V28	303.144	7.4155	0.98896	2.0e-4	2.5e-3	2.5e-3	2.3e-5	1.1e-3	1.1e-3	4.3e-6	1.1e-4	1.1e-4	0.98894
V29	303.145	7.4253	0.98862	7.9e-5	2.5e-3	2.5e-3	3.9e-5	1.1e-3	1.1e-3	2.7e-6	9.6e-5[+]	9.6e-5[+]	0.98863
V30	303.145	7.4287	0.98855	1.1e-4	2.5e-3	2.5e-3	2.6e-5	1.1e-3	1.1e-3	7.7e-6	1.0e-4[+]	1.0e-4[+]	0.98855
V31	303.145	7.4304	0.98856	2.4e-4	2.6e-3	2.6e-3	2.5e-5	1.1e-3	1.1e-3	9.2e-6	9.8e-5[+]	9.8e-5[+]	0.98853
V32	303.145	7.4316	0.98854	9.7e-5	2.5e-3	2.5e-3	3.0e-5	1.1e-3	1.1e-3	7.4e-6	1.0e-4[+]	1.0e-4[+]	0.98853
V33	303.145	7.4328	0.98855	2.2e-4	2.5e-3	2.5e-3	1.7e-5	1.1e-3	1.1e-3	6.0e-6	9.5e-5[+]	9.5e-5[+]	0.98855
V34	303.144	7.4341	0.98861	1.1e-4	2.5e-3	2.5e-3	1.4e-5	1.1e-3	1.1e-3	2.4e-6	1.5e-4[+]	1.5e-4[+]	0.98862

[+] The derivatives $\frac{\partial y_{CO_2}}{\partial p}$ used in Eq. (5) to obtain $\bar{u}_{tot}(y_{CO_2})$ were calculated using the scaling law in Eq. (6) with the parameters in Table 4 instead of the UMR-PRU fitted model. See Table S.2 in the Supplementary Material for the values of the derivatives, and Section 4.3 for details.

[a] Sample standard deviation of the mean of the temperatures, $s(\bar{T}_f)$, mean of the standard systematic uncertainty of the temperature, $\bar{u}_c(\bar{T})$, total standard uncertainty of the temperature, $\bar{u}_c(\bar{T}_f)$, sample standard deviation of the mean of the pressures, $s(\bar{p}_f)$, mean of the standard systematic uncertainty of the pressure, $\bar{u}_c(\bar{p})$, total standard uncertainty of the pressure, $\bar{u}_c(\bar{p}_f)$, sample standard deviation of the mean of the mole fractions, $s(\bar{x}_{CO_2})$, mean of the total standard uncertainty of the mole fractions, $\bar{u}_{tot}(\bar{y}_{CO_2})$, mean of the total combined uncertainties of the mole fractions, $\bar{u}_c(\bar{y}_{CO_2})$, and UMR-PRU calculated mole fraction, $\bar{y}_{CO_2,calc}$.

[b] Span-Wagner CO_2 vapor pressure is 5.7256 ± 0.0017 MPa.

[c] Span-Wagner CO_2 vapor pressure is 6.4317 ± 0.0019 MPa.

[d] Span-Wagner CO_2 vapor pressure is 7.2131 ± 0.0021 MPa.

Table 4: Parameters of the scaling law in Eq. (6) fitted to critical region data from this work for the three different average temperatures.

T(K)	Used Points	n_p	$10^4 \cdot \hat{\lambda}_1$ (MPa^{-1})	$10^3 \cdot \hat{\lambda}_2$ (MPa^{-1})	$10^5 \cdot \hat{\mu}$ ($MPa^{-\beta}$)	$\hat{z}_{CO_2,c}$ (-)	$\hat{p}_c$ (MPa)	$S_E(\hat{z}_{CO_2,c})$ (-)	$u(\hat{z}_{CO_2,c})$ (-)	$S_E(\hat{p}_c)$ (MPa)	$u(\hat{p}_c)$ (MPa)
293.130	L9-L14, V9-V14	12	2.3192	3.2924	7.8298	0.8829	7.933	8.6e-4	0.00086	0.001	0.00101
298.142	L21-L24, V21-V24	8	3.1311	1.8708	1.3064	0.9349	7.702	6.6e-4	0.00067	0.001	0.00101
303.145	L29-L34, V29,V30, V32-V34	11	4.4845	0.3604	-19.3810	0.9889	7.435	3.6e-4	0.00037	0.001	0.00101

Table 5: Pure component parameters for SRK, PR and UMR-PRU.

Component	Ref.	T_c (K)	P_c (MPa)	ω (-)
CO_2	[37]	304.21	7.3815	0.2276
Methane	[37]	190.56	4.599	0.0115

Table 6: Pure component parameters for PC-SAFT.

Component	Ref.	m (-)	ε/k (K)	σ (Å)
CO_2	This work[a]	2.6246	148.39	2.6264
Methane	[25]	1.0000	150.03	3.7039

[a] PC-SAFT parameters were determined by fitting vapor pressure data and liquid density data [37] in the T_r -range of 0.71 to 0.999, with an average absolute error of 0.03% in vapor pressure, 14% in saturated liquid molar volume, ΔT_c=-2.0·10^{-5} K and Δp_c=-1.7·10^{-5} MPa, where, $\Delta T_c = T_c^{calc} - T_c^{exp}$ and $\Delta p_c = p_c^{calc} - p_c^{exp}$.

Table 7: Binary interaction parameters for SRK, PR, PC-SAFT and UMR-PRU fitted to the experimental data of this work, through Eq. (9), for each isotherm.

$\bar{T}$ (K)	n_p	k_{ij}			UMR-PRU*		%Δp[a]				100·Δy_{CO_2}[b]			
		PR	SRK	PC-SAFT	u_{nm}[c]	u_{mn}[c]	PR	SRK	PC-SAFT	UMR-PRU	PR	SRK	PC-SAFT	UMR-PRU
293.130	12	0.1236	0.1319	0.0876	439.69	-136.68	0.62	0.60	0.75	0.29	0.98	1.15	1.01	0.82
298.142	8	0.1251	0.1604	0.0933	635.80	-226.23	0.27	0.44	0.31	0.16	0.43	0.51	0.47	0.34
303.145	11	0.1603	0.1774	0.1200	830.36	-305.00	0.04	0.03	0.09	0.06	0.04	0.04	0.05	0.04
Overall	37	-	-	-	-	-	0.34	0.38	0.42	0.18	0.55	0.58	0.52	0.43

[a] $\%\Delta p = 100 \cdot \frac{1}{n_p}\sum_{i=1}^{n_p} \frac{|\bar{p}_f{}^{exp} - \mathrm{p}^{calc}|}{\bar{p}_f{}^{exp}}$, where $\bar{p}_f{}^{exp}$ is the experimental bubble point pressure and p^{calc} the calculated bubble point pressure for each model.

[b] $\%\Delta y_{CO_2} = 100 \cdot \frac{1}{n_p} \cdot \sum_{i=1}^{n_p} \frac{|\bar{y}_{CO_2}^{exp} - y_{CO_2}^{calc}|}{\bar{y}_{CO_2}^{exp}}$, where $y_{CO_2}^{exp}$ and $y_{CO_2}^{calc}$ are the experimental and calculated CO_2 concentration in vapor phase at pressure $\bar{p}_f$.

[c] n, m: UNIFAC groups of the UMR-PRU model, where n represents CO_2 and m represents CH_4.

* UNIFAC van der Waals volume (R) and surface area (Q) group parameters for the UMR-PRU model are: R_{CO2}=1.296, Q_{CO2}=1.261, R_{CH4}=1.129, Q_{CH4}=1.124.

Table 8: Deviations of the UMR-PRU model from the estimated by the scaling law critical point data.

$\bar{T}$ (K)	293.13 K		298.142 K		303.145 K	
	p_c (MPa)	$z_{CO_2,c}$ (-)	p_c (MPa)	$z_{CO_2,c}$ (-)	p_c (MPa)	$z_{CO_2,c}$ (-)
Exp.	7.933	0.8829	7.702	0.9350	7.435	0.98895
UMR-PRU	8.121	0.8676	7.824	0.9258	7.486	0.98625
%AAD*	2.37	1.73	1.59	0.97	0.69	0.27

* $\%\mathrm{AAD} = 100 \cdot \frac{1}{n_p}\sum_{i=1}^{n_p} \frac{|\mathrm{x}^{exp} - \mathrm{x}^{calc}|}{x^{exp}}$, where x represents the critical point pressure, p_c, or the composition at the critical point, $z_{CO_2,c}$

Table A.1: Cubic EoS parameters for the SRK and PR used in Eqs. A.3 – A.5 in the Appendix.

	d_0	d_1	d_2	d_3	d_4
SRK	0.48508	1.55171	-0.15613	0.42748	0.08664
PR	0.37464	1.54226	-0.26992	0.45724	0.07780

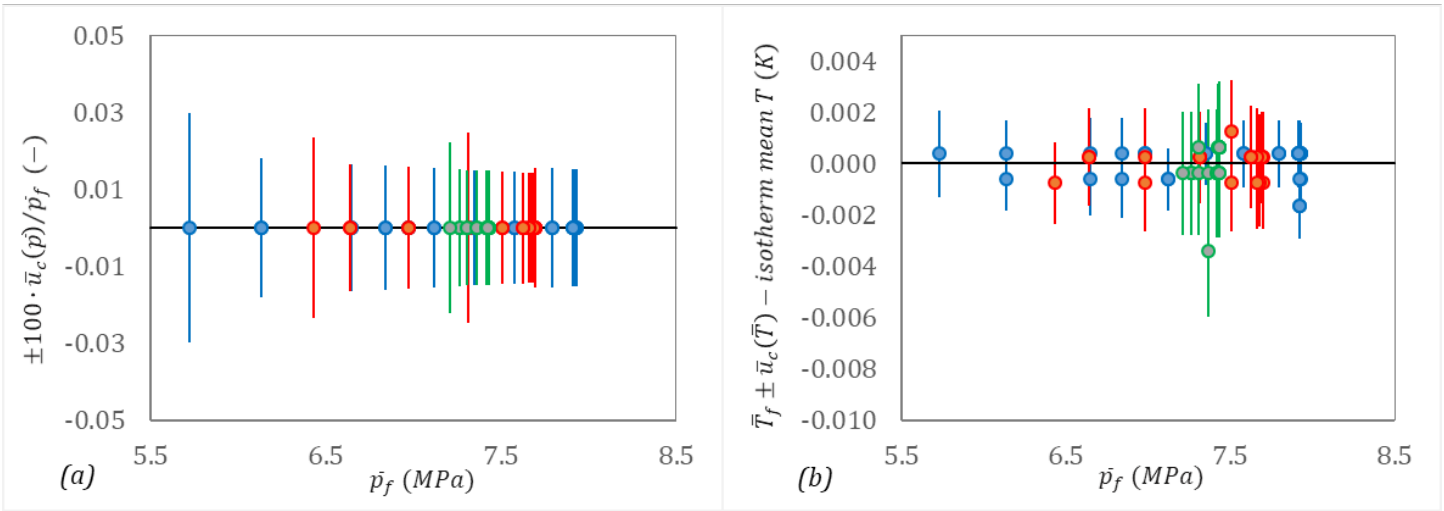

Figure 1

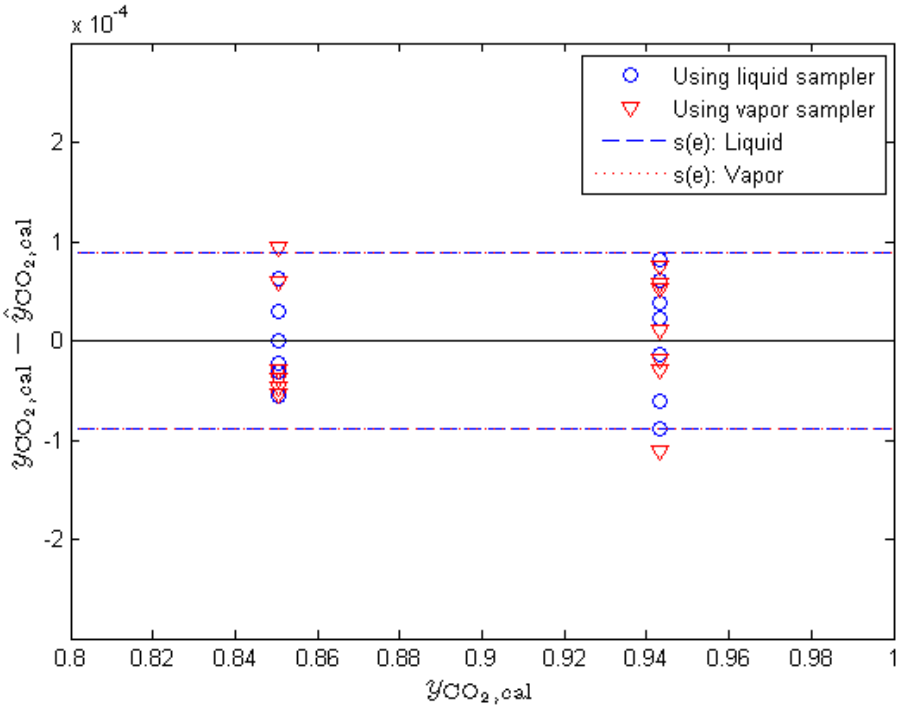

Figure 2

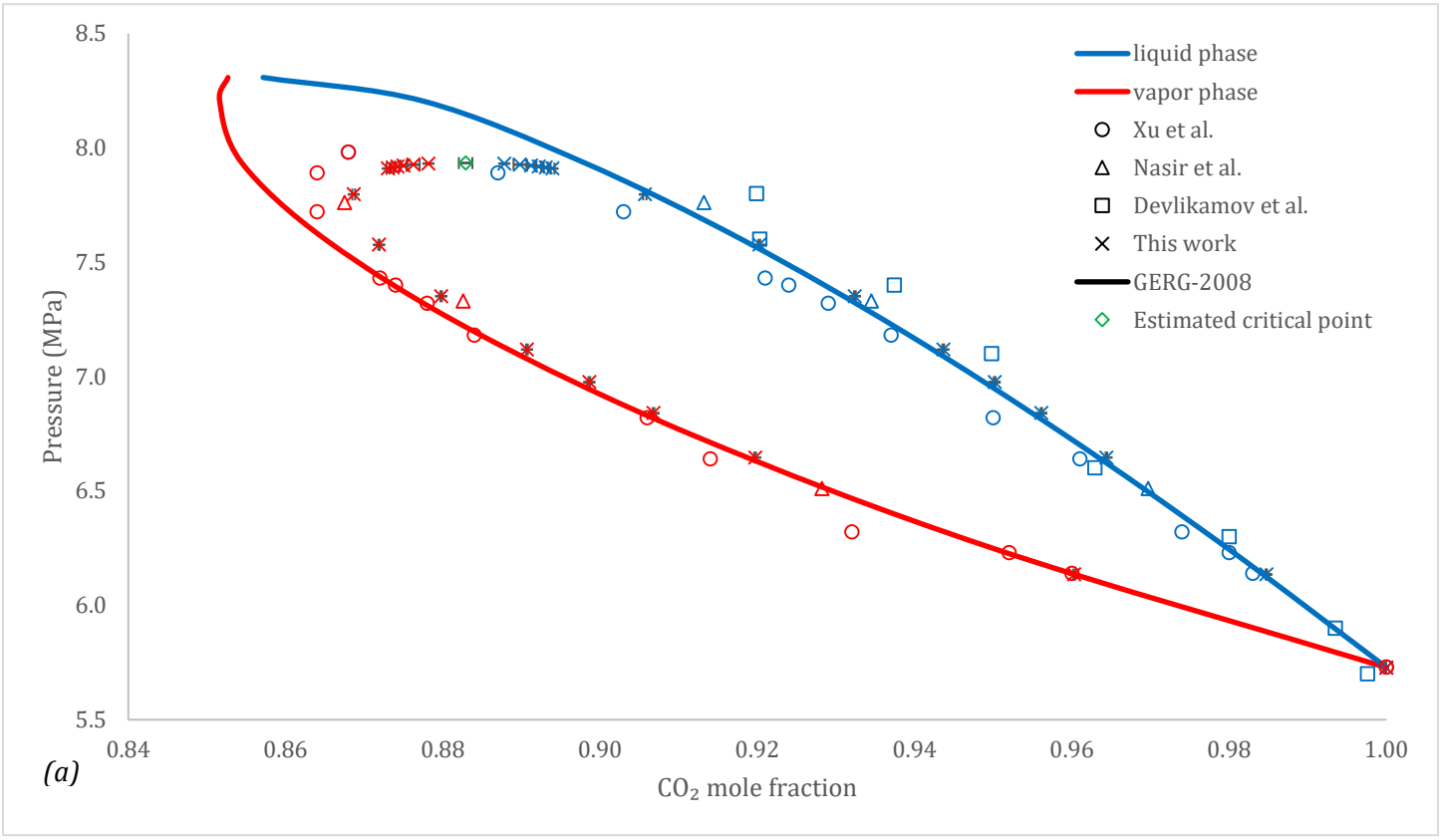
8.5
8.0
7.5
7.0
6.5
6.0
5.5
Pressure (MPa)
0.84
0.86
0.88
0.90
0.92
0.94
0.96
0.98
1.00
CO2 mole fraction
liquid phase
vapor phase
Xu et al.
Nasir et al.
Devlikamov et al.
This work
GERG-2008
Estimated critical point

(a)

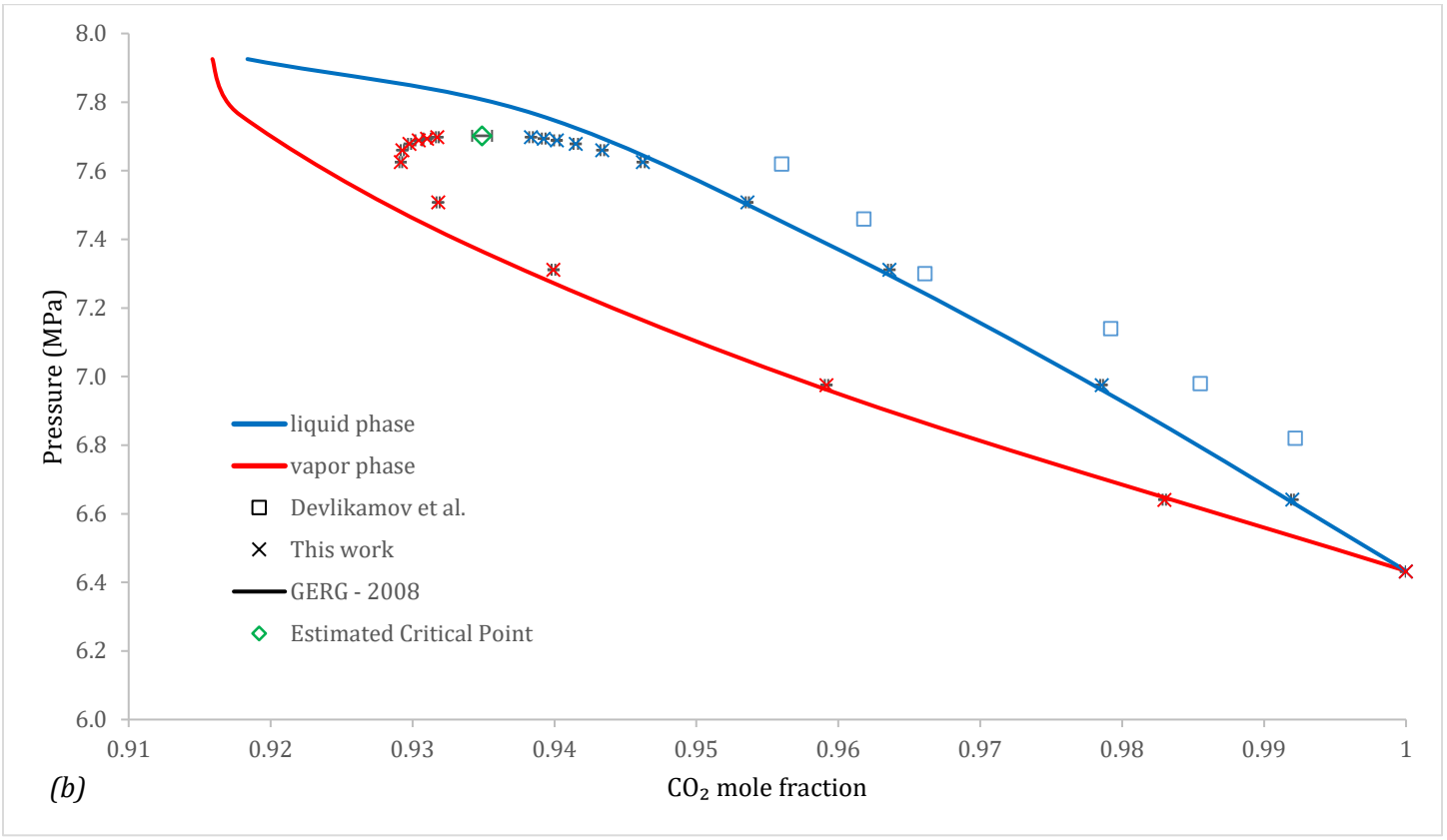
8.0
7.8
7.6
7.4
7.2
7.0
6.8
6.6
6.4
6.2
6.0
Pressure (MPa)
0.91
0.92
0.93
0.94
0.95
0.96
0.97
0.98
0.99
1
CO2 mole fraction
liquid phase
vapor phase
Devlikamov et al.
This work
GERG - 2008
Estimated Critical Point

(b)

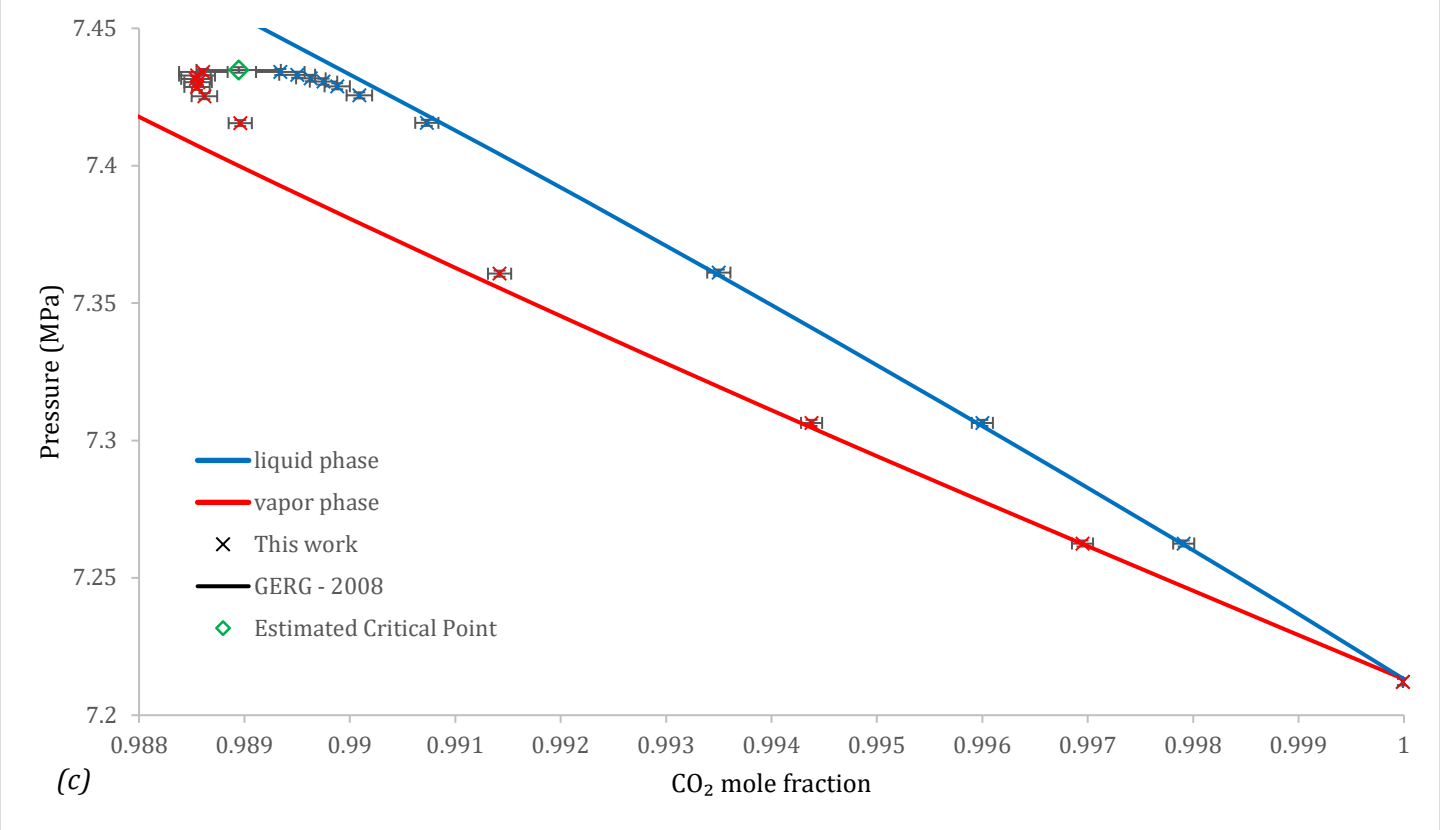
7.45
7.4
7.35
7.3
7.25
7.2
Pressure (MPa)
0.988
0.989
0.99
0.991
0.992
0.993
0.994
0.995
0.996
0.997
0.998
0.999
1
CO2 mole fraction
liquid phase
vapor phase
This work
GERG - 2008
Estimated Critical Point
(c)

Figure 3

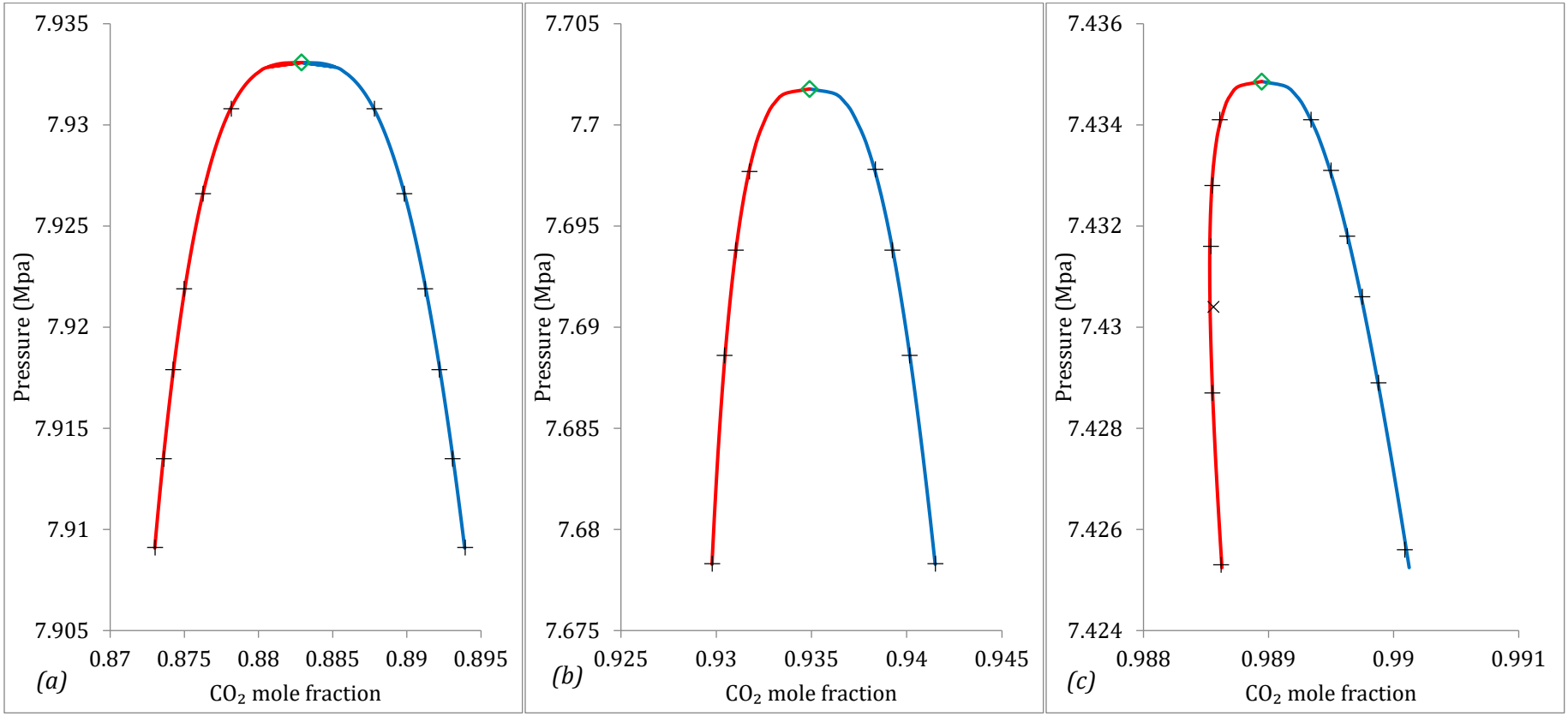
7.935
7.93
7.925
7.92
7.915
7.91
7.905
Pressure (Mpa)
0.87
0.875
0.88
0.885
0.89
0.895
(a)
CO2 mole fraction
7.705
7.7
7.695
7.69
7.685
7.68
7.675
Pressure (Mpa)
0.925
0.93
0.935
0.94
0.945
(b)
CO2 mole fraction
7.436
7.434
7.432
7.43
7.428
7.426
7.424
Pressure (Mpa)
0.988
0.989
0.99
0.991
(c)
CO2 mole fraction

Figure 4

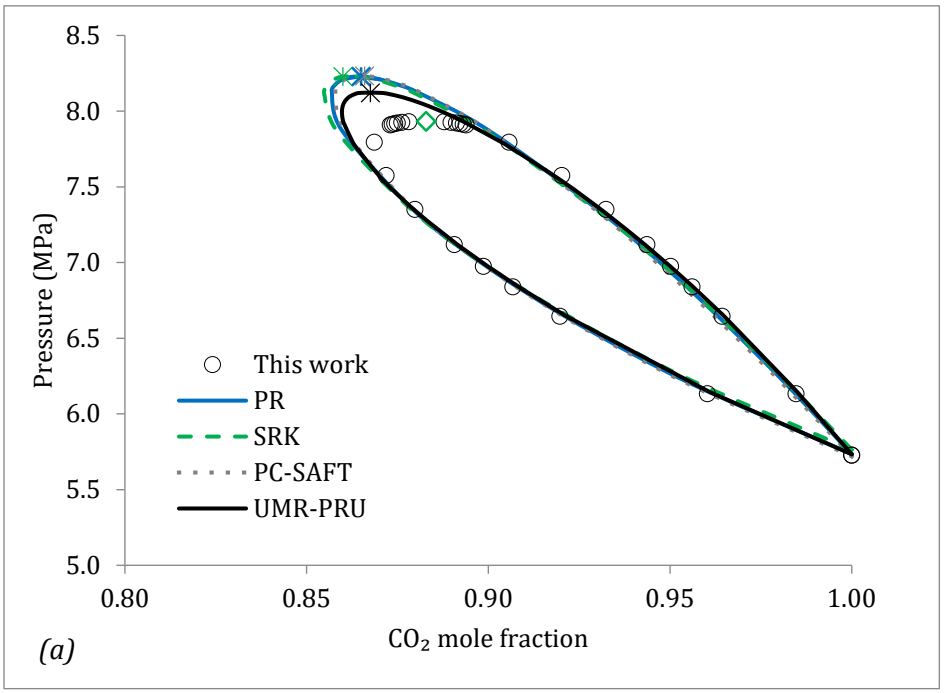
8.5
8.0
7.5
7.0
6.5
6.0
5.5
5.0
Pressure (MPa)
0.80
0.85
0.90
0.95
1.00
CO2 mole fraction
This work
PR
SRK
PC-SAFT
UMR-PRU
(a)

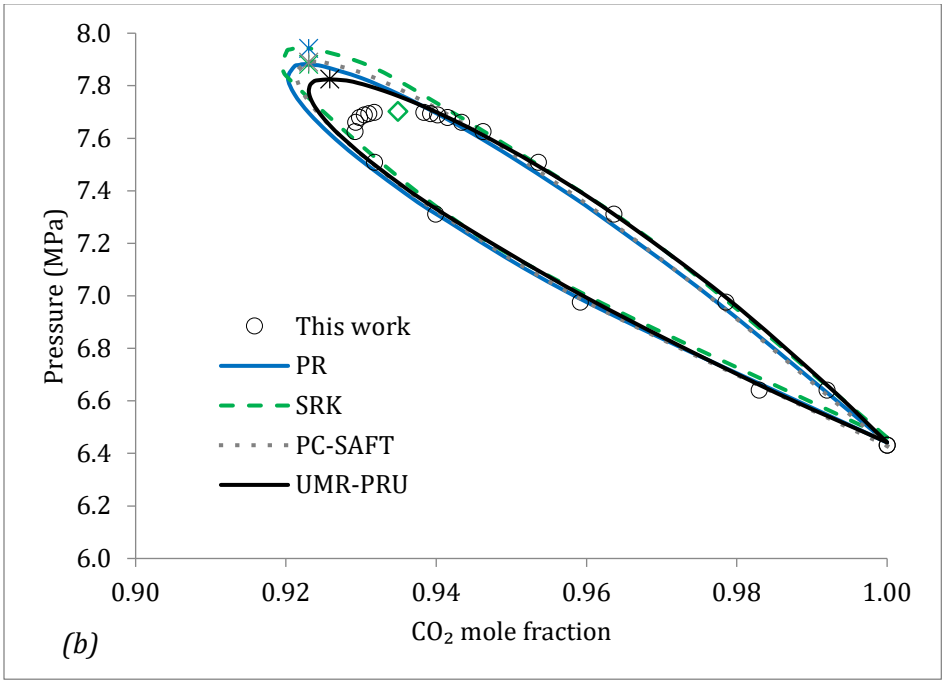
8.0
7.8
7.6
7.4
7.2
7.0
6.8
6.6
6.4
6.2
6.0
Pressure (MPa)
0.90
0.92
0.94
0.96
0.98
1.00
CO2 mole fraction
This work
PR
SRK
PC-SAFT
UMR-PRU
(b)

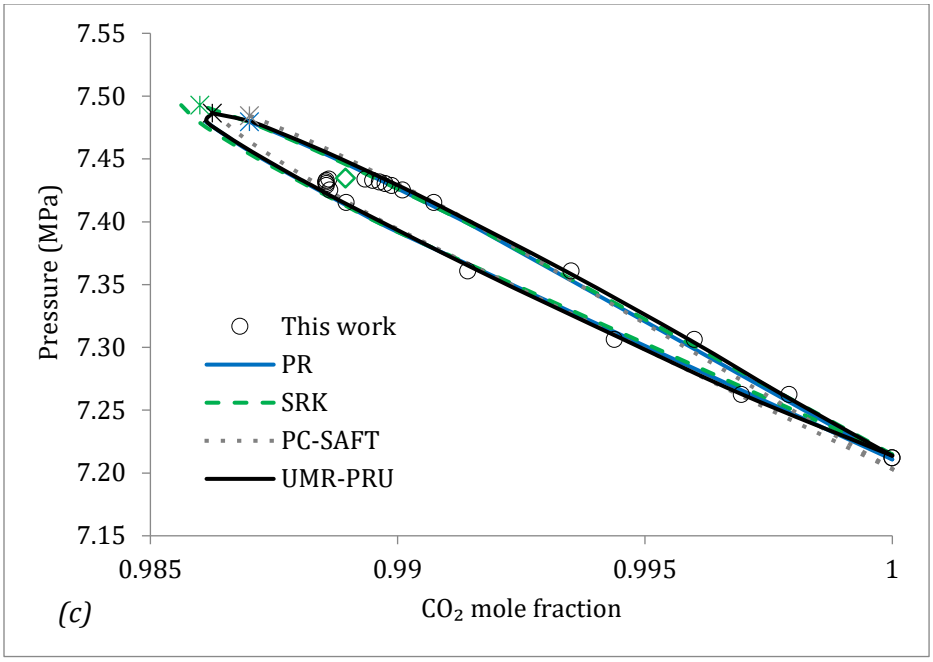
7.55
7.50
7.45
7.40
7.35
7.30
7.25
7.20
7.15
Pressure (MPa)
This work
PR
SRK
PC-SAFT
UMR-PRU
0.985
0.99
0.995
1
CO2 mole fraction
(c)

Figure 5

Vapor - liquid equilibrium of the carbon dioxide/methane mixture at three isotherms

Eirini Petropoulou[1], Epaminondas Voutsas[1], Snorre Foss Westman[2], Anders Austegard[2], Hans Georg Jacob Stang[2], Sigurd Weidemann Løvseth[2]

[1]*Laboratory of Thermodynamics and Transport Phenomena*
School of Chemical Engineering, National Technical University of Athens
9, Heroon Polytechniou Str., Zografou Campus, 15780 Athens, Greece

[2]*SINTEF Energy Research*
Postboks 4761Torgard
N-7465 Trondheim
Norway

Supplementary Material

Appendix B: Detailed experimental data

For ease of reading, a summary of the symbols used in the tables detailed experimental data tables is given in Table S.6. Detailed VLE data for the liquid phase samples are given in Table S.1 and for the vapor phase samples in Table S.2. Each row in the tables corresponds to one composition sample. A series of samples taken at the same VLE experiment is identified by the same ID which corresponds to those of Tables 2 and 3 respectively.

Table S.1: Experimental VLE data for the liquid phase of CO_2/CH_4 mixture at mean temperature, $\bar{T}$, mean pressure, $\bar{p}$, and sample liquid phase mole fraction, x_{CO_2}.

ID	Data			Temperature (K)				Pressure (MPa)				Composition (-)			Composition Derivatives	
	$\bar{T}$ (K)	$\bar{p}$ (MPa)	x_{CO_2} (-)	$s(T)$	$s(\bar{T})$	$u(T)$	$u_c(\bar{T})$	$s(p)$	$s(\bar{p})$	$u(p)$	$u_c(\bar{p})$	$u(x_{CO_2})$	$u_{tot}(x_{CO_2})$	$x_{CO_2,calc}$	$\frac{\partial x_{CO_2}}{\partial T}$ (K^{-1})	$\frac{\partial x_{CO_2}}{\partial p}$ (MPa^{-1})
P1	293.130	5.7273	0.99999	1.3e-3	1.1e-4	1.1e-3	1.1e-3	1.3e-4	1.6e-5	1.2e-3	1.2e-3					
L1	293.130	6.1347	0.98473	6.1e-4	8.0e-5	1.1e-3	1.1e-3	9.7e-5	1.9e-5	1.1e-3	1.1e-3	8.9e-5	9.9e-5	0.98538	0.00494	-0.03770
	293.127	6.1349	0.98472	2.1e-3	5.7e-4	1.1e-3	1.2e-3	9.8e-5	6.6e-6	1.1e-3	1.1e-3	8.9e-5	9.8e-5	0.98536	0.00494	-0.03770
	293.129	6.1349	0.98473	9.2e-4	3.7e-4	1.1e-3	1.1e-3	8.3e-5	3.8e-6	1.1e-3	1.1e-3	8.9e-5	9.8e-5	0.98537	0.00494	-0.03770
	293.130	6.1348	0.98471	8.0e-4	1.5e-4	1.1e-3	1.1e-3	8.0e-5	9.9e-6	1.1e-3	1.1e-3	8.9e-5	9.8e-5	0.98538	0.00494	-0.03770
	293.130	6.1348	0.98472	7.4e-4	2.2e-4	1.0e-3	1.1e-3	8.6e-5	6.2e-6	1.1e-3	1.1e-3	8.9e-5	9.8e-5	0.98538	0.00494	-0.03770
L2	293.129	6.6459	0.96438	1.2e-3	1.1e-4	1.4e-3	1.4e-3	9.5e-5	9.5e-6	1.1e-3	1.1e-3	8.9e-5	1.0e-4	0.96486	0.00536	-0.04290
	293.129	6.6459	0.96440	1.4e-3	1.9e-4	1.5e-3	1.5e-3	8.8e-5	1.2e-5	1.1e-3	1.1e-3	8.9e-5	1.0e-4	0.96486	0.00536	-0.04290
	293.129	6.6459	0.96437	1.2e-3	1.1e-4	1.3e-3	1.3e-3	8.1e-5	9.0e-6	1.1e-3	1.1e-3	8.9e-5	1.0e-4	0.96486	0.00536	-0.04290
	293.130	6.6459	0.96439	1.2e-3	2.3e-4	1.2e-3	1.3e-3	8.7e-5	1.6e-5	1.1e-3	1.1e-3	8.9e-5	1.0e-4	0.96486	0.00536	-0.04290
	293.129	6.6458	0.96439	8.1e-4	8.4e-5	1.3e-3	1.3e-3	9.0e-5	1.1e-5	1.1e-3	1.1e-3	8.9e-5	1.0e-4	0.96486	0.00536	-0.04290
L3	293.130	6.8402	0.95614	2.1e-3	5.9e-4	1.5e-3	1.6e-3	1.3e-4	2.1e-5	1.1e-3	1.1e-3	8.9e-5	1.0e-4	0.95629	0.00554	-0.04540
	293.130	6.8401	0.95614	1.9e-3	6.6e-4	1.2e-3	1.3e-3	1.5e-4	3.3e-5	1.1e-3	1.1e-3	8.9e-5	1.0e-4	0.95629	0.00554	-0.04540
	293.131	6.8401	0.95609	1.5e-3	4.4e-4	1.2e-3	1.3e-3	1.2e-4	2.9e-5	1.1e-3	1.1e-3	8.9e-5	1.0e-4	0.95630	0.00554	-0.04540
	293.131	6.8402	0.95609	1.3e-3	2.7e-4	1.3e-3	1.3e-3	1.2e-4	7.2e-6	1.1e-3	1.1e-3	8.9e-5	1.0e-4	0.95629	0.00554	-0.04540
	293.130	6.8402	0.95609	1.6e-3	2.2e-4	1.2e-3	1.2e-3	1.4e-4	1.9e-5	1.1e-3	1.1e-3	8.9e-5	1.0e-4	0.95629	0.00554	-0.04540
L4	293.128	6.9756	0.95019	2.0e-3	4.3e-4	1.1e-3	1.2e-3	1.5e-4	2.3e-5	1.1e-3	1.1e-3	8.9e-5	1.0e-4	0.95000	0.00568	-0.04740
	293.129	6.9756	0.95019	1.8e-3	3.1e-4	1.1e-3	1.2e-3	1.5e-4	1.8e-5	1.1e-3	1.1e-3	8.9e-5	1.0e-4	0.95000	0.00568	-0.04740
	293.131	6.9755	0.95020	7.6e-4	2.8e-4	1.0e-3	1.1e-3	1.3e-4	1.7e-5	1.1e-3	1.1e-3	8.9e-5	1.0e-4	0.95002	0.00568	-0.04740
	293.131	6.9755	0.95015	6.6e-4	1.0e-4	1.0e-3	1.0e-3	1.7e-4	2.3e-5	1.1e-3	1.1e-3	8.9e-5	1.0e-4	0.95002	0.00568	-0.04740
	293.131	6.9755	0.95014	9.2e-4	2.2e-4	1.0e-3	1.0e-3	1.7e-4	3.2e-5	1.1e-3	1.1e-3	8.9e-5	1.0e-4	0.95002	0.00568	-0.04740
L5	293.128	7.1184	0.94367	2.2e-3	7.0e-4	1.1e-3	1.3e-3	1.6e-4	2.0e-5	1.1e-3	1.1e-3	8.9e-5	1.1e-4	0.94306	0.00583	-0.04980
	293.129	7.1183	0.94363	1.5e-3	2.5e-4	1.1e-3	1.2e-3	1.5e-4	3.6e-5	1.1e-3	1.1e-3	8.9e-5	1.1e-4	0.94307	0.00583	-0.04980

ID	Data			Temperature (K)				Pressure (MPa)				Composition (-)			Composition Derivatives	
	$\bar{T}$ (K)	$\bar{p}$ (MPa)	x_{CO_2} (-)	$s(T)$	$s(\bar{T})$	$u(T)$	$u_c(\bar{T})$	$s(p)$	$s(\bar{p})$	$u(p)$	$u_c(\bar{p})$	$u(x_{CO_2})$	$u_{tot}(x_{CO_2})$	$x_{CO_2,calc}$	$\frac{\partial x_{CO_2}}{\partial T}$ (K^{-1})	$\frac{\partial x_{CO_2}}{\partial p}$ (MPa^{-1})
	293.129	7.1184	0.94365	1.3e-3	2.5e-4	1.2e-3	1.2e-3	1.4e-4	1.4e-5	1.1e-3	1.1e-3	8.9e-5	1.1e-4	0.94306	0.00583	-0.04980
	293.130	7.1183	0.94363	8.3e-4	1.4e-4	1.2e-3	1.2e-3	1.6e-4	4.1e-5	1.1e-3	1.1e-3	8.9e-5	1.1e-4	0.94307	0.00583	-0.04980
	293.130	7.1183	0.94364	1.1e-3	3.5e-4	1.1e-3	1.1e-3	1.5e-4	1.1e-5	1.1e-3	1.1e-3	8.9e-5	1.1e-4	0.94307	0.00583	-0.04980
L6	293.129	7.3508	0.93242	1.1e-3	2.5e-4	1.2e-3	1.2e-3	1.6e-4	1.5e-5	1.1e-3	1.1e-3	8.9e-5	1.1e-4	0.93096	0.00607	-0.05460
	293.129	7.3509	0.93238	6.7e-4	1.4e-4	1.2e-3	1.2e-3	1.7e-4	1.5e-5	1.1e-3	1.1e-3	8.9e-5	1.1e-4	0.93095	0.00607	-0.05460
	293.130	7.3508	0.93235	7.7e-4	7.6e-5	1.2e-3	1.2e-3	1.7e-4	1.8e-5	1.1e-3	1.1e-3	8.9e-5	1.1e-4	0.93097	0.00607	-0.05460
	293.130	7.3508	0.93239	9.1e-4	2.5e-4	1.1e-3	1.1e-3	1.5e-4	1.5e-5	1.1e-3	1.1e-3	8.9e-5	1.1e-4	0.93097	0.00607	-0.05460
	293.130	7.3508	0.93243	8.4e-4	1.1e-4	1.2e-3	1.2e-3	1.4e-4	1.6e-5	1.1e-3	1.1e-3	8.9e-5	1.1e-4	0.93097	0.00607	-0.05460
L7	293.130	7.5758	0.92022	1.6e-3	2.9e-4	1.4e-3	1.4e-3	1.4e-4	7.7e-6	1.1e-3	1.1e-3	8.9e-5	1.1e-4	0.91800	0.00631	-0.06110
	293.130	7.5758	0.92024	1.1e-3	1.6e-4	1.2e-3	1.3e-3	1.4e-4	8.3e-6	1.1e-3	1.1e-3	8.9e-5	1.1e-4	0.91800	0.00631	-0.06110
	293.130	7.5758	0.92024	9.4e-4	1.2e-4	1.1e-3	1.2e-3	1.6e-4	1.2e-5	1.1e-3	1.1e-3	8.9e-5	1.1e-4	0.91800	0.00631	-0.06110
	293.130	7.5758	0.92025	1.0e-3	1.3e-4	1.3e-3	1.3e-3	1.7e-4	1.7e-5	1.1e-3	1.1e-3	8.9e-5	1.1e-4	0.91800	0.00631	-0.06110
	293.130	7.5758	0.92024	1.0e-3	2.1e-4	1.3e-3	1.3e-3	1.6e-4	1.1e-5	1.1e-3	1.1e-3	8.9e-5	1.1e-4	0.91800	0.00631	-0.06110
L8	293.130	7.7962	0.90566	1.4e-3	3.8e-4	1.3e-3	1.3e-3	1.6e-4	2.1e-5	1.1e-3	1.1e-3	8.9e-5	1.2e-4	0.90350	0.00649	-0.07160
	293.130	7.7962	0.90565	1.7e-3	2.6e-4	1.3e-3	1.3e-3	1.7e-4	1.1e-5	1.2e-3	1.2e-3	8.9e-5	1.2e-4	0.90350	0.00649	-0.07160
	293.131	7.7961	0.90571	5.6e-4	9.5e-5	1.1e-3	1.1e-3	1.7e-4	1.2e-5	1.2e-3	1.2e-3	8.9e-5	1.2e-4	0.90351	0.00649	-0.07160
	293.131	7.7962	0.90569	8.1e-4	1.6e-4	1.2e-3	1.2e-3	1.8e-4	8.9e-6	1.2e-3	1.2e-3	8.9e-5	1.2e-4	0.90350	0.00649	-0.07160
	293.130	7.7961	0.90568	1.1e-3	1.4e-4	1.5e-3	1.5e-3	1.7e-4	1.4e-5	1.2e-3	1.2e-3	8.9e-5	1.2e-4	0.90350	0.00649	-0.07160
L9	293.128	7.9091	0.89394	1.8e-3	4.0e-4	1.3e-3	1.3e-3	1.5e-4	2.5e-5	1.2e-3	1.2e-3	8.9e-5	2.1e-4	0.89490	0.00144^{+}	-0.16730
	293.130	7.9091	0.89394	9.6e-4	2.8e-4	1.1e-3	1.1e-3	1.3e-4	1.1e-5	1.2e-3	1.2e-3	8.9e-5	2.1e-4	0.89491	0.00144^{+}	-0.16730
	293.130	7.9091	0.89395	1.4e-3	2.4e-4	1.2e-3	1.2e-3	1.4e-4	1.3e-5	1.2e-3	1.2e-3	8.9e-5	2.1e-4	0.89491	0.00144^{+}	-0.16730
	293.130	7.9091	0.89396	1.2e-3	3.7e-4	1.3e-3	1.3e-3	1.3e-4	9.2e-6	1.2e-3	1.2e-3	8.9e-5	2.1e-4	0.89491	0.00144^{+}	-0.16730
L10	293.130	7.9135	0.89306	6.7e-4	6.8e-5	1.0e-3	1.0e-3	1.4e-4	3.0e-5	1.2e-3	1.2e-3	8.9e-5	2.4e-4	0.89455	0.06302^{+}	-0.18810
	293.130	7.9136	0.89311	8.2e-4	2.9e-4	1.1e-3	1.1e-3	1.3e-4	1.2e-5	1.2e-3	1.2e-3	8.9e-5	2.5e-4	0.89454	0.06302^{+}	-0.18810
	293.130	7.9135	0.89306	8.6e-4	1.3e-4	1.0e-3	1.0e-3	1.3e-4	1.4e-5	1.2e-3	1.2e-3	8.9e-5	2.4e-4	0.89455	0.06302^{+}	-0.18810
	293.130	7.9135	0.89317	5.9e-4	6.6e-5	1.0e-3	1.0e-3	1.4e-4	3.8e-5	1.2e-3	1.2e-3	8.9e-5	2.4e-4	0.89455	0.06302^{+}	-0.18810
L11	293.128	7.9179	0.89215	2.4e-3	1.1e-3	1.1e-3	1.5e-3	1.5e-4	1.5e-5	1.2e-3	1.2e-3	8.9e-5	2.7e-4	0.89417	-0.00014^{+}	-0.21810

ID	Data			Temperature (K)				Pressure (MPa)				Composition (-)			Composition Derivatives	
	$\bar{T}$ (K)	$\bar{p}$ (MPa)	x_{CO_2} (-)	$s(T)$	$s(\bar{T})$	$u(T)$	$u_c(\bar{T})$	$s(p)$	$s(\bar{p})$	$u(p)$	$u_c(\bar{p})$	$u(x_{CO_2})$	$u_{tot}(x_{CO_2})$	$x_{CO_2,calc}$	$\frac{\partial x_{CO_2}}{\partial T}$ (K^{-1})	$\frac{\partial x_{CO_2}}{\partial p}$ (MPa^{-1})
	293.128	7.9179	0.89221	1.3e-3	2.2e-4	1.1e-3	1.1e-3	1.3e-4	7.2e-6	1.2e-3	1.2e-3	8.9e-5	2.7e-4	0.89417	-0.00014^{+}	-0.21810
	293.128	7.9179	0.89220	1.9e-3	6.7e-4	1.1e-3	1.3e-3	1.3e-4	2.5e-5	1.2e-3	1.2e-3	8.9e-5	2.7e-4	0.89417	-0.00014^{+}	-0.21810
	293.128	7.9179	0.89227	1.3e-3	4.5e-4	1.1e-3	1.2e-3	1.7e-4	2.6e-5	1.2e-3	1.2e-3	8.9e-5	2.7e-4	0.89417	-0.00014^{+}	-0.21810
L12	293.129	7.9219	0.89124	2.1e-3	9.4e-4	1.1e-3	1.5e-3	1.1e-4	1.1e-5	1.2e-3	1.2e-3	8.9e-5	3.2e-4	0.89385	0.00416^{+}	-0.26190
	293.129	7.9220	0.89116	2.0e-3	7.1e-4	1.1e-3	1.3e-3	1.3e-4	1.0e-5	1.2e-3	1.2e-3	8.9e-5	3.2e-4	0.89384	0.00416^{+}	-0.26190
	293.130	7.9219	0.89126	6.1e-4	1.2e-4	1.1e-3	1.1e-3	1.3e-4	8.9e-6	1.2e-3	1.2e-3	8.9e-5	3.2e-4	0.89386	0.00416^{+}	-0.26190
	293.126	7.9219	0.89122	8.0e-4	9.3e-5	1.1e-3	1.1e-3	1.3e-4	1.2e-5	1.2e-3	1.2e-3	8.9e-5	3.2e-4	0.89383	0.00416^{+}	-0.26190
L13	293.130	7.9267	0.88977	8.2e-4	1.7e-4	1.1e-3	1.1e-3	1.4e-4	1.7e-5	1.2e-3	1.2e-3	8.9e-5	5.1e-4	0.89346	-0.23635^{+}	-0.36730
	293.130	7.9266	0.88984	1.0e-3	3.7e-4	1.0e-3	1.1e-3	1.2e-4	8.7e-6	1.2e-3	1.2e-3	8.9e-5	5.1e-4	0.89347	-0.23635^{+}	-0.36730
	293.130	7.9266	0.88987	8.4e-4	1.4e-4	1.1e-3	1.1e-3	1.4e-4	9.5e-6	1.2e-3	1.2e-3	8.9e-5	5.1e-4	0.89347	-0.23635^{+}	-0.36730
	293.130	7.9266	0.88980	7.1e-4	1.5e-4	1.1e-3	1.1e-3	1.4e-4	2.1e-5	1.2e-3	1.2e-3	8.9e-5	5.1e-4	0.89347	-0.23635^{+}	-0.36730
L14	293.129	7.9308	0.88776	1.8e-3	3.5e-4	1.1e-3	1.2e-3	1.0e-4	1.3e-5	1.2e-3	1.2e-3	8.9e-5	8.3e-4	0.89311	0.00599^{+}	-0.71320
	293.128	7.9308	0.88782	1.2e-3	4.6e-4	1.1e-3	1.2e-3	1.2e-4	6.7e-6	1.2e-3	1.2e-3	8.9e-5	8.3e-4	0.89310	0.00599^{+}	-0.71320
	293.130	7.9308	0.88786	1.4e-3	5.9e-4	1.1e-3	1.2e-3	1.2e-4	1.3e-5	1.2e-3	1.2e-3	8.9e-5	8.3e-4	0.89311	0.00599^{+}	-0.71320
	293.130	7.9308	0.88781	1.1e-3	2.6e-4	1.2e-3	1.2e-3	1.2e-4	1.4e-5	1.2e-3	1.2e-3	8.9e-5	8.3e-4	0.89311	0.00599^{+}	-0.71320
P2	298.141	6.4316	0.99999	6.7e-4	7.6e-5	1.4e-3	1.4e-3	1.0e-4	3.4e-5	1.1e-3	1.1e-3					
L15	298.142	6.6411	0.99200	1.3e-3	4.9e-4	1.9e-3	2.0e-3	1.2e-4	2.9e-5	1.1e-3	1.1e-3	8.9e-5	9.9e-5	0.99271	0.00535	-0.03723
	298.141	6.6410	0.99200	7.5e-4	1.4e-4	1.9e-3	1.9e-3	8.2e-5	6.6e-6	1.1e-3	1.1e-3	8.9e-5	9.9e-5	0.99271	0.00535	-0.03723
	298.141	6.6411	0.99200	8.5e-4	3.3e-4	1.8e-3	1.9e-3	9.0e-5	1.2e-5	1.1e-3	1.1e-3	8.9e-5	9.9e-5	0.99270	0.00535	-0.03723
	298.142	6.6411	0.99200	5.9e-4	4.8e-5	1.9e-3	1.9e-3	9.3e-5	1.3e-5	1.1e-3	1.1e-3	8.9e-5	9.9e-5	0.99271	0.00535	-0.03723
	298.142	6.6410	0.99200	4.7e-4	7.2e-5	1.9e-3	1.9e-3	8.7e-5	8.9e-6	1.1e-3	1.1e-3	8.9e-5	9.9e-5	0.99271	0.00535	-0.03723
L16	298.142	6.9754	0.97855	9.2e-4	3.1e-4	1.9e-3	1.9e-3	1.2e-4	5.1e-6	1.1e-3	1.1e-3	8.9e-5	1.0e-4	0.97936	0.00585	-0.04294
	298.142	6.9755	0.97855	8.0e-4	2.1e-4	1.8e-3	1.8e-3	1.4e-4	2.2e-5	1.1e-3	1.1e-3	8.9e-5	1.0e-4	0.97936	0.00585	-0.04294
	298.142	6.9755	0.97856	5.6e-4	8.2e-5	1.8e-3	1.8e-3	1.3e-4	1.1e-5	1.1e-3	1.1e-3	8.9e-5	1.0e-4	0.97936	0.00585	-0.04294
	298.142	6.9755	0.97855	4.9e-4	1.0e-4	1.9e-3	1.9e-3	1.2e-4	1.1e-5	1.1e-3	1.1e-3	8.9e-5	1.0e-4	0.97936	0.00585	-0.04294
	298.143	6.9755	0.97855	4.7e-4	5.2e-5	2.0e-3	2.0e-3	1.3e-4	2.0e-5	1.1e-3	1.1e-3	8.9e-5	1.0e-4	0.97936	0.00585	-0.04294
L17	298.142	7.3114	0.96362	3.3e-4	5.0e-5	1.8e-3	1.8e-3	9.6e-5	1.9e-5	1.1e-3	1.1e-3	8.9e-5	1.1e-4	0.96361	0.00645	-0.05147

ID	Data			Temperature (K)				Pressure (MPa)				Composition (-)			Composition Derivatives	
	$\bar{T}$ (K)	$\bar{p}$ (MPa)	x_{CO_2} (-)	$s(T)$	$s(\bar{T})$	$u(T)$	$u_c(\bar{T})$	$s(p)$	$s(\bar{p})$	$u(p)$	$u_c(\bar{p})$	$u(x_{CO_2})$	$u_{tot}(x_{CO_2})$	$x_{CO_2,calc}$	$\frac{\partial x_{CO_2}}{\partial T}$ (K^{-1})	$\frac{\partial x_{CO_2}}{\partial p}$ (MPa^{-1})
	298.142	7.3114	0.96358	5.4e-4	1.2e-4	2.0e-3	2.0e-3	1.1e-4	1.2e-5	1.1e-3	1.1e-3	8.9e-5	1.1e-4	0.96361	0.00645	-0.05147
	298.142	7.3114	0.96362	4.8e-4	8.7e-5	1.7e-3	1.7e-3	1.1e-4	1.5e-5	1.1e-3	1.1e-3	8.9e-5	1.1e-4	0.96361	0.00645	-0.05147
	298.142	7.3114	0.96360	3.8e-4	7.5e-5	1.9e-3	1.9e-3	1.1e-4	1.2e-5	1.1e-3	1.1e-3	8.9e-5	1.1e-4	0.96361	0.00645	-0.05147
	298.142	7.3114	0.96363	4.0e-4	8.5e-5	1.7e-3	1.7e-3	1.2e-4	1.3e-5	1.1e-3	1.1e-3	8.9e-5	1.1e-4	0.96361	0.00645	-0.05147
L18	298.140	7.5078	0.95358	1.1e-3	2.3e-4	1.6e-3	1.6e-3	1.8e-4	5.2e-5	1.1e-3	1.1e-3	8.9e-5	1.1e-4	0.95276	0.00683	-0.05956
	298.140	7.5079	0.95361	1.1e-3	1.8e-4	1.7e-3	1.7e-3	1.3e-4	1.3e-5	1.1e-3	1.1e-3	8.9e-5	1.1e-4	0.95275	0.00683	-0.05956
	298.141	7.5079	0.95358	1.9e-3	4.0e-4	2.0e-3	2.0e-3	1.3e-4	1.0e-5	1.1e-3	1.1e-3	8.9e-5	1.1e-4	0.95276	0.00683	-0.05956
	298.142	7.5079	0.95359	4.3e-4	8.7e-5	1.9e-3	1.9e-3	1.2e-4	1.4e-5	1.1e-3	1.1e-3	8.9e-5	1.1e-4	0.95277	0.00683	-0.05956
	298.142	7.5079	0.95360	7.7e-4	3.1e-4	1.9e-3	1.9e-3	1.3e-4	1.7e-5	1.1e-3	1.1e-3	8.9e-5	1.1e-4	0.95277	0.00683	-0.05956
L19	298.142	7.6250	0.94625	3.9e-4	1.3e-4	1.9e-3	1.9e-3	1.1e-4	1.2e-5	1.1e-3	1.1e-3	8.9e-5	1.4e-4	0.94536	0.03851	-0.06800
	298.141	7.6250	0.94619	6.2e-4	2.0e-4	1.8e-3	1.9e-3	1.1e-4	6.6e-6	1.1e-3	1.1e-3	8.9e-5	1.4e-4	0.94535	0.03851	-0.06800
	298.142	7.6250	0.94626	5.5e-4	1.5e-4	2.0e-3	2.0e-3	1.3e-4	1.3e-5	1.1e-3	1.1e-3	8.9e-5	1.4e-4	0.94536	0.03851	-0.06800
	298.142	7.6250	0.94616	6.0e-4	1.1e-4	2.0e-3	2.0e-3	1.4e-4	2.2e-5	1.1e-3	1.1e-3	8.9e-5	1.4e-4	0.94536	0.03851	-0.06800
	298.142	7.6250	0.94623	6.8e-4	1.7e-4	2.1e-3	2.1e-3	1.3e-4	2.3e-5	1.1e-3	1.1e-3	8.9e-5	1.4e-4	0.94536	0.03851	-0.06800
L20	298.142	7.6599	0.94338	5.9e-4	1.1e-4	1.7e-3	1.7e-3	1.2e-4	1.6e-5	1.1e-3	1.1e-3	8.9e-5	1.3e-4	0.94294	0.00493	-0.08700
	298.142	7.6599	0.94338	5.0e-4	1.0e-4	1.8e-3	1.8e-3	1.1e-4	8.0e-6	1.1e-3	1.1e-3	8.9e-5	1.3e-4	0.94294	0.00493	-0.08700
	298.140	7.6599	0.94337	6.8e-4	2.0e-4	1.7e-3	1.7e-3	1.1e-4	7.4e-6	1.1e-3	1.1e-3	8.9e-5	1.3e-4	0.94293	0.00493	-0.08700
	298.141	7.6602	0.94336	1.3e-3	5.0e-4	1.8e-3	1.9e-3	1.9e-4	6.9e-5	1.1e-3	1.1e-3	8.9e-5	1.3e-4	0.94291	0.00493	-0.08700
	298.142	7.6600	0.94335	4.3e-4	7.8e-5	1.8e-3	1.8e-3	1.4e-4	2.2e-5	1.1e-3	1.1e-3	8.9e-5	1.3e-4	0.94293	0.00493	-0.08700
L21	298.141	7.6783	0.94151	9.4e-4	2.7e-4	1.8e-3	1.9e-3	1.3e-4	1.3e-5	1.1e-3	1.1e-3	8.9e-5	1.6e-4	0.94160	0.02602^{+}	-0.11300
	298.141	7.6783	0.94150	8.3e-4	1.8e-4	1.8e-3	1.8e-3	1.4e-4	2.3e-5	1.1e-3	1.1e-3	8.9e-5	1.6e-4	0.94160	0.02602^{+}	-0.11300
	298.142	7.6783	0.94153	5.0e-4	4.5e-5	1.7e-3	1.7e-3	1.5e-4	1.4e-5	1.1e-3	1.1e-3	8.9e-5	1.6e-4	0.94161	0.02602^{+}	-0.11300
	298.141	7.6783	0.94149	6.0e-4	1.2e-4	1.7e-3	1.7e-3	1.4e-4	1.2e-5	1.1e-3	1.1e-3	8.9e-5	1.6e-4	0.94160	0.02602^{+}	-0.11300
	298.142	7.6782	0.94150	4.1e-4	4.0e-5	1.7e-3	1.7e-3	1.2e-4	1.0e-5	1.1e-3	1.1e-3	8.9e-5	1.6e-4	0.94162	0.02602^{+}	-0.11300
L22	298.142	7.6886	0.94019	4.1e-4	6.8e-5	1.7e-3	1.7e-3	1.3e-4	1.6e-5	1.1e-3	1.1e-3	8.9e-5	1.9e-4	0.94085	0.00867^{+}	-0.15100
	298.142	7.6886	0.94013	4.4e-4	1.2e-4	1.8e-3	1.8e-3	1.0e-4	8.2e-6	1.1e-3	1.1e-3	8.9e-5	1.9e-4	0.94085	0.00867^{+}	-0.15100
	298.142	7.6886	0.94014	5.0e-4	1.2e-4	1.8e-3	1.8e-3	1.3e-4	1.3e-5	1.1e-3	1.1e-3	8.9e-5	1.9e-4	0.94085	0.00867^{+}	-0.15100

ID	Data			Temperature (K)				Pressure (MPa)				Composition (-)			Composition Derivatives	
	$\bar{T}$ (K)	$\bar{p}$ (MPa)	x_{CO_2} (-)	$s(T)$	$s(\bar{T})$	$u(T)$	$u_c(\bar{T})$	$s(p)$	$s(\bar{p})$	$u(p)$	$u_c(\bar{p})$	$u(x_{CO_2})$	$u_{tot}(x_{CO_2})$	$x_{CO_2,calc}$	$\frac{\partial x_{CO_2}}{\partial T}$ (K^{-1})	$\frac{\partial x_{CO_2}}{\partial p}$ (MPa^{-1})
	298.142	7.6886	0.94020	4.1e-4	5.0e-5	1.8e-3	1.8e-3	1.2e-4	7.2e-6	1.1e-3	1.1e-3	8.9e-5	1.9e-4	0.94085	0.00867^{+}	-0.15100
	298.141	7.6886	0.94015	4.4e-4	1.2e-4	1.8e-3	1.8e-3	1.1e-4	6.9e-6	1.1e-3	1.1e-3	8.9e-5	1.9e-4	0.94084	0.00867^{+}	-0.15100
L23	298.142	7.6938	0.93929	4.2e-4	1.4e-4	1.7e-3	1.7e-3	1.3e-4	7.5e-6	1.1e-3	1.1e-3	8.9e-5	1.2e-4	0.94046	0.00707^{+}	-0.07564
	298.142	7.6938	0.93926	4.1e-4	1.0e-4	1.8e-3	1.8e-3	1.1e-4	8.2e-6	1.1e-3	1.1e-3	8.9e-5	1.2e-4	0.94046	0.00707^{+}	-0.07564
	298.142	7.6938	0.93926	4.2e-4	1.6e-4	1.8e-3	1.8e-3	1.3e-4	1.2e-5	1.1e-3	1.1e-3	8.9e-5	1.2e-4	0.94046	0.00707^{+}	-0.07564
	298.142	7.6938	0.93919	5.0e-4	7.5e-5	1.8e-3	1.8e-3	1.2e-4	1.0e-5	1.1e-3	1.1e-3	8.9e-5	1.2e-4	0.94046	0.00707^{+}	-0.07564
	298.142	7.6938	0.93921	3.8e-4	9.7e-5	1.8e-3	1.8e-3	1.3e-4	9.9e-6	1.1e-3	1.1e-3	8.9e-5	1.2e-4	0.94046	0.00707^{+}	-0.07564
L24	298.142	7.6978	0.93836	3.7e-4	6.3e-5	1.7e-3	1.7e-3	1.1e-4	5.5e-6	1.1e-3	1.1e-3	8.9e-5	1.3e-4	0.94015	0.00707^{+}	-0.07626
	298.141	7.6977	0.93834	5.0e-4	8.1e-5	1.7e-3	1.7e-3	1.4e-4	1.1e-5	1.1e-3	1.1e-3	8.9e-5	1.3e-4	0.94015	0.00707^{+}	-0.07626
	298.140	7.6977	0.93836	3.7e-4	4.6e-5	1.8e-3	1.8e-3	1.1e-4	7.1e-6	1.1e-3	1.1e-3	8.9e-5	1.3e-4	0.94015	0.00707^{+}	-0.07626
	298.142	7.6978	0.93833	8.2e-4	1.3e-4	1.8e-3	1.8e-3	1.3e-4	2.4e-5	1.1e-3	1.1e-3	8.9e-5	1.3e-4	0.94015	0.00707^{+}	-0.07626
	298.140	7.6978	0.93835	9.0e-4	2.5e-4	1.8e-3	1.8e-3	1.4e-4	1.2e-5	1.1e-3	1.1e-3	8.9e-5	1.3e-4	0.94014	0.00707^{+}	-0.07626
P3	303.144	7.2121	0.99999	4.2e-4	3.9e-5	2.4e-3	2.4e-3	1.1e-4	1.1e-5	1.2e-3	1.2e-3					
L25	303.144	7.2623	0.99790	5.6e-4	9.3e-5	2.3e-3	2.3e-3	1.0e-4	5.3e-6	1.1e-3	1.1e-3	8.9e-5	1.0e-4	0.99778	0.00664	-0.04231
	303.145	7.2624	0.99791	4.5e-4	1.1e-4	2.5e-3	2.5e-3	1.1e-4	1.4e-5	1.1e-3	1.1e-3	8.9e-5	1.0e-4	0.99779	0.00664	-0.04231
	303.144	7.2625	0.99791	5.5e-4	5.3e-5	2.4e-3	2.4e-3	1.3e-4	2.8e-5	1.1e-3	1.1e-3	8.9e-5	1.0e-4	0.99778	0.00664	-0.04231
	303.144	7.2625	0.99791	9.6e-4	2.0e-4	2.4e-3	2.4e-3	1.1e-4	1.1e-5	1.1e-3	1.1e-3	8.9e-5	1.0e-4	0.99778	0.00664	-0.04231
	303.143	7.2625	0.99790	1.1e-3	1.9e-4	2.1e-3	2.1e-3	1.2e-4	1.8e-5	1.1e-3	1.1e-3	8.9e-5	1.0e-4	0.99777	0.00664	-0.04231
L26	303.146	7.3064	0.99600	1.8e-3	3.8e-4	2.3e-3	2.4e-3	2.8e-4	5.6e-5	1.1e-3	1.1e-3	8.9e-5	1.0e-4	0.99589	0.00677	-0.04421
	303.144	7.3061	0.99600	1.0e-3	3.2e-4	2.4e-3	2.4e-3	1.5e-4	4.9e-5	1.1e-3	1.1e-3	8.9e-5	1.0e-4	0.99589	0.00677	-0.04421
	303.146	7.3065	0.99600	2.0e-3	7.0e-4	2.4e-3	2.5e-3	2.3e-4	6.9e-5	1.1e-3	1.1e-3	8.9e-5	1.0e-4	0.99589	0.00677	-0.04421
	303.144	7.3063	0.99599	5.9e-4	1.2e-4	2.4e-3	2.4e-3	1.1e-4	9.9e-6	1.1e-3	1.1e-3	8.9e-5	1.0e-4	0.99588	0.00677	-0.04421
L27	303.144	7.3612	0.99350	5.4e-4	1.4e-4	2.4e-3	2.4e-3	1.4e-4	4.0e-5	1.1e-3	1.1e-3	8.9e-5	1.1e-4	0.99338	0.00693	-0.04720
	303.144	7.3611	0.99350	4.9e-4	1.3e-4	2.5e-3	2.5e-3	1.1e-4	5.7e-6	1.1e-3	1.1e-3	8.9e-5	1.1e-4	0.99338	0.00693	-0.04720
	303.142	7.3611	0.99350	1.3e-3	4.4e-4	2.5e-3	2.5e-3	1.1e-4	1.4e-5	1.1e-3	1.1e-3	8.9e-5	1.1e-4	0.99337	0.00693	-0.04720
	303.144	7.3610	0.99350	5.4e-4	9.7e-5	2.3e-3	2.3e-3	1.1e-4	5.6e-6	1.1e-3	1.1e-3	8.9e-5	1.0e-4	0.99339	0.00693	-0.04720
	303.143	7.3609	0.99350	1.4e-3	3.0e-4	2.3e-3	2.3e-3	1.0e-4	4.8e-6	1.1e-3	1.1e-3	8.9e-5	1.0e-4	0.99338	0.00693	-0.04720

ID	Data			Temperature (K)				Pressure (MPa)				Composition (-)			Composition Derivatives	
	$\bar{T}$ (K)	$\bar{p}$ (MPa)	x_{CO_2} (-)	$s(T)$	$s(\bar{T})$	$u(T)$	$u_c(\bar{T})$	$s(p)$	$s(\bar{p})$	$u(p)$	$u_c(\bar{p})$	$u(x_{CO_2})$	$u_{tot}(x_{CO_2})$	$x_{CO_2,calc}$	$\frac{\partial x_{CO_2}}{\partial T}$ (K^{-1})	$\frac{\partial x_{CO_2}}{\partial p}$ (MPa^{-1})
L28	303.145	7.4156	0.99073	5.8e-4	9.1e-5	2.5e-3	2.5e-3	9.5e-5	1.6e-5	1.1e-3	1.1e-3	8.9e-5	1.1e-4	0.99071	0.00443	-0.05300
	303.144	7.4156	0.99073	5.8e-4	1.2e-4	2.4e-3	2.4e-3	8.9e-5	1.2e-5	1.1e-3	1.1e-3	8.9e-5	1.1e-4	0.99070	0.00443	-0.05300
	303.144	7.4157	0.99073	7.4e-4	2.8e-4	2.6e-3	2.6e-3	8.3e-5	8.1e-6	1.1e-3	1.1e-3	8.9e-5	1.1e-4	0.99069	0.00443	-0.05300
	303.144	7.4157	0.99073	6.4e-4	1.2e-4	2.5e-3	2.5e-3	8.9e-5	6.0e-6	1.1e-3	1.1e-3	8.9e-5	1.1e-4	0.99069	0.00443	-0.05300
	303.142	7.4156	0.99072	9.5e-4	8.3e-5	2.5e-3	2.5e-3	9.6e-5	1.9e-5	1.1e-3	1.1e-3	8.9e-5	1.1e-4	0.99069	0.00443	-0.05300
L29	303.145	7.4257	0.99012	6.5e-4	1.1e-4	2.6e-3	2.6e-3	1.1e-4	1.4e-5	1.1e-3	1.1e-3	8.9e-5	1.1e-4	0.99018	-0.00109^{+}	-0.06400
	303.145	7.4256	0.99012	5.5e-4	1.0e-4	2.5e-3	2.5e-3	1.0e-4	8.9e-6	1.1e-3	1.1e-3	8.9e-5	1.1e-4	0.99019	-0.00109^{+}	-0.06400
	303.145	7.4256	0.99009	4.5e-4	4.6e-5	2.4e-3	2.4e-3	9.5e-5	1.0e-5	1.1e-3	1.1e-3	8.9e-5	1.1e-4	0.99019	-0.00109^{+}	-0.06400
	303.145	7.4256	0.99008	5.6e-4	1.1e-4	2.5e-3	2.5e-3	1.1e-4	6.6e-6	1.1e-3	1.1e-3	8.9e-5	1.1e-4	0.99019	-0.00109^{+}	-0.06400
	303.145	7.4255	0.99003	6.5e-4	2.4e-4	2.6e-3	2.6e-3	9.0e-5	2.7e-6	1.1e-3	1.1e-3	8.9e-5	1.1e-4	0.99019	-0.00109^{+}	-0.06400
L30	303.145	7.4291	0.98987	5.0e-4	1.4e-4	2.6e-3	2.6e-3	9.5e-5	7.4e-6	1.1e-3	1.1e-3	8.9e-5	1.2e-4	0.99000	0.00576^{+}	-0.07500
	303.145	7.4290	0.98987	9.4e-4	2.3e-4	2.5e-3	2.5e-3	1.0e-4	1.4e-5	1.1e-3	1.1e-3	8.9e-5	1.2e-4	0.99001	0.00576^{+}	-0.07500
	303.145	7.4289	0.98988	5.1e-4	1.0e-4	2.7e-3	2.7e-3	9.9e-5	1.3e-5	1.1e-3	1.1e-3	8.9e-5	1.2e-4	0.99001	0.00576^{+}	-0.07500
	303.145	7.4289	0.98988	7.1e-4	1.3e-4	2.6e-3	2.6e-3	1.1e-4	7.3e-6	1.1e-3	1.1e-3	8.9e-5	1.2e-4	0.99001	0.00576^{+}	-0.07500
	303.145	7.4289	0.98988	3.7e-4	3.4e-5	2.6e-3	2.6e-3	1.0e-4	5.5e-6	1.1e-3	1.1e-3	8.9e-5	1.2e-4	0.99001	0.00576^{+}	-0.07500
L31	303.145	7.4306	0.98973	5.6e-4	1.5e-4	2.5e-3	2.5e-3	1.0e-4	9.4e-6	1.1e-3	1.1e-3	8.9e-5	1.3e-4	0.98992	0.00596^{+}	-0.08400
	303.145	7.4307	0.98975	4.6e-4	1.9e-5	2.6e-3	2.6e-3	1.0e-4	1.4e-5	1.1e-3	1.1e-3	8.9e-5	1.3e-4	0.98992	0.00596^{+}	-0.08400
	303.145	7.4306	0.98975	4.8e-4	6.4e-5	2.6e-3	2.6e-3	9.5e-5	6.7e-6	1.1e-3	1.1e-3	8.9e-5	1.3e-4	0.98992	0.00596^{+}	-0.08400
	303.145	7.4306	0.98975	4.8e-4	6.0e-5	2.6e-3	2.6e-3	9.9e-5	1.8e-5	1.1e-3	1.1e-3	8.9e-5	1.3e-4	0.98992	0.00596^{+}	-0.08400
	303.145	7.4306	0.98975	2.7e-4	3.1e-5	2.5e-3	2.5e-3	1.2e-4	3.7e-5	1.1e-3	1.1e-3	8.9e-5	1.3e-4	0.98992	0.00596^{+}	-0.08400
L32	303.145	7.4320	0.98962	4.8e-4	9.5e-5	2.6e-3	2.6e-3	1.0e-4	6.0e-6	1.1e-3	1.1e-3	8.9e-5	1.4e-4	0.98985	-0.00856^{+}	-0.09700
	303.145	7.4318	0.98962	5.4e-4	1.2e-4	2.4e-3	2.5e-3	1.3e-4	2.0e-5	1.1e-3	1.1e-3	8.9e-5	1.4e-4	0.98986	-0.00856^{+}	-0.09700
	303.145	7.4319	0.98963	2.8e-4	4.0e-5	2.6e-3	2.6e-3	9.9e-5	9.2e-6	1.1e-3	1.1e-3	8.9e-5	1.4e-4	0.98985	-0.00856^{+}	-0.09700
	303.145	7.4318	0.98964	4.2e-4	8.0e-5	2.4e-3	2.4e-3	8.7e-5	4.1e-6	1.1e-3	1.1e-3	8.9e-5	1.4e-4	0.98986	-0.00856^{+}	-0.09700
	303.144	7.4317	0.98964	3.5e-4	5.6e-5	2.5e-3	2.5e-3	1.0e-4	1.5e-5	1.1e-3	1.1e-3	8.9e-5	1.4e-4	0.98985	-0.00856^{+}	-0.09700
L33	303.144	7.4331	0.98948	1.0e-3	4.3e-4	2.5e-3	2.6e-3	1.1e-4	1.6e-5	1.1e-3	1.1e-3	8.9e-5	1.7e-4	0.98978	0.01910^{+}	-0.12400
	303.145	7.4331	0.98949	4.4e-4	5.7e-5	2.6e-3	2.6e-3	1.0e-4	1.9e-5	1.1e-3	1.1e-3	8.9e-5	1.7e-4	0.98979	0.01910^{+}	-0.12400

ID	Data			Temperature (K)				Pressure (MPa)				Composition (-)			Composition Derivatives	
	$\bar{T}$ (K)	$\bar{p}$ (MPa)	x_{CO_2} (-)	$s(T)$	$s(\bar{T})$	$u(T)$	$u_c(\bar{T})$	$s(p)$	$s(\bar{p})$	$u(p)$	$u_c(\bar{p})$	$u(x_{CO_2})$	$u_{tot}(x_{CO_2})$	$x_{CO_2,calc}$	$\frac{\partial x_{CO_2}}{\partial T}$ (K^{-1})	$\frac{\partial x_{CO_2}}{\partial p}$ (MPa^{-1})
	303.145	7.4331	0.98951	4.3e-4	1.2e-4	2.6e-3	2.7e-3	1.1e-4	9.8e-6	1.1e-3	1.1e-3	8.9e-5	1.7e-4	0.98979	0.01910[+]	-0.12400
	303.145	7.4331	0.98950	3.7e-4	3.4e-5	2.5e-3	2.5e-3	9.7e-5	8.4e-6	1.1e-3	1.1e-3	8.9e-5	1.7e-4	0.98979	0.01910[+]	-0.12400
	303.145	7.4330	0.98950	6.3e-4	1.4e-4	2.6e-3	2.6e-3	1.1e-4	2.5e-5	1.1e-3	1.1e-3	8.9e-5	1.7e-4	0.98979	0.01910[+]	-0.12400
L34	303.144	7.4343	0.98929	7.2e-4	1.3e-4	2.4e-3	2.4e-3	1.0e-4	5.1e-6	1.1e-3	1.1e-3	8.9e-5	2.3e-4	0.98971	0.01428[+]	-0.19100
	303.144	7.4341	0.98933	9.7e-4	1.6e-4	2.5e-3	2.5e-3	1.3e-4	3.2e-5	1.1e-3	1.1e-3	8.9e-5	2.3e-4	0.98973	0.01428[+]	-0.19100
	303.144	7.4340	0.98933	4.3e-4	4.3e-5	2.5e-3	2.5e-3	1.1e-4	1.4e-5	1.1e-3	1.1e-3	8.9e-5	2.4e-4	0.98973	0.01428[+]	-0.19100
	303.145	7.4341	0.98935	4.4e-4	5.9e-5	2.5e-3	2.5e-3	9.0e-5	8.9e-6	1.1e-3	1.1e-3	8.9e-5	2.4e-4	0.98973	0.01428[+]	-0.19100
	303.144	7.4341	0.98935	8.8e-4	1.4e-4	2.4e-3	2.4e-3	1.3e-4	2.0e-5	1.1e-3	1.1e-3	8.9e-5	2.3e-4	0.98973	0.01428[+]	-0.19100

[+] The derivatives $\frac{\partial x_{CO_2}}{\partial p}$ used in Eq. (5) to obtain $\bar{u}_{tot}(x_{CO_2})$ were calculated using the scaling law in Eq. (6) with the parameters in Table 4 instead of the UMR-PRU fitted model.

Table S.2: Experimental VLE data for the vapor phase of CO_2/CH_4 mixture at mean temperature, $\bar{T}$, mean pressure, $\bar{p}$, and sample liquid phase mole fraction, y_{CO_2}.

ID	Data			Temperature (K)				Pressure (MPa)				Composition (-)			Composition Derivatives	
	$\bar{T}$ (K)	$\bar{p}$ (MPa)	y_{CO_2} (-)	$s(T)$	$s(\bar{T})$	$u(T)$	$u_c(\bar{T})$	$s(p)$	$s(\bar{p})$	$u(p)$	$u_c(\bar{p})$	$u(y_{CO_2})$	$u_{tot}(y_{CO_2})$	$y_{CO_2,calc}$	$\frac{\partial y_{CO_2}}{\partial T}$ (K^{-1})	$\frac{\partial y_{CO_2}}{\partial p}$ (MPa^{-1})
P1	293.130	5.7273	0.99999	1.3e-3	1.1e-4	1.1e-3	1.1e-3	1.3e-4	1.6e-5	1.2e-3	1.2e-3					
V1	293.128	6.1347	0.96047	1.4e-3	4.7e-4	1.0e-3	1.1e-3	8.9e-5	1.2e-5	1.1e-3	1.1e-3	8.9e-5	1.3e-4	0.96183	0.00669	-0.08730
	293.130	6.1346	0.96038	1.2e-3	2.7e-4	1.0e-3	1.1e-3	1.0e-4	1.1e-5	1.1e-3	1.1e-3	8.9e-5	1.3e-4	0.96187	0.00669	-0.08730
	293.128	6.1346	0.96028	1.7e-3	6.4e-4	1.1e-3	1.3e-3	9.9e-5	1.3e-5	1.1e-3	1.1e-3	8.9e-5	1.3e-4	0.96184	0.00669	-0.08730
	293.130	6.1345	0.96026	8.3e-4	1.3e-4	1.2e-3	1.2e-3	1.1e-4	1.6e-5	1.1e-3	1.1e-3	8.9e-5	1.3e-4	0.96188	0.00669	-0.08730
	293.129	6.1345	0.96027	1.1e-3	4.2e-4	1.2e-3	1.2e-3	9.5e-5	1.7e-5	1.1e-3	1.1e-3	8.9e-5	1.3e-4	0.96186	0.00669	-0.08730
	293.130	6.1344	0.96028	1.6e-3	4.2e-4	1.2e-3	1.3e-3	1.1e-4	8.8e-6	1.1e-3	1.1e-3	8.9e-5	1.3e-4	0.96189	0.00669	-0.08730
V2	293.130	6.6458	0.91974	1.2e-3	1.4e-4	1.4e-3	1.4e-3	8.3e-5	4.3e-6	1.1e-3	1.1e-3	8.9e-5	1.2e-4	0.92146	0.01289	-0.07090
	293.130	6.6458	0.91971	1.5e-3	3.1e-4	1.3e-3	1.4e-3	8.7e-5	6.6e-6	1.1e-3	1.1e-3	8.9e-5	1.2e-4	0.92146	0.01289	-0.07090
	293.129	6.6458	0.91970	3.3e-3	6.7e-4	1.4e-3	1.5e-3	9.1e-5	1.2e-5	1.1e-3	1.1e-3	8.9e-5	1.2e-4	0.92145	0.01289	-0.07090
	293.130	6.6457	0.91971	1.6e-3	1.8e-4	1.3e-3	1.3e-3	9.1e-5	7.7e-6	1.1e-3	1.1e-3	8.9e-5	1.2e-4	0.92147	0.01289	-0.07090
	293.131	6.6458	0.91971	1.5e-3	2.2e-4	1.2e-3	1.2e-3	9.2e-5	9.5e-6	1.1e-3	1.1e-3	8.9e-5	1.2e-4	0.92147	0.01289	-0.07090
V3	293.130	6.8401	0.90680	1.4e-3	2.6e-4	1.3e-3	1.3e-3	1.5e-4	1.5e-5	1.1e-3	1.1e-3	8.9e-5	1.2e-4	0.90828	0.01269	-0.06470
	293.128	6.8401	0.90679	2.6e-3	6.8e-4	2.1e-3	2.2e-3	9.7e-5	7.9e-6	1.1e-3	1.1e-3	8.9e-5	1.2e-4	0.90826	0.01269	-0.06470
	293.129	6.8401	0.90679	2.9e-3	5.2e-4	1.4e-3	1.4e-3	1.0e-4	1.5e-5	1.1e-3	1.1e-3	8.9e-5	1.2e-4	0.90827	0.01269	-0.06470
	293.131	6.8402	0.90680	1.1e-3	1.4e-4	1.2e-3	1.2e-3	1.2e-4	1.2e-5	1.1e-3	1.1e-3	8.9e-5	1.2e-4	0.90829	0.01269	-0.06470
	293.128	6.8401	0.90680	1.8e-3	4.9e-4	1.2e-3	1.3e-3	1.2e-4	1.1e-5	1.1e-3	1.1e-3	8.9e-5	1.2e-4	0.90826	0.01269	-0.06470
	293.130	6.8401	0.90676	1.2e-3	1.7e-4	1.2e-3	1.2e-3	1.5e-4	3.0e-5	1.1e-3	1.1e-3	8.9e-5	1.2e-4	0.90828	0.01269	-0.06470
V4	293.130	6.9755	0.89872	1.4e-3	1.9e-4	1.2e-3	1.2e-3	1.2e-4	2.6e-5	1.1e-3	1.1e-3	8.9e-5	1.1e-4	0.89981	0.01254	-0.06040
	293.130	6.9755	0.89867	9.4e-4	1.4e-4	1.1e-3	1.1e-3	1.3e-4	2.4e-5	1.1e-3	1.1e-3	8.9e-5	1.1e-4	0.89981	0.01254	-0.06040
	293.131	6.9755	0.89864	1.1e-3	1.9e-4	1.1e-3	1.2e-3	1.5e-4	2.7e-5	1.1e-3	1.1e-3	8.9e-5	1.1e-4	0.89982	0.01254	-0.06040
	293.131	6.9755	0.89860	9.0e-4	1.4e-4	1.0e-3	1.0e-3	1.9e-4	2.5e-5	1.1e-3	1.1e-3	8.9e-5	1.1e-4	0.89982	0.01254	-0.06040
	293.130	6.9755	0.89861	9.2e-4	1.7e-4	1.1e-3	1.1e-3	1.3e-4	9.6e-6	1.1e-3	1.1e-3	8.9e-5	1.1e-4	0.89981	0.01254	-0.06040
	293.130	6.9755	0.89861	9.0e-4	2.4e-4	1.0e-3	1.1e-3	1.2e-4	9.1e-6	1.1e-3	1.1e-3	8.9e-5	1.1e-4	0.89981	0.01254	-0.06040

ID	Data			Temperature (K)				Pressure (MPa)				Composition (-)			Composition Derivatives	
	$\bar{T}$ (K)	$\bar{p}$ (MPa)	y_{CO_2} (-)	$s(T)$	$s(\bar{T})$	$u(T)$	$u_c(\bar{T})$	$s(p)$	$s(\bar{p})$	$u(p)$	$u_c(\bar{p})$	$u(y_{CO_2})$	$u_{tot}(y_{CO_2})$	$y_{CO_2,calc}$	$\frac{\partial y_{CO_2}}{\partial T}$ (K^{-1})	$\frac{\partial y_{CO_2}}{\partial p}$ (MPa^{-1})
V5	293.129	7.1184	0.89084	2.4e-3	1.0e-3	1.1e-3	1.5e-3	1.2e-4	1.0e-5	1.1e-3	1.1e-3	8.9e-5	1.1e-4	0.89149	0.01239	-0.05570
	293.128	7.1183	0.89072	1.2e-3	3.5e-4	1.1e-3	1.2e-3	1.2e-4	9.4e-6	1.1e-3	1.1e-3	8.9e-5	1.1e-4	0.89149	0.01239	-0.05570
	293.130	7.1183	0.89071	1.2e-3	1.7e-4	1.1e-3	1.1e-3	1.3e-4	1.7e-5	1.1e-3	1.1e-3	8.9e-5	1.1e-4	0.89151	0.01239	-0.05570
	293.130	7.1184	0.89068	9.3e-4	1.7e-4	1.1e-3	1.1e-3	1.2e-4	1.2e-5	1.1e-3	1.1e-3	8.9e-5	1.1e-4	0.89151	0.01239	-0.05570
	293.129	7.1182	0.89067	1.1e-3	3.5e-4	1.1e-3	1.2e-3	1.4e-4	3.2e-5	1.1e-3	1.1e-3	8.9e-5	1.1e-4	0.89151	0.01239	-0.05570
	293.130	7.1183	0.89067	6.8e-4	1.2e-4	1.1e-3	1.1e-3	1.2e-4	1.8e-5	1.1e-3	1.1e-3	8.9e-5	1.1e-4	0.89151	0.01239	-0.05570
V6	293.129	7.3508	0.87991	1.1e-3	2.4e-4	1.1e-3	1.2e-3	1.3e-4	1.2e-5	1.1e-3	1.1e-3	8.9e-5	1.1e-4	0.87947	0.01214	-0.04760
	293.129	7.3509	0.87986	1.0e-3	2.5e-4	1.3e-3	1.3e-3	1.2e-4	1.1e-5	1.1e-3	1.1e-3	8.9e-5	1.1e-4	0.87947	0.01214	-0.04760
	293.128	7.3508	0.87976	1.2e-3	3.8e-4	1.2e-3	1.2e-3	1.5e-4	2.4e-5	1.1e-3	1.1e-3	8.9e-5	1.1e-4	0.87946	0.01214	-0.04760
	293.130	7.3508	0.87974	1.1e-3	1.7e-4	1.2e-3	1.2e-3	1.2e-4	1.5e-5	1.1e-3	1.1e-3	8.9e-5	1.1e-4	0.87948	0.01214	-0.04760
	293.130	7.3508	0.87978	1.1e-3	2.4e-4	1.1e-3	1.2e-3	1.2e-4	1.3e-5	1.1e-3	1.1e-3	8.9e-5	1.1e-4	0.87948	0.01214	-0.04760
	293.130	7.3508	0.87977	8.8e-4	1.7e-4	1.1e-3	1.2e-3	1.3e-4	1.7e-5	1.1e-3	1.1e-3	8.9e-5	1.1e-4	0.87948	0.01214	-0.04760
V7	293.130	7.5758	0.87196	1.3e-3	1.9e-4	1.2e-3	1.2e-3	1.3e-4	1.6e-5	1.1e-3	1.1e-3	8.9e-5	1.0e-4	0.86979	0.01193	-0.03820
	293.130	7.5758	0.87194	8.4e-4	9.5e-5	1.3e-3	1.3e-3	1.3e-4	1.3e-5	1.1e-3	1.1e-3	8.9e-5	1.0e-4	0.86979	0.01193	-0.03820
	293.130	7.5758	0.87190	7.6e-4	7.5e-5	1.2e-3	1.2e-3	1.3e-4	1.4e-5	1.1e-3	1.1e-3	8.9e-5	1.0e-4	0.86979	0.01193	-0.03820
	293.129	7.5758	0.87189	1.4e-3	2.8e-4	1.2e-3	1.2e-3	1.2e-4	9.0e-6	1.1e-3	1.1e-3	8.9e-5	1.0e-4	0.86978	0.01193	-0.03820
	293.130	7.5758	0.87184	1.1e-3	1.6e-4	1.2e-3	1.2e-3	1.1e-4	1.2e-5	1.1e-3	1.1e-3	8.9e-5	1.0e-4	0.86979	0.01193	-0.03820
	293.129	7.5758	0.87182	1.5e-3	4.2e-4	1.2e-3	1.3e-3	1.3e-4	2.6e-5	1.1e-3	1.1e-3	8.9e-5	1.0e-4	0.86978	0.01193	-0.03820
V8	293.130	7.7961	0.86866	1.5e-3	4.2e-4	1.1e-3	1.2e-3	1.2e-4	2.0e-5	1.2e-3	1.2e-3	8.9e-5	9.5e-5	0.86268	0.01179	-0.02530
	293.131	7.7961	0.86866	6.5e-4	9.2e-5	1.2e-3	1.2e-3	1.2e-4	1.2e-5	1.1e-3	1.1e-3	8.9e-5	9.5e-5	0.86269	0.01179	-0.02530
	293.131	7.7961	0.86866	5.3e-4	9.1e-5	1.1e-3	1.1e-3	1.3e-4	1.6e-5	1.1e-3	1.1e-3	8.9e-5	9.5e-5	0.86269	0.01179	-0.02530
	293.130	7.7961	0.86865	7.0e-4	9.1e-5	1.1e-3	1.1e-3	1.2e-4	9.2e-6	1.1e-3	1.1e-3	8.9e-5	9.5e-5	0.86268	0.01179	-0.02530
	293.130	7.7961	0.86868	4.1e-4	1.0e-4	1.2e-3	1.2e-3	1.2e-4	1.1e-5	1.1e-3	1.1e-3	8.9e-5	9.5e-5	0.86268	0.01179	-0.02530
	293.131	7.7961	0.86862	7.4e-4	2.4e-4	1.0e-3	1.1e-3	1.3e-4	2.0e-5	1.1e-3	1.1e-3	8.9e-5	9.5e-5	0.86269	0.01179	-0.02530
V9	293.130	7.9091	0.87301	1.4e-3	2.8e-4	1.1e-3	1.1e-3	1.1e-4	1.3e-5	1.2e-3	1.2e-3	8.9e-5	1.8e-4	0.86039	-0.05839^{+}	0.12100
	293.130	7.9091	0.87304	1.6e-3	5.7e-4	1.2e-3	1.3e-3	1.2e-4	1.6e-5	1.2e-3	1.2e-3	8.9e-5	1.8e-4	0.86039	-0.05839^{+}	0.12100
	293.130	7.9091	0.87303	6.2e-4	1.3e-4	1.0e-3	1.0e-3	1.2e-4	2.5e-5	1.2e-3	1.2e-3	8.9e-5	1.8e-4	0.86039	-0.05839^{+}	0.12100

ID	Data			Temperature (K)				Pressure (MPa)				Composition (-)			Composition Derivatives	
	$\bar{T}$ (K)	$\bar{p}$ (MPa)	y_{CO_2} (-)	$s(T)$	$s(\bar{T})$	$u(T)$	$u_c(\bar{T})$	$s(p)$	$s(\bar{p})$	$u(p)$	$u_c(\bar{p})$	$u(y_{CO_2})$	$u_{tot}(y_{CO_2})$	$y_{CO_2,calc}$	$\frac{\partial y_{CO_2}}{\partial T}$ (K^{-1})	$\frac{\partial y_{CO_2}}{\partial p}$ (MPa^{-1})
	293.130	7.9091	0.87299	7.1e-4	1.3e-4	1.1e-3	1.1e-3	1.1e-4	9.7e-6	1.2e-3	1.2e-3	8.9e-5	1.8e-4	0.86039	-0.05839^{+}	0.12100
	293.130	7.9091	0.87302	5.6e-4	9.1e-5	1.1e-3	1.1e-3	1.1e-4	1.5e-5	1.2e-3	1.2e-3	8.9e-5	1.8e-4	0.86039	-0.05839^{+}	0.12100
	293.130	7.9091	0.87305	1.4e-3	2.4e-4	1.1e-3	1.1e-3	1.3e-4	1.0e-5	1.2e-3	1.2e-3	8.9e-5	1.8e-4	0.86039	-0.05839^{+}	0.12100
V10	293.130	7.9135	0.87361	6.1e-4	1.7e-4	1.0e-3	1.0e-3	1.4e-4	3.4e-5	1.2e-3	1.2e-3	8.9e-5	1.9e-4	0.86033	0.01785^{+}	0.14140
	293.130	7.9135	0.87358	6.9e-4	9.0e-5	1.1e-3	1.1e-3	1.1e-4	1.4e-5	1.2e-3	1.2e-3	8.9e-5	1.9e-4	0.86033	0.01785^{+}	0.14140
	293.130	7.9135	0.87362	5.6e-4	1.6e-4	1.0e-3	1.0e-3	1.3e-4	3.1e-5	1.2e-3	1.2e-3	8.9e-5	1.9e-4	0.86033	0.01785^{+}	0.14140
	293.130	7.9135	0.87360	9.6e-4	1.8e-4	1.1e-3	1.1e-3	1.1e-4	9.8e-6	1.2e-3	1.2e-3	8.9e-5	1.9e-4	0.86033	0.01785^{+}	0.14140
	293.130	7.9135	0.87361	5.2e-4	1.2e-4	1.1e-3	1.1e-3	1.3e-4	1.5e-5	1.2e-3	1.2e-3	8.9e-5	1.9e-4	0.86033	0.01785^{+}	0.14140
V11	293.128	7.9179	0.87424	2.1e-3	7.5e-4	1.1e-3	1.3e-3	1.2e-4	2.1e-5	1.2e-3	1.2e-3	8.9e-5	2.2e-4	0.86025	-0.00054^{+}	0.17170
	293.130	7.9179	0.87423	9.5e-4	2.5e-4	1.1e-3	1.1e-3	1.1e-4	1.5e-5	1.2e-3	1.2e-3	8.9e-5	2.2e-4	0.86027	-0.00054^{+}	0.17170
	293.128	7.9179	0.87423	1.8e-3	5.6e-4	1.2e-3	1.3e-3	1.1e-4	2.4e-5	1.2e-3	1.2e-3	8.9e-5	2.2e-4	0.86025	-0.00054^{+}	0.17170
	293.128	7.9179	0.87429	1.7e-3	3.7e-4	1.1e-3	1.1e-3	1.2e-4	8.8e-6	1.2e-3	1.2e-3	8.9e-5	2.2e-4	0.86025	-0.00054^{+}	0.17170
	293.128	7.9179	0.87423	1.6e-3	5.9e-4	1.1e-3	1.3e-3	1.2e-4	2.2e-5	1.2e-3	1.2e-3	8.9e-5	2.2e-4	0.86025	-0.00054^{+}	0.17170
	293.128	7.9179	0.87425	2.5e-3	1.1e-3	1.1e-3	1.6e-3	1.2e-4	1.8e-5	1.2e-3	1.2e-3	8.9e-5	2.2e-4	0.86025	-0.00054^{+}	0.17170
V12	293.130	7.9220	0.87497	9.3e-4	1.4e-4	1.2e-3	1.2e-3	1.1e-4	9.3e-6	1.2e-3	1.2e-3	8.9e-5	2.7e-4	0.86022	0.00291^{+}	0.21610
	293.127	7.9219	0.87499	2.4e-3	9.3e-4	1.1e-3	1.5e-3	1.1e-4	6.2e-6	1.2e-3	1.2e-3	8.9e-5	2.7e-4	0.86018	0.00291^{+}	0.21610
	293.130	7.9220	0.87500	5.6e-4	4.9e-5	1.2e-3	1.2e-3	1.1e-4	1.4e-5	1.2e-3	1.2e-3	8.9e-5	2.7e-4	0.86022	0.00291^{+}	0.21610
	293.130	7.9219	0.87501	4.2e-4	4.1e-5	1.1e-3	1.1e-3	1.2e-4	2.5e-5	1.2e-3	1.2e-3	8.9e-5	2.7e-4	0.86022	0.00291^{+}	0.21610
	293.130	7.9219	0.87495	1.2e-3	3.2e-4	1.1e-3	1.1e-3	1.3e-4	1.4e-5	1.2e-3	1.2e-3	8.9e-5	2.7e-4	0.86022	0.00291^{+}	0.21610
	293.130	7.9219	0.87500	5.4e-4	7.8e-5	1.1e-3	1.1e-3	1.1e-4	1.2e-5	1.2e-3	1.2e-3	8.9e-5	2.7e-4	0.86022	0.00291^{+}	0.21610
V13	293.130	7.9266	0.87625	7.2e-4	1.4e-4	1.1e-3	1.1e-3	9.9e-5	1.5e-5	1.2e-3	1.2e-3	8.9e-5	3.8e-4	0.86016	-0.02519^{+}	0.32120
	293.130	7.9267	0.87625	8.2e-4	1.2e-4	1.1e-3	1.1e-3	1.2e-4	1.2e-5	1.2e-3	1.2e-3	8.9e-5	3.8e-4	0.86016	-0.02519^{+}	0.32120
	293.130	7.9266	0.87627	5.4e-4	1.4e-4	1.1e-3	1.1e-3	9.7e-5	9.0e-6	1.2e-3	1.2e-3	8.9e-5	3.8e-4	0.86016	-0.02519^{+}	0.32120
	293.130	7.9266	0.87626	6.1e-4	1.5e-4	1.1e-3	1.1e-3	1.1e-4	1.2e-5	1.2e-3	1.2e-3	8.9e-5	3.8e-4	0.86016	-0.02519^{+}	0.32120
	293.130	7.9267	0.87627	1.1e-3	1.9e-4	1.2e-3	1.2e-3	1.0e-4	1.8e-5	1.2e-3	1.2e-3	8.9e-5	3.8e-4	0.86016	-0.02519^{+}	0.32120
	293.130	7.9266	0.87625	1.0e-3	1.9e-4	1.1e-3	1.1e-3	1.1e-4	1.2e-5	1.2e-3	1.2e-3	8.9e-5	3.8e-4	0.86016	-0.02519^{+}	0.32120
V14	293.129	7.9308	0.87818	1.1e-3	2.3e-4	1.2e-3	1.3e-3	9.4e-5	7.5e-6	1.2e-3	1.2e-3	8.9e-5	7.9e-4	0.86010	-0.06007^{+}	0.67090

ID	Data			Temperature (K)				Pressure (MPa)				Composition (-)			Composition Derivatives	
	$\bar{T}$ (K)	$\bar{p}$ (MPa)	y_{CO_2} (-)	$s(T)$	$s(\bar{T})$	$u(T)$	$u_c(\bar{T})$	$s(p)$	$s(\bar{p})$	$u(p)$	$u_c(\bar{p})$	$u(y_{CO_2})$	$u_{tot}(y_{CO_2})$	$y_{CO_2,calc}$	$\frac{\partial y_{CO_2}}{\partial T}$ (K^{-1})	$\frac{\partial y_{CO_2}}{\partial p}$ (MPa^{-1})
	293.130	7.9308	0.87815	4.8e-4	1.3e-4	1.1e-3	1.1e-3	9.8e-5	7.5e-6	1.2e-3	1.2e-3	8.9e-5	7.9e-4	0.86011	-0.06007^{+}	0.67090
	293.130	7.9308	0.87810	5.6e-4	7.3e-5	1.2e-3	1.2e-3	9.3e-5	3.1e-6	1.2e-3	1.2e-3	8.9e-5	7.9e-4	0.86011	-0.06007^{+}	0.67090
	293.130	7.9308	0.87820	9.5e-4	2.4e-4	1.1e-3	1.2e-3	1.1e-4	1.3e-5	1.2e-3	1.2e-3	8.9e-5	7.9e-4	0.86011	-0.06007^{+}	0.67090
	293.130	7.9308	0.87817	9.0e-4	1.2e-4	1.1e-3	1.1e-3	1.0e-4	1.2e-5	1.2e-3	1.2e-3	8.9e-5	7.9e-4	0.86011	-0.06007^{+}	0.67090
	293.129	7.9308	0.87819	1.0e-3	4.0e-4	1.1e-3	1.2e-3	1.0e-4	8.4e-6	1.2e-3	1.2e-3	8.9e-5	7.9e-4	0.86010	-0.06007^{+}	0.67090
P2	298.141	6.4316	0.99999	6.7e-4	7.6e-5	1.4e-3	1.4e-3	1.0e-4	3.4e-5	1.1e-3	1.1e-3					
V15	298.142	6.6410	0.98298	8.5e-4	2.2e-4	1.9e-3	1.9e-3	1.1e-4	1.6e-5	1.1e-3	1.1e-3	8.9e-5	1.2e-4	0.98448	0.01174	-0.07411
	298.142	6.6410	0.98298	1.2e-3	1.1e-4	1.8e-3	1.8e-3	1.5e-4	1.4e-5	1.1e-3	1.1e-3	8.9e-5	1.2e-4	0.98448	0.01174	-0.07411
	298.142	6.6410	0.98296	1.2e-3	3.7e-4	1.8e-3	1.8e-3	1.6e-4	3.9e-5	1.1e-3	1.1e-3	8.9e-5	1.2e-4	0.98448	0.01174	-0.07411
	298.142	6.6409	0.98296	9.3e-4	2.6e-4	1.8e-3	1.8e-3	1.4e-4	2.9e-5	1.1e-3	1.1e-3	8.9e-5	1.2e-4	0.98448	0.01174	-0.07411
	298.142	6.6410	0.98297	1.0e-3	2.7e-4	1.9e-3	1.9e-3	1.5e-4	2.9e-5	1.1e-3	1.1e-3	8.9e-5	1.2e-4	0.98448	0.01174	-0.07411
	298.142	6.6409	0.98298	1.2e-3	5.0e-4	1.9e-3	1.9e-3	1.3e-4	4.3e-5	1.1e-3	1.1e-3	8.9e-5	1.2e-4	0.98448	0.01174	-0.07411
V16	298.142	6.9755	0.95918	5.1e-4	9.7e-5	1.9e-3	1.9e-3	1.1e-4	8.1e-6	1.1e-3	1.1e-3	8.9e-5	1.2e-4	0.96113	0.01175	-0.06515
	298.141	6.9754	0.95917	8.9e-4	3.1e-4	1.8e-3	1.8e-3	1.1e-4	1.4e-5	1.1e-3	1.1e-3	8.9e-5	1.2e-4	0.96112	0.01175	-0.06515
	298.142	6.9753	0.95917	1.3e-3	4.6e-4	1.8e-3	1.8e-3	1.6e-4	3.5e-5	1.1e-3	1.1e-3	8.9e-5	1.2e-4	0.96114	0.01175	-0.06515
	298.141	6.9754	0.95919	1.4e-3	4.8e-4	1.8e-3	1.9e-3	2.2e-4	6.6e-5	1.1e-3	1.1e-3	8.9e-5	1.2e-4	0.96112	0.01175	-0.06515
	298.141	6.9754	0.95917	9.5e-4	1.5e-4	1.9e-3	1.9e-3	1.7e-4	1.9e-5	1.1e-3	1.1e-3	8.9e-5	1.2e-4	0.96112	0.01175	-0.06515
	298.141	6.9754	0.95917	6.7e-4	1.8e-4	1.7e-3	1.7e-3	1.2e-4	9.9e-6	1.1e-3	1.1e-3	8.9e-5	1.2e-4	0.96112	0.01175	-0.06515
V17	298.142	7.3114	0.93996	5.5e-4	9.7e-5	1.8e-3	1.8e-3	1.1e-4	1.0e-5	1.1e-3	1.1e-3	8.9e-5	1.1e-4	0.94107	0.01160	-0.05374
	298.142	7.3114	0.93992	6.1e-4	1.0e-4	1.9e-3	1.9e-3	1.1e-4	1.8e-5	1.1e-3	1.1e-3	8.9e-5	1.1e-4	0.94107	0.01160	-0.05374
	298.142	7.3114	0.93991	3.9e-4	6.8e-5	1.7e-3	1.7e-3	9.5e-5	1.3e-5	1.1e-3	1.1e-3	8.9e-5	1.1e-4	0.94107	0.01160	-0.05374
	298.142	7.3114	0.93989	5.5e-4	1.9e-4	1.7e-3	1.7e-3	1.0e-4	1.1e-5	1.1e-3	1.1e-3	8.9e-5	1.1e-4	0.94107	0.01160	-0.05374
	298.142	7.3063	0.93994	5.8e-4	1.4e-4	1.9e-3	1.9e-3	1.9e-1	4.1e-3	1.1e-3	4.2e-3	8.9e-5	2.5e-4	0.94135	0.01160	-0.05374
	298.142	7.3114	0.93993	4.7e-4	1.1e-4	1.8e-3	1.8e-3	1.3e-4	2.3e-5	1.1e-3	1.1e-3	8.9e-5	1.1e-4	0.94107	0.01160	-0.05374
V18	298.143	7.5079	0.93183	3.8e-4	3.7e-5	2.0e-3	2.0e-3	1.2e-4	9.1e-6	1.1e-3	1.1e-3	8.9e-5	1.0e-4	0.93140	0.01148	-0.04421
	298.143	7.5078	0.93179	4.9e-4	4.0e-5	1.9e-3	1.9e-3	9.8e-5	8.9e-6	1.1e-3	1.1e-3	8.9e-5	1.0e-4	0.93141	0.01148	-0.04421
	298.143	7.5078	0.93181	6.4e-4	2.1e-4	1.9e-3	1.9e-3	1.2e-4	2.0e-5	1.1e-3	1.1e-3	8.9e-5	1.0e-4	0.93141	0.01148	-0.04421

ID	Data			Temperature (K)				Pressure (MPa)				Composition (-)			Composition Derivatives	
	$\bar{T}$ (K)	$\bar{p}$ (MPa)	y_{CO_2} (-)	$s(T)$	$s(\bar{T})$	$u(T)$	$u_c(\bar{T})$	$s(p)$	$s(\bar{p})$	$u(p)$	$u_c(\bar{p})$	$u(y_{CO_2})$	$u_{tot}(y_{CO_2})$	$y_{CO_2,calc}$	$\frac{\partial y_{CO_2}}{\partial T}$ (K^{-1})	$\frac{\partial y_{CO_2}}{\partial p}$ (MPa^{-1})
	298.143	7.5078	0.93178	5.2e-4	1.3e-4	2.0e-3	2.0e-3	9.7e-5	1.2e-5	1.1e-3	1.1e-3	8.9e-5	1.0e-4	0.93141	0.01148	-0.04421
	298.143	7.5078	0.93178	5.1e-4	9.2e-5	2.0e-3	2.0e-3	9.5e-5	7.4e-6	1.1e-3	1.1e-3	8.9e-5	1.0e-4	0.93141	0.01148	-0.04421
	298.143	7.5078	0.93182	4.2e-4	4.4e-5	2.0e-3	2.0e-3	9.8e-5	6.2e-6	1.1e-3	1.1e-3	8.9e-5	1.0e-4	0.93141	0.01148	-0.04421
V19	298.142	7.6250	0.92918	5.4e-4	1.8e-4	1.8e-3	1.8e-3	1.0e-4	5.4e-6	1.1e-3	1.1e-3	8.9e-5	9.6e-5	0.92669	-0.01910	0.00600
	298.142	7.6251	0.92918	3.7e-4	5.5e-5	1.8e-3	1.8e-3	8.8e-5	9.6e-6	1.1e-3	1.1e-3	8.9e-5	9.6e-5	0.92669	-0.01910	0.00600
	298.142	7.6250	0.92917	4.2e-4	1.1e-4	1.8e-3	1.8e-3	1.0e-4	9.6e-6	1.1e-3	1.1e-3	8.9e-5	9.6e-5	0.92669	-0.01910	0.00600
	298.142	7.6250	0.92917	4.5e-4	8.0e-5	1.8e-3	1.8e-3	1.1e-4	1.7e-5	1.1e-3	1.1e-3	8.9e-5	9.6e-5	0.92669	-0.01910	0.00600
	298.140	7.6250	0.92918	7.7e-4	1.9e-4	1.8e-3	1.8e-3	1.1e-4	9.1e-6	1.1e-3	1.1e-3	8.9e-5	9.6e-5	0.92667	-0.01910	0.00600
	298.142	7.6250	0.92908	6.6e-4	9.7e-5	2.1e-3	2.1e-3	1.1e-4	1.4e-5	1.1e-3	1.1e-3	8.9e-5	9.8e-5	0.92669	-0.01910	0.00600
V20	298.142	7.6599	0.92930	5.4e-4	2.3e-4	1.9e-3	1.9e-3	1.0e-4	2.0e-5	1.1e-3	1.1e-3	8.9e-5	1.1e-4	0.92551	-0.02494	0.02400
	298.142	7.6599	0.92930	4.3e-4	3.6e-5	1.7e-3	1.7e-3	1.1e-4	8.8e-6	1.1e-3	1.1e-3	8.9e-5	1.0e-4	0.92551	-0.02494	0.02400
	298.141	7.6599	0.92929	1.0e-3	3.7e-4	1.7e-3	1.8e-3	1.1e-4	1.1e-5	1.1e-3	1.1e-3	8.9e-5	1.0e-4	0.92550	-0.02494	0.02400
	298.142	7.6599	0.92925	4.5e-4	1.3e-4	1.9e-3	1.9e-3	1.1e-4	1.1e-5	1.1e-3	1.1e-3	8.9e-5	1.1e-4	0.92551	-0.02494	0.02400
	298.142	7.6599	0.92929	6.4e-4	2.2e-4	2.0e-3	2.0e-3	1.2e-4	1.4e-5	1.1e-3	1.1e-3	8.9e-5	1.1e-4	0.92551	-0.02494	0.02400
	298.142	7.6599	0.92924	2.8e-4	5.5e-5	2.0e-3	2.0e-3	1.1e-4	8.8e-6	1.1e-3	1.1e-3	8.9e-5	1.1e-4	0.92551	-0.02494	0.02400
V21	298.142	7.6783	0.92983	3.4e-4	6.2e-5	1.8e-3	1.8e-3	1.1e-4	1.0e-5	1.1e-3	1.1e-3	8.9e-5	1.1e-4	0.92495	0.01176^{+}	0.05000
	298.142	7.6783	0.92975	4.4e-4	1.2e-4	1.7e-3	1.7e-3	9.3e-5	4.4e-6	1.1e-3	1.1e-3	8.9e-5	1.1e-4	0.92495	0.01176^{+}	0.05000
	298.142	7.6783	0.92980	3.7e-4	3.9e-5	1.8e-3	1.8e-3	1.0e-4	8.2e-6	1.1e-3	1.1e-3	8.9e-5	1.1e-4	0.92495	0.01176^{+}	0.05000
	298.140	7.6783	0.92979	6.8e-4	2.3e-4	1.7e-3	1.7e-3	1.0e-4	8.7e-6	1.1e-3	1.1e-3	8.9e-5	1.1e-4	0.92493	0.01176^{+}	0.05000
	298.142	7.6783	0.92974	4.0e-4	6.1e-5	1.7e-3	1.7e-3	1.0e-4	7.5e-6	1.1e-3	1.1e-3	8.9e-5	1.1e-4	0.92495	0.01176^{+}	0.05000
	298.142	7.6783	0.92984	4.8e-4	9.7e-5	1.7e-3	1.7e-3	1.0e-4	4.7e-6	1.1e-3	1.1e-3	8.9e-5	1.1e-4	0.92495	0.01176^{+}	0.05000
V22	298.142	7.6886	0.93047	4.8e-4	5.9e-5	1.8e-3	1.8e-3	9.9e-5	9.3e-6	1.1e-3	1.1e-3	8.9e-5	2.5e-4	0.92466	0.11798^{+}	0.08900
	298.142	7.6886	0.93040	6.5e-4	8.1e-5	1.8e-3	1.8e-3	1.0e-4	1.8e-5	1.1e-3	1.1e-3	8.9e-5	2.5e-4	0.92466	0.11798^{+}	0.08900
	298.142	7.6886	0.93040	4.1e-4	8.3e-5	1.8e-3	1.8e-3	9.5e-5	8.4e-6	1.1e-3	1.1e-3	8.9e-5	2.5e-4	0.92466	0.11798^{+}	0.08900
	298.142	7.6886	0.93046	4.5e-4	9.9e-5	1.6e-3	1.6e-3	1.0e-4	5.4e-6	1.1e-3	1.1e-3	8.9e-5	2.3e-4	0.92466	0.11798^{+}	0.08900
	298.142	7.6886	0.93045	3.9e-4	7.9e-5	1.7e-3	1.7e-3	1.0e-4	1.0e-5	1.1e-3	1.1e-3	8.9e-5	2.4e-4	0.92466	0.11798^{+}	0.08900
	298.142	7.6886	0.93044	4.6e-4	4.5e-5	1.7e-3	1.7e-3	1.1e-4	1.1e-5	1.1e-3	1.1e-3	8.9e-5	2.4e-4	0.92466	0.11798^{+}	0.08900

ID	Data			Temperature (K)				Pressure (MPa)				Composition (-)			Composition Derivatives	
	$\bar{T}$ (K)	$\bar{p}$ (MPa)	y_{CO_2} (-)	$s(T)$	$s(\bar{T})$	$u(T)$	$u_c(\bar{T})$	$s(p)$	$s(\bar{p})$	$u(p)$	$u_c(\bar{p})$	$u(y_{CO_2})$	$u_{tot}(y_{CO_2})$	$y_{CO_2,calc}$	$\frac{\partial y_{CO_2}}{\partial T}$ (K^{-1})	$\frac{\partial y_{CO_2}}{\partial p}$ (MPa^{-1})
V23	298.142	7.6938	0.93103	5.2e-4	7.3e-5	1.8e-3	1.8e-3	9.8e-5	8.9e-6	1.1e-3	1.1e-3	8.9e-5	9.7e-5	0.92451	0.01151$^+$	-0.02707
	298.142	7.6938	0.93103	4.0e-4	8.6e-5	1.6e-3	1.6e-3	1.0e-4	1.0e-5	1.1e-3	1.1e-3	8.9e-5	9.6e-5	0.92451	0.01151$^+$	-0.02707
	298.142	7.6938	0.93105	4.1e-4	6.4e-5	1.7e-3	1.7e-3	1.0e-4	1.6e-5	1.1e-3	1.1e-3	8.9e-5	9.7e-5	0.92451	0.01151$^+$	-0.02707
	298.142	7.6938	0.93104	5.4e-4	1.0e-4	1.8e-3	1.8e-3	1.1e-4	1.8e-5	1.1e-3	1.1e-3	8.9e-5	9.7e-5	0.92451	0.01151$^+$	-0.02707
	298.142	7.6938	0.93100	5.0e-4	3.5e-5	1.8e-3	1.8e-3	3.8e-4	3.6e-5	1.1e-3	1.1e-3	8.9e-5	9.7e-5	0.92451	0.01151$^+$	-0.02707
	298.142	7.6911	0.92999	6.2e-4	7.5e-5	1.9e-3	1.9e-3	1.4e-4	1.7e-5	1.2e-3	1.2e-3	8.9e-5	9.8e-5	0.92459	0.01151$^+$	-0.02707
V24	298.142	7.6977	0.93168	5.2e-4	1.4e-4	1.8e-3	1.8e-3	9.1e-5	1.1e-5	1.1e-3	1.1e-3	8.9e-5	9.7e-5	0.92441	0.01152$^+$	-0.02642
	298.142	7.6977	0.93177	4.3e-4	6.2e-5	1.8e-3	1.8e-3	1.1e-4	4.9e-6	1.1e-3	1.1e-3	8.9e-5	9.7e-5	0.92441	0.01152$^+$	-0.02642
	298.142	7.6977	0.93174	4.2e-4	9.4e-5	1.6e-3	1.6e-3	1.2e-4	1.5e-5	1.1e-3	1.1e-3	8.9e-5	9.6e-5	0.92441	0.01152$^+$	-0.02642
	298.142	7.6977	0.93175	4.5e-4	1.5e-4	1.8e-3	1.8e-3	1.0e-4	1.2e-5	1.1e-3	1.1e-3	8.9e-5	9.7e-5	0.92441	0.01152$^+$	-0.02642
	298.142	7.6978	0.93177	4.4e-4	9.8e-5	1.6e-3	1.6e-3	1.0e-4	1.6e-5	1.1e-3	1.1e-3	8.9e-5	9.6e-5	0.92441	0.01152$^+$	-0.02642
P3	303.144	7.2121	0.99999	4.2e-4	3.9e-5	2.4e-3	2.4e-3	1.1e-4	1.1e-5	1.2e-3	1.2e-3					
V25	303.144	7.2624	0.99694	8.1e-4	1.6e-4	2.4e-3	2.4e-3	1.1e-4	4.6e-6	1.1e-3	1.1e-3	8.9e-5	1.1e-4	0.99697	0.00927	-0.05566
	303.143	7.2625	0.99695	1.3e-3	4.0e-4	2.4e-3	2.4e-3	1.3e-4	1.4e-5	1.1e-3	1.1e-3	8.9e-5	1.1e-4	0.99696	0.00927	-0.05566
	303.144	7.2625	0.99695	5.2e-4	8.2e-5	2.2e-3	2.2e-3	1.3e-4	8.7e-6	1.1e-3	1.1e-3	8.9e-5	1.1e-4	0.99697	0.00927	-0.05566
	303.144	7.2625	0.99695	4.8e-4	5.1e-5	2.4e-3	2.4e-3	1.2e-4	1.4e-5	1.1e-3	1.1e-3	8.9e-5	1.1e-4	0.99697	0.00927	-0.05566
	303.144	7.2625	0.99694	5.8e-4	1.6e-4	2.4e-3	2.4e-3	1.2e-4	7.5e-6	1.1e-3	1.1e-3	8.9e-5	1.1e-4	0.99697	0.00927	-0.05566
	303.144	7.2625	0.99696	6.7e-4	1.1e-4	2.4e-3	2.4e-3	1.3e-4	1.9e-5	1.1e-3	1.1e-3	8.9e-5	1.1e-4	0.99697	0.00927	-0.05566
V26	303.144	7.3064	0.99438	9.0e-4	2.9e-4	2.5e-3	2.5e-3	1.3e-4	1.5e-5	1.1e-3	1.1e-3	8.9e-5	1.1e-4	0.99455	0.00936	-0.05436
	303.145	7.3065	0.99437	5.0e-4	9.9e-5	2.4e-3	2.4e-3	1.1e-4	4.8e-6	1.1e-3	1.1e-3	8.9e-5	1.1e-4	0.99455	0.00936	-0.05436
	303.145	7.3064	0.99437	3.8e-4	5.9e-5	2.4e-3	2.4e-3	1.1e-4	5.6e-6	1.1e-3	1.1e-3	8.9e-5	1.1e-4	0.99456	0.00936	-0.05436
	303.145	7.3064	0.99437	3.6e-4	5.2e-5	2.4e-3	2.4e-3	1.3e-4	1.5e-5	1.1e-3	1.1e-3	8.9e-5	1.1e-4	0.99456	0.00936	-0.05436
	303.144	7.3064	0.99438	5.6e-4	1.7e-4	2.3e-3	2.3e-3	1.2e-4	1.1e-5	1.1e-3	1.1e-3	8.9e-5	1.1e-4	0.99455	0.00936	-0.05436
	303.144	7.3064	0.99438	9.0e-4	3.2e-4	2.4e-3	2.5e-3	1.3e-4	1.3e-5	1.1e-3	1.1e-3	8.9e-5	1.1e-4	0.99455	0.00936	-0.05436
V27	303.142	7.3607	0.99141	1.5e-3	6.6e-4	2.2e-3	2.3e-3	1.7e-4	4.5e-5	1.1e-3	1.1e-3	8.9e-5	1.1e-4	0.99164	0.00947	-0.05209
	303.139	7.3608	0.99143	9.4e-4	3.9e-4	2.4e-3	2.5e-3	2.2e-4	5.9e-5	1.1e-3	1.1e-3	8.9e-5	1.1e-4	0.99160	0.00947	-0.05209
	303.143	7.3607	0.99143	1.2e-3	5.0e-4	2.4e-3	2.5e-3	1.3e-4	1.9e-5	1.1e-3	1.1e-3	8.9e-5	1.1e-4	0.99165	0.00947	-0.05209

ID	Data			Temperature (K)				Pressure (MPa)				Composition (-)			Composition Derivatives	
	$\bar{T}$ (K)	$\bar{p}$ (MPa)	y_{CO_2} (-)	$s(T)$	$s(\bar{T})$	$u(T)$	$u_c(\bar{T})$	$s(p)$	$s(\bar{p})$	$u(p)$	$u_c(\bar{p})$	$u(y_{CO_2})$	$u_{tot}(y_{CO_2})$	$y_{CO_2,calc}$	$\frac{\partial y_{CO_2}}{\partial T}$ (K^{-1})	$\frac{\partial y_{CO_2}}{\partial p}$ (MPa^{-1})
	303.140	7.3607	0.99140	1.3e-3	3.4e-4	2.5e-3	2.5e-3	2.1e-4	5.8e-5	1.1e-3	1.1e-3	8.9e-5	1.1e-4	0.99162	0.00947	-0.05209
V28	303.145	7.4156	0.98894	7.3e-4	1.6e-4	2.4e-3	2.4e-3	9.5e-5	8.3e-6	1.1e-3	1.1e-3	8.9e-5	1.1e-4	0.98890	-0.02040	-0.03700
	303.143	7.4156	0.98897	4.5e-4	6.3e-5	2.5e-3	2.5e-3	8.8e-5	9.5e-6	1.1e-3	1.1e-3	8.9e-5	1.1e-4	0.98888	-0.02040	-0.03700
	303.144	7.4155	0.98895	5.7e-4	7.2e-5	2.5e-3	2.5e-3	8.9e-5	1.0e-5	1.1e-3	1.1e-3	8.9e-5	1.1e-4	0.98889	-0.02040	-0.03700
	303.144	7.4155	0.98897	1.0e-3	4.1e-4	2.4e-3	2.5e-3	9.9e-5	7.2e-6	1.1e-3	1.1e-3	8.9e-5	1.1e-4	0.98889	-0.02040	-0.03700
	303.144	7.4155	0.98896	9.0e-4	1.2e-4	2.4e-3	2.4e-3	9.1e-5	1.4e-5	1.1e-3	1.1e-3	8.9e-5	1.1e-4	0.98889	-0.02040	-0.03700
	303.144	7.4154	0.98896	8.1e-4	2.3e-4	2.6e-3	2.6e-3	9.1e-5	4.1e-6	1.1e-3	1.1e-3	8.9e-5	1.1e-4	0.98890	-0.02040	-0.03700
V29	303.145	7.4254	0.98863	4.3e-4	6.8e-5	2.6e-3	2.6e-3	1.1e-4	1.3e-5	1.1e-3	1.1e-3	8.9e-5	9.6e-5	0.98843	0.00636^{+}	-0.02600
	303.145	7.4254	0.98863	8.8e-4	1.9e-4	2.7e-3	2.7e-3	1.0e-4	6.6e-6	1.1e-3	1.1e-3	8.9e-5	9.6e-5	0.98843	0.00636^{+}	-0.02600
	303.144	7.4253	0.98862	1.0e-3	2.1e-4	2.5e-3	2.5e-3	1.1e-4	2.5e-5	1.1e-3	1.1e-3	8.9e-5	9.6e-5	0.98842	0.00636^{+}	-0.02600
	303.145	7.4252	0.98861	3.8e-4	4.3e-5	2.5e-3	2.5e-3	1.1e-4	8.8e-6	1.1e-3	1.1e-3	8.9e-5	9.5e-5	0.98844	0.00636^{+}	-0.02600
	303.145	7.4252	0.98862	9.7e-4	1.3e-4	2.5e-3	2.5e-3	1.1e-4	1.9e-5	1.1e-3	1.1e-3	8.9e-5	9.6e-5	0.98844	0.00636^{+}	-0.02600
	303.145	7.4252	0.98863	4.0e-4	8.2e-5	2.5e-3	2.5e-3	1.1e-4	2.6e-5	1.1e-3	1.1e-3	8.9e-5	9.6e-5	0.98844	0.00636^{+}	-0.02600
V30	303.145	7.4288	0.98855	4.2e-4	4.9e-5	2.5e-3	2.5e-3	1.0e-4	1.1e-5	1.1e-3	1.1e-3	8.9e-5	1.0e-4	0.98827	-0.01580^{+}	-0.01600
	303.145	7.4288	0.98853	3.6e-4	2.8e-5	2.6e-3	2.6e-3	1.1e-4	1.3e-5	1.1e-3	1.1e-3	8.9e-5	1.0e-4	0.98827	-0.01580^{+}	-0.01600
	303.145	7.4287	0.98858	3.8e-4	3.6e-5	2.5e-3	2.5e-3	1.1e-4	1.1e-5	1.1e-3	1.1e-3	8.9e-5	1.0e-4	0.98827	-0.01580^{+}	-0.01600
	303.145	7.4287	0.98855	4.1e-4	1.1e-4	2.6e-3	2.6e-3	1.1e-4	1.8e-5	1.1e-3	1.1e-3	8.9e-5	1.0e-4	0.98827	-0.01580^{+}	-0.01600
	303.145	7.4287	0.98854	6.4e-4	2.0e-4	2.5e-3	2.5e-3	1.2e-4	1.2e-5	1.1e-3	1.1e-3	8.9e-5	9.9e-5	0.98827	-0.01580^{+}	-0.01600
	303.145	7.4286	0.98857	8.7e-4	1.9e-4	2.4e-3	2.4e-3	1.1e-4	1.8e-5	1.1e-3	1.1e-3	8.9e-5	9.9e-5	0.98828	-0.01580^{+}	-0.01600
V31	303.144	7.4305	0.98855	6.2e-4	1.6e-4	2.6e-3	2.6e-3	1.0e-4	1.5e-5	1.1e-3	1.1e-3	8.9e-5	9.8e-5	0.98818	-0.01487^{+}	-0.00700
	303.145	7.4304	0.98857	3.6e-4	5.0e-5	2.6e-3	2.6e-3	1.0e-4	9.4e-6	1.1e-3	1.1e-3	8.9e-5	9.8e-5	0.98819	-0.01487^{+}	-0.00700
	303.145	7.4304	0.98855	4.1e-4	1.4e-4	2.6e-3	2.6e-3	1.0e-4	1.3e-5	1.1e-3	1.1e-3	8.9e-5	9.8e-5	0.98819	-0.01487^{+}	-0.00700
	303.145	7.4304	0.98851	3.7e-4	6.2e-5	2.6e-3	2.6e-3	9.6e-5	1.5e-5	1.1e-3	1.1e-3	8.9e-5	9.8e-5	0.98819	-0.01487^{+}	-0.00700
	303.145	7.4304	0.98856	5.7e-4	1.4e-4	2.5e-3	2.6e-3	9.5e-5	9.0e-6	1.1e-3	1.1e-3	8.9e-5	9.7e-5	0.98819	-0.01487^{+}	-0.00700
	303.144	7.4303	0.98856	8.4e-4	3.0e-4	2.7e-3	2.7e-3	1.0e-4	1.3e-5	1.1e-3	1.1e-3	8.9e-5	9.8e-5	0.98819	-0.01487^{+}	-0.00700
V32	303.145	7.4317	0.98852	3.3e-4	5.0e-5	2.5e-3	2.5e-3	9.5e-5	1.9e-5	1.1e-3	1.1e-3	8.9e-5	1.0e-4	0.98813	-0.01999^{+}	0.00500
	303.145	7.4317	0.98856	3.1e-4	2.8e-5	2.4e-3	2.4e-3	1.1e-4	1.3e-5	1.1e-3	1.1e-3	8.9e-5	1.0e-4	0.98813	-0.01999^{+}	0.00500

ID	Data			Temperature (K)				Pressure (MPa)				Composition (-)			Composition Derivatives	
	$\bar{T}$ (K)	$\bar{p}$ (MPa)	y_{CO_2} (-)	$s(T)$	$s(\bar{T})$	$u(T)$	$u_c(\bar{T})$	$s(p)$	$s(\bar{p})$	$u(p)$	$u_c(\bar{p})$	$u(y_{CO_2})$	$u_{tot}(y_{CO_2})$	$y_{CO_2,calc}$	$\frac{\partial y_{CO_2}}{\partial T}$ (K^{-1})	$\frac{\partial y_{CO_2}}{\partial p}$ (MPa^{-1})
	303.145	7.4316	0.98857	6.6e-4	1.7e-4	2.5e-3	2.5e-3	8.8e-5	4.0e-6	1.1e-3	1.1e-3	8.9e-5	1.0e-4	0.98814	-0.01999[+]	0.00500
	303.145	7.4317	0.98854	5.2e-4	1.7e-4	2.6e-3	2.6e-3	1.1e-4	1.5e-5	1.1e-3	1.1e-3	8.9e-5	1.0e-4	0.98813	-0.01999[+]	0.00500
	303.145	7.4316	0.98852	5.0e-4	1.2e-4	2.5e-3	2.5e-3	1.1e-4	2.3e-5	1.1e-3	1.1e-3	8.9e-5	1.0e-4	0.98814	-0.01999[+]	0.00500
	303.145	7.4315	0.98854	5.1e-4	1.5e-4	2.7e-3	2.7e-3	1.1e-4	1.0e-5	1.1e-3	1.1e-3	8.9e-5	1.0e-4	0.98814	-0.01999[+]	0.00500
V33	303.145	7.4329	0.98858	5.2e-4	6.6e-5	2.6e-3	2.6e-3	1.0e-4	8.5e-6	1.1e-3	1.1e-3	8.9e-5	9.5e-5	0.98808	-0.00252[+]	0.02700
	303.145	7.4329	0.98857	4.0e-4	1.0e-4	2.5e-3	2.5e-3	1.1e-4	1.2e-5	1.1e-3	1.1e-3	8.9e-5	9.5e-5	0.98808	-0.00252[+]	0.02700
	303.144	7.4328	0.98856	4.3e-4	5.5e-5	2.4e-3	2.4e-3	9.8e-5	5.2e-6	1.1e-3	1.1e-3	8.9e-5	9.5e-5	0.98807	-0.00252[+]	0.02700
	303.145	7.4328	0.98854	7.1e-4	1.3e-4	2.4e-3	2.5e-3	1.0e-4	1.2e-5	1.1e-3	1.1e-3	8.9e-5	9.5e-5	0.98808	-0.00252[+]	0.02700
	303.145	7.4328	0.98854	3.9e-4	6.8e-5	2.7e-3	2.7e-3	1.0e-4	9.2e-6	1.1e-3	1.1e-3	8.9e-5	9.5e-5	0.98808	-0.00252[+]	0.02700
	303.145	7.4328	0.98855	4.4e-4	7.6e-5	2.6e-3	2.6e-3	1.2e-4	1.9e-5	1.1e-3	1.1e-3	8.9e-5	9.5e-5	0.98808	-0.00252[+]	0.02700
V34	303.145	7.4341	0.98860	4.4e-4	1.4e-4	2.3e-3	2.3e-3	9.7e-5	1.7e-5	1.1e-3	1.1e-3	8.9e-5	1.5e-4	0.98802	-0.00733[+]	0.10200
	303.145	7.4341	0.98861	9.6e-4	3.2e-4	2.6e-3	2.6e-3	1.0e-4	8.0e-6	1.1e-3	1.1e-3	8.9e-5	1.5e-4	0.98802	-0.00733[+]	0.10200
	303.144	7.4341	0.98860	9.3e-4	3.0e-4	2.7e-3	2.7e-3	9.0e-5	4.8e-6	1.1e-3	1.1e-3	8.9e-5	1.5e-4	0.98801	-0.00733[+]	0.10200
	303.144	7.4341	0.98861	5.8e-4	1.8e-4	2.4e-3	2.4e-3	9.0e-5	5.9e-6	1.1e-3	1.1e-3	8.9e-5	1.5e-4	0.98801	-0.00733[+]	0.10200
	303.144	7.4340	0.98860	6.6e-4	7.3e-5	2.4e-3	2.4e-3	9.3e-5	5.9e-6	1.1e-3	1.1e-3	8.9e-5	1.5e-4	0.98802	-0.00733[+]	0.10200
	303.144	7.4341	0.98861	8.8e-4	3.2e-4	2.5e-3	2.5e-3	1.0e-4	1.3e-5	1.1e-3	1.1e-3	8.9e-5	1.5e-4	0.98801	-0.00733[+]	0.10200

[+] The derivatives $\frac{\partial y_{CO_2}}{\partial p}$ used in Eq. (5) to obtain $\bar{u}_{tot}(y_{CO_2})$ were calculated using the scaling law in Eq. (6) with the parameters in Table 4 instead of the UMR-PRU fitted model.

Appendix C: Supplementary Tables

Table S.3: Molar masses of atomic elements and compounds with uncertainties

Component *i*	M_i	$u(M_i)$	Unit
C[a]	0.0120108	0.0000003	kg·mol^{-1}
C[b]	0.0120108	0.0000001	kg·mol^{-1}
O	0.0159994	0.0000001	kg·mol^{-1}
CO_2	0.0440096	0.0000003	kg·mol^{-1}
CH_4	0.0160427	0.0000002	kg·mol^{-1}
CO_2 + *imp*	0.0440095		kg·mol^{-1}
CH_4 + *imp*	0.0160427		kg·mol^{-1}
$CO_{2,eff}$	0.0440096		kg·mol^{-1}
$CH_{4,eff}$	0.0160428		kg·mol^{-1}

[a] in CO_2 molecule

[b] in CH_4 molecule

Table S.4: CO_2/CH_4 calibration gas mixtures: CO_2 mole fractions and corresponding standard uncertainties.

$y_{CO_2.cal}$	$u(y_{CO_2.cal}, m)$	$u(y_{CO_2.cal}, M_{eff})$	$u(y_{CO_2.cal}, ads)$	$u_c(y_{CO_2.cal})$
0.850481	$3.4 \cdot 10^{-6}$	$6.3 \cdot 10^{-6}$	$2.5 \cdot 10^{-6}$	$7.6 \cdot 10^{-6}$
0.943293	$3.9 \cdot 10^{-6}$	$7.8 \cdot 10^{-6}$	$2.8 \cdot 10^{-6}$	$9.1 \cdot 10^{-6}$

Table S.5: Fitted parameters for the vapor and liquid correlation between the GC response and the number of moles, along with the standard uncertainty of composition analysis.

Variable	L ROLSI	V ROLSI
$10^3 \cdot c_1$	0.00546	0.00334
c_2	2.13036	2.22570
c_3	1.49009	1.48217
$10^3 \cdot c_4$	0.18510	0.22991
c_5	1.95232	1.94099
$u(x_{CO_2}) = u(y_{CO_2}) = s(e)$	$89.41 \cdot 10^{-6}$	$89.41 \cdot 10^{-6}$
n	13	13

Table S.6: Summary of symbols used in Tables S.1 and S.2.

Symbol	Definition
ID	Identifier for a series of samples. L, V and P corresponds to liquid, vapor and CO_2 vapor pressure series, respectively.
$\bar{T}$	Mean temperature before the sample is withdrawn from the cell.
$\bar{p}$	Mean pressure before the sample is withdrawn from the cell.
x_{CO_2}	Liquid phase CO_2 mole fraction
y_{CO_2}	Vapor phase CO_2 mole fraction
$s(T)$	Sample standard deviation of the measured temperatures used to calculate $\bar{T}$. See Eq. (7) in Westman et al. [12].
$s(\bar{T})$	Standard random uncertainty of $\bar{T}$, considering the autocorrelation of the measurements of T. See Eq. (6) in Westman et al. [12].
$u(T)$	Standard systematic uncertainty of $\bar{T}$. Details in section 3.1 in Westman et al. [12].
$u_c(\bar{T})$	Combined systematic uncertainty of $\bar{T}$ calculated through $\sqrt{s^2(\bar{T}) + u^2(T)}$
$s(p)$	Sample standard deviation of the measured pressures used to calculate $\bar{p}$. See Eq. (7) in Westman et al. [12].
$s(\bar{p})$	Standard random uncertainty of $\bar{p}$., considering the autocorrelation of the measurements of p. See Eq. (6) in Westman et al. [12].
$u(p)$	Standard systematic uncertainty of $\bar{p}$. See Section 3.5 in Westman et al. [12].
$u_c(\bar{p})$	Combined systematic uncertainty of $\bar{p}$ calculated through $\sqrt{s^2(\bar{p}) + u^2(p)}$
$u(z_{CO_2})^*$	Standard uncertainty of a sample from composition analysis alone. See Section 3.3 and Table S.3.
$u_{tot}(z_{CO_2})^*$	Total standard uncertainty of a sample, caused by additional contribution from the uncertainty in temperature and pressure. See Eq. (5). Marker $^+$ indicates that the derivative $\frac{\partial z_{CO_2}}{\partial p}$ used in Eq. (5) was calculated using the scaling law in Eq. (6) with the parameters in Table 4 instead of the fitted UMR-PRU model.
$z_{CO_2,calc}{}^*$	VLE CO_2 mole fraction at ($\bar{T}$, $\bar{p}$), calculated using the fitted UMR-PRU model. See Section 4.5.
$\frac{\partial z_{CO_2}}{\partial T}{}^*$	Partial derivative of phase composition at VLE with respect to temperature used in Eq. (5), calculated using the fitted UMR-PRU model.
$\frac{\partial z_{CO_2}}{\partial p}{}^*$	Partial derivative of phase composition at VLE with respect to pressure used in Eq. (5), calculated using the fitted UMR-PRU model.

* z_{CO_2} refers to x_{CO_2} in Table S.1 and y_{CO_2} in Table S.2